Southeastern Geology: Volume 37, No. 2 October 1997

Editor in Chief: S. Duncan Heron, Jr.

Abstract

Academic journal published quarterly by the Department of Geology, Duke University.

SOUTHEASTERN GEOLOGY

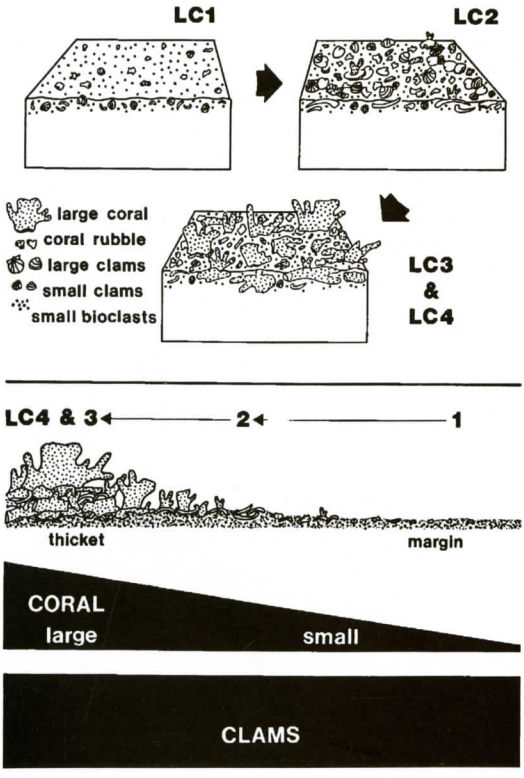

VOL. 37, NO. 2 OCTOBER 1997

SOUTHEASTERN GEOLOGY

PUBLISHED

at

DUKE UNIVERSITY

Editor in Chief:

Duncan Heron

This journal publishes the results of original research on all phases of geology, geophysics, geochemistry and environmental geology as related to the Southeast. Send manuscripts to **DUNCAN HERON, DUKE UNIVERSITY, BOX 90233, DURHAM, NORTH CAROLINA 27708-0233**. Phone: 919-684-5321, Fax: 919-684-5833, Email: heron@geo.duke.edu Please observe the following:

1) Type the manuscript with double space lines and submit in duplicate.
2) Cite references and prepare bibliographic lists in accordance with the method found within the pages of this journal.
3) Submit line drawings and complex tables reduced to final publication size (no bigger than 8 x 5 3/8 inches).
4) Make certain that all photographs are sharp, clear, and of good contrast.
5) Stratigraphic terminology should abide by the North American Stratigraphic Code (American Association Petroleum Geologists Bulletin, v. 67, p. 841-875).

Subscriptions to *Southeastern Geology* for volume 37 are: individuals - $18.00 (paid by personal check); corporations and libraries - $23.00; foreign $27. Inquires should be sent to: **SOUTHEASTERN GEOLOGY, DUKE UNIVERSITY, BOX 90233, DURHAM, NORTH CAROLINA 27708-0233**. Make checks payable to: *Southeastern Geology.*

Information about SOUTHEASTERN GEOLOGY is on the World Wide Web including a seachable author-title index 1958-1996. The URL for the Web site is:

http://www.geo.duke.edu/seglgy.htm

SOUTHEASTERN GEOLOGY is a peer review journal.

ISSN 0038-3678

SOUTHEASTERN GEOLOGY

Table of Contents

Volume 37, No. 2

October 1997

SOUTHEASTERN GEOLOGY
V. 37, No. 2, October 1997, p. 55-72

SIGNIFICANCE OF YOUNG PALEOCENE RB-SR AND K-AR GLAUCONITE DATES FROM THE LANG SYNE FORMATION, SAVANNAH RIVER SITE, SOUTH CAROLINA

W. BURLEIGH HARRIS

Department of Earth Sciences
University of North Carolina at Wilmington
Wilmington, NC 28403

PAUL D. FULLAGAR

Department of Geology
University of North Carolina at Chapel Hill
Chapel Hill, NC 27514

LAURA L. TOVO

Westinghouse Savannah River Company
Savannah River Technology Center
Analytical Development Section
Aiken, SC 29808

ABSTRACT

Twenty hand-picked glauconitic micas from the late Paleocene (Selandian/Thanetian) Lang Syne Formation in three core holes from the Savannah River Site, yield a nearly linear array of data points which corresponds to a Rb-Sr date of 51.5 ± 0.1 Ma and an initial $^{87}Sr/^{86}Sr$ ratio of 0.70822 ± 0.0001. This date is about 10-15% younger than the suggested biostratigraphic age of the unit.

All updip samples have model dates that are too young, whereas some downdip samples are also young, but several have dates that agree with the suggested biostratigraphic age. Electron microprobe analysis of the spatial distribution of Fe_2O_3, Al_2O_3, K_2O, P_2O_5 and CaO in updip samples indicates that they are mature, have no unusual distribution of oxides and low concentrations of CaO. In addition, these samples also have low concentrations of Sr and high Rb/Sr ratios. All downdip samples have higher concentrations of P_2O_5 and CaO. Concentrations of CaO appear in most cases to follow P_2O_5, but CaO also occurs where concentrations of P_2O_5 are low in grain interiors. In addition, downdip samples also have higher Sr concentrations and lower Rb/Sr ratios than updip samples. Downdip samples with dates that agree with the biostratigraphic age have the highest P_2O_5, CaO, and Sr concentrations and the lowest Rb/Sr ratios.

K-Ar conventional dates of three of the glauconitic micas, one updip and two downdip, are generally concordant with the Rb-Sr model dates (49.8 ± 1.9 Ma - updip; 47.5 ± 1.8 Ma - downdip); however, one downdip sample yields a date of 58.8 ± 2.3 Ma which agrees with the biostratigraphic age of the unit.

The concordance of Rb-Sr model dates from the Lang Syne Formation in three core holes indicates that a regional geologic event is probably responsible for resetting the dates of the samples. The early Eocene was a time at which the largest sea level drop in the early Tertiary occurred; it is suggested that most of the glauconitic micas re-equilibrated during diagenesis with ground water during the 51.5 Ma lowstand of sea level.

INTRODUCTION

The term glauconite is used for any green sand-size grain that occurs in sediments or sedimentary rocks, or for a specific clay mineral rich in Fe and K that is similar to illite. Because of this ambiguity Odin and Matter (1981) introduced the term glaucony for any green sand-size grain (facies) and glauconite mica for the specific mineral. On the basis of K_2O concentration, Odin and Matter (1981) recognized five types of glaucony: nascent, little evolved, highly evolved, and relict. Nascent and little-evolved glaucony contained less than 6% K_2O, was referred to as glauconitic smectite, contained incompletely glauconitized mineral precursors, and commonly yields dates older than deposition. Evolved to highly evolved glaucony represented recrystallization of glauconitic smectite, contained greater than 6% K_2O and was referred to as glauconitic mica. They suggested that evolved to highly evolved glaucony offers the best possibility of providing depositional ages as vestiges of the mineral precursors are destroyed during its formation.

Odin and Matter (1981) suggested that the optimum conditions for glauconitization are those of semi-confinement as the interiors of grains are more glauconitized (greater evolved) than the grain exteriors. Hence, inter-grain variation in maturity and glaucony mineralogy is common and often complicates any attempts to interpret obtained dates. Velde (1976) demonstrated through electron microprobe analysis that glaucony maturity varies between grains within the same sample as well as within the same grains. Odin and Fullagar (1988) indicated that knowledge of the conditions of formation, evolution and diagenesis of glaucony are "... necessary to interpret radiometric ages obtained from this material." In this paper, glauconitic smectite or glauconitic mica is used when the exact nature of the grains has been determined by X-ray diffraction studies, and glaucony is used in the facies sense of Odin and Matter (1981).

Glaucony dates have been used by various workers to determine the time of sediment deposition and to place age-constraints on the geologic time scale (Odin, 1982). However, Obradovich (1988, p. 757) has remained skeptical of the chronostratigraphic utility of glauconies, and stated that "...outright acceptance of published results... can result in erroneous age estimates of various biostratigraphic levels and stage and epoch boundaries". The contention is that glauconies may produce precise dates but they are usually younger than the time of deposition as indicated by dates of coeval volcanic minerals. Although few direct comparisons have been made between dates of glauconitic mica and coeval volcanic minerals, an example of the concordance has been reported (Harris and Fullagar, 1989). Nevertheless, glauconitic mica dates have been generally dismissed for dating the time of sediment deposition (Obradovich, 1989). Certainly, glaucony dates that are younger than the time of sedimentation are known to exist. Various reasons used to explain these young dates include, they: 1) reflect diagenetic and fluid migrational history (Smalley and others, 1987), 2) represent diagenesis (Morton and Long, 1980; Grant and others, 1984), 3) mark emergence above sea-level or regional uplift (Laskowski and others, 1980; Morton and Long, 1984)), 4) record tectonism (Conrad and others, 1982), or 5) represent the time of ore formation (Stein and Kish, 1985, 1991). Consistent among all proposals is that they rely upon cation exchange reactions with some type of fluid, either meteoric, juvenile, ground water, or hydothermal to reset mineral dates.

This paper presents Rb-Sr and K-Ar glauconitic mica dates for the Paleocene Lang Syne Formation from the updip part of the Southeast Georgia Embayment at the Savannah River Site, South Carolina. Dates which are significantly younger than the suggested biostratigraphic age of the unit are interpreted to record a regional diagenetic event that may be related to eustatic lowering of sea level during the late Paleocene to early Eocene.

GEOLOGIC SETTING

The Savannah River Site (SRS), located approximately 32 km east of the Fall Line in the inner coastal plain of South Carolina, Aiken,

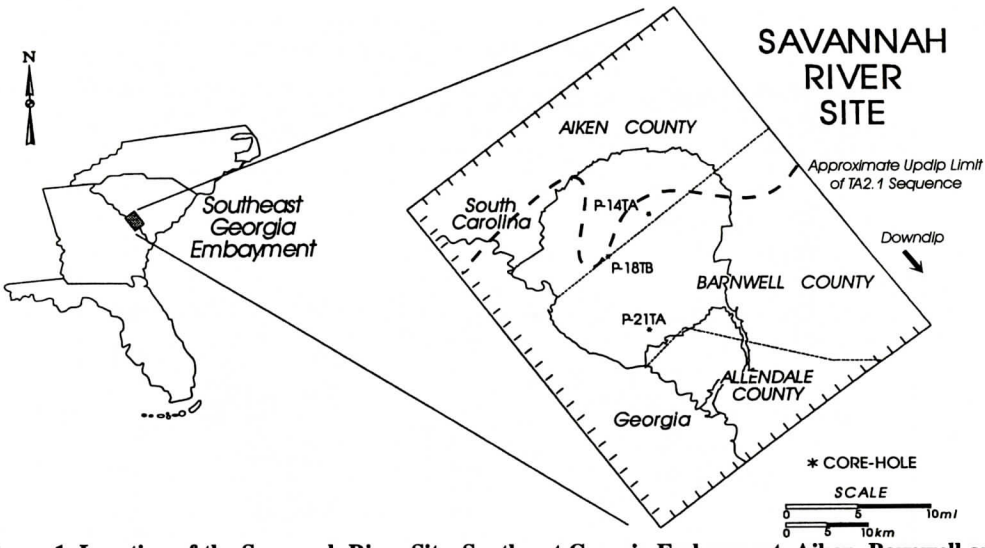

Figure 1. Location of the Savannah River Site, Southeast Georgia Embayment, Aiken, Barnwell and Allendale Counties, South Carolina. Also shown are the three core holes and the approximate updip limit of the depositional sequence that provided the samples dated in this study. Appendix 1 gives the latitude and longitude of core hole locations.

Barnwell, and Allendale Counties, covers an area of almost 800 sq. km in the updip Southeast Georgia Embayment (Figure 1). The coastal plain section on the SRS consists of a wedge of Cretaceous and Cenozoic sediments that thickens from about 200 m along the northwestern border to over 400 m along the southeastern border. Although regional dip is to the southeast at about 9 m/km, beds locally dip and thicken in other directions. Over most of the SRS, Cretaceous sediments are unconformable on Precambrian and Paleozoic crystalline rocks of the Appalachian orogen including slate, phyllite, schist, gneiss, volcanic and metavolcanic rocks, granite and mafic rocks (Fallaw and Price, 1995). In the southeastern part of the SRS they lie on Triassic-Jurassic? sediments of the Newark Supergroup within the Dunbarton basin.

Stratigraphy

Paleogene units on the SRS consist predominantly of Paleocene and lower Eocene siliciclastic sediments and middle and upper Eocene mixed siliciclastic-carbonate sediments (Figure 2). The oldest Paleocene unit recognized in the area was called the Ellenton Formation by Siple (1967) as defined by Prowell and others (1985). Recently this name was abandoned by Fallaw and Price (1992, 1995), because it included two different sedimentary sequences deposited during separate cycles of relative sea level. Fallaw and Price (1995) extended the Sawdust Landing Formation which is used for Danian age sediments in the Santee River area, South Carolina, south into the Savannah River area and applied it to all sediments that are early Paleocene in age. For upper Paleocene sediments, they introduced the name Lang Syne Formation which is also used in the Santee River area for sediments generally considered Thanetian in age. In this paper we follow Fallaw and Price (1995) and use the terms Sawdust Landing and Lang Syne Formations for lower and upper Paleocene sediments on the SRS.

Sawdust Landing Formation.

This formation consists of basal, poorly sorted muscovite-rich quartz sand with occasional quartz pebbles and partially lignitized wood fragments, and upper dark, organic, sometimes fissile clay or claystone that often contains inter-laminae of fine quartz sand or silt-sized muscovite flakes. Thin quartz silt and sand layers become more abundant toward the top (Figure 3). Edwards (1992) suggested an early

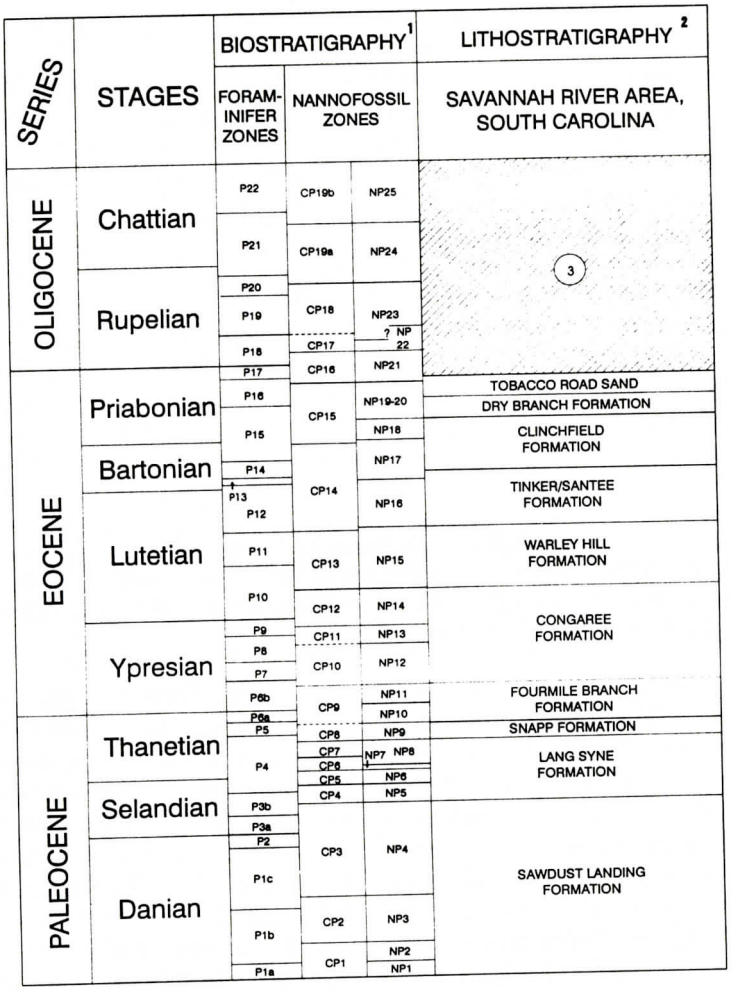

Figure 2. Biostratigraphy and lithostratigraphy in the Savannah River area, South Carolina. (1) Biostratigraphic zonation is from Berggren and others (1995); (2) lithostratigraphy is after Fallaw and Price (1995); (3) possible Oligocene/Miocene sediments reported by Zullo and others (1982).

Paleocene age for the formation, and dinoflagellates and pollen from the lower part of the formation indicate that it is latest Danian (Clark, 1989, personal communication). Fallaw and Price (1992, 1995) on the basis of a few palynological dates assigned the Sawdust Landing Formation on the SRS to Martini's (1971) calcareous nannofossil zones NP1 to perhaps NP4, and either Haq and others' (1987) TA1.2 or TA1.3 global coastal onlap cycle (Figure 3). Harris and others (1993) identified a single lower Paleocene depositional sequence which represented their lowermost Ellenton Formation (Sawdust Landing Formation of Fallaw and Price, 1995) and assigned it to Haq and others' (1987) TA1.3 global coastal onlap cycle.

Lang Syne Formation

The Lang Syne Formation is composed of lower organic-rich quartz sand, glauconitic quartz sand or pebbly quartz sand, and upper siliceous mudstone, laminated organic claystone, or fossiliferous clay or limestone (Figure 3). Fossiliferous clay and limestone become more abundant downdip to the southeast whereas siliceous mudstone is more abundant on the SRS. Siliceous mudstone is usually massive, particularly where it contains appreciable

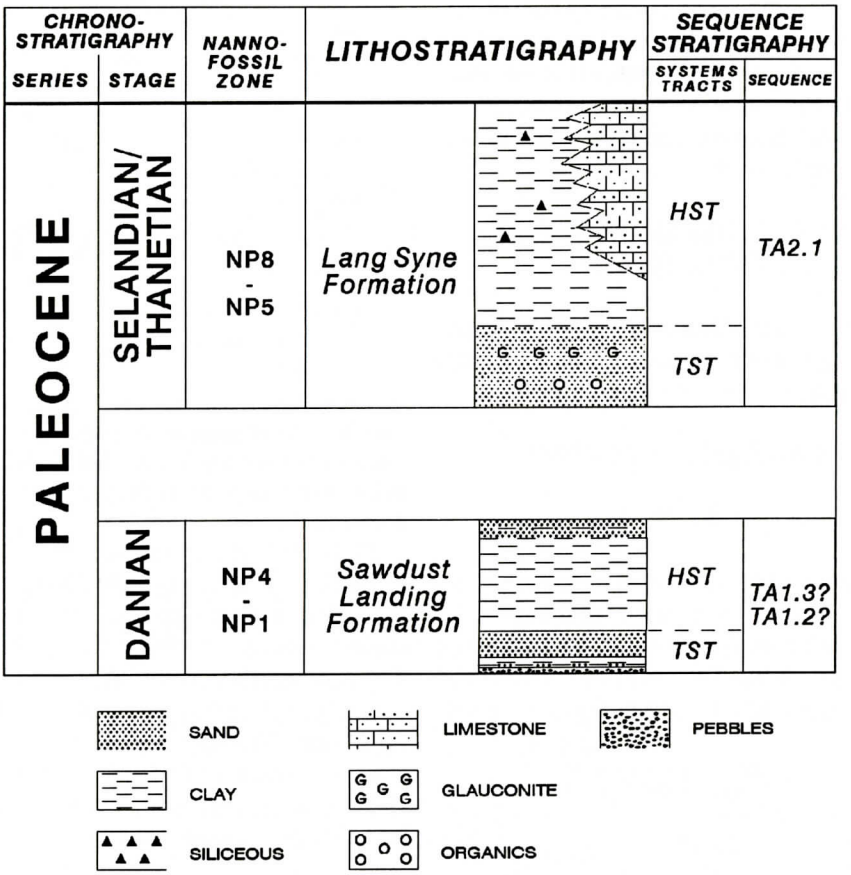

Figure 3. Chronostratigraphy, biostratigraphy, and sequence stratigraphy of the Paleocene Lang Syne Formation, Savannah River Site, South Carolina. The Lang Syne Formation provided the samples dated in this study. TST = transgressive systems tract, HST = highstand systems tract.

amounts of cristobalite, whereas the laminated organic claystone is fissile. Invertebrates, dinoflagellates, and calcareous nannofossils (*Heliolithus riedelli*) indicate that the formation is assignable to calcareous nannofossil zone NP8. Fallaw and Price (1992, 1995) indicate that numerous palynological assemblages have been recovered from the Lang Syne Formation on the SRS which indicate assignment to nannoplankton zones NP4-8 or NP5-8. Harris and others (1993) identified a single upper Paleocene depositional sequence which represented their uppermost Ellenton Formation (Lang Syne Formation of Fallaw and Price, 1995) and assigned it to Haq and others' (1987) TA2.1 cycle (Figure 3). As coastal onlap cycle TA2.1 includes calcareous nannofossil zones NP5-8, the material dated in this study is compared to suggested ages for these zones.

Glaucony quartz sand of the lower part of the Selandian/Thanetian Lang Syne Formation (TA2.1 depositional sequence) in three core holes, P-14TA, P-18TB, and P-21TA provided the material that is dated and discussed in this paper (Figure 1). Core hole P-14TA is interpreted to represent a depositional updip position, core hole P-18TB an intermediate position, and core hole P-21TA a depositional downdip position. The location of core hole P-18 was selected to be close to Siple's (1967) original Ellenton Formation (Price, 1997, personal communication). The Lang Syne Formation is assigned to

the Crouch Branch aquifer in core hole P-14TA, and the Crouch Branch confining unit in core holes P-18TB and P-21TA by Aadland and others (1995). Thayer (1997, personal communication) indicates that formation waters in the Crouch Branch aquifer and confining unit have a pH that averages 5.

SAMPLE PREPARATION AND ANALYTICAL TECHNIQUES

Sample preparation and analytical procedures are given in Appendix 1. Table 1 gives the analytical data for the samples dated.

RADIOMETRIC DATES

Rb-Sr

Regression analysis of data for twenty glauconitic mica splits from three core holes in the Lang Syne Formation yield a Rb-Sr date of 51.5 ± 0.1 Ma, an initial $^{87}Sr/^{86}Sr$ ratio of 0.70822 ± 0.0001, and an MSWD of 8.8 (Figure 4). If only

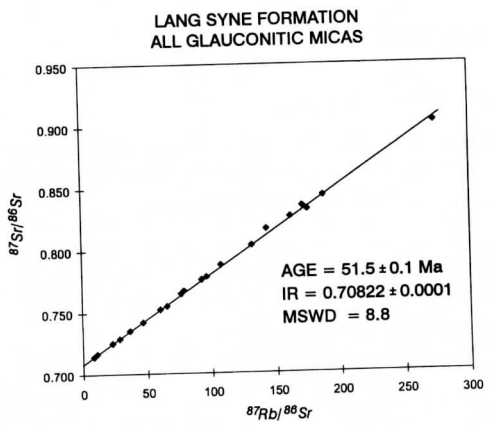

Figure 4. Rb-Sr errochron plot of $^{87}Rb/^{86}Sr$ versus $^{87}Sr/^{86}Sr$ of all glauconitic mica from the Lang Syne Formation. Data points are significantly larger than analytical uncertainties.

samples in the updip core hole (P-14TA) are considered, twelve glauconitic micas yield a Rb-Sr date of 50.8 ± 0.2 Ma, an initial $^{87}Sr/^{86}Sr$ ratio of 0.70968 ± 0.0004, and an MSWD of 10.5 (Figure 5). In the downdip core hole (P-21TA), six glauconitic micas yield a Rb-Sr date

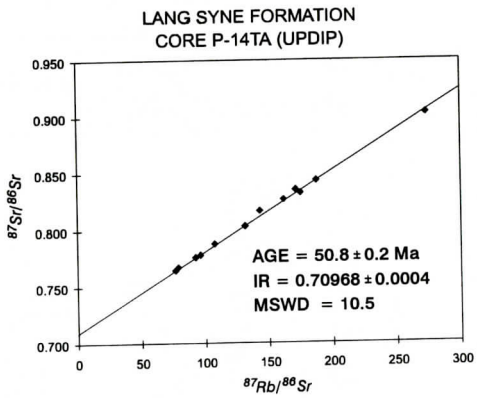

Figure 5. Rb-Sr errochron plot of $^{87}Rb/^{86}Sr$ versus $^{87}Sr/^{86}Sr$ of glauconitic mica from the updip Lang Syne Formation (core hole P-14TA). Data points are significantly larger than analytical uncertainties.

of 50.1 ± 0.5 Ma, an initial $^{87}Sr/^{86}Sr$ ratio of 0.70862 ± 0.00017, and an MSWD of 1.9 (Figure 6). The date that is based on all of the glauconitic micas (51.5 Ma) as well as the date of the updip samples (50.8 Ma) have high MSWD values indicating that these dates are based on errochrons. The date of 50.1 Ma for samples from core hole P-21TA has a low MSWD value (1.9), thus suggesting that this date could be based on an isochron.

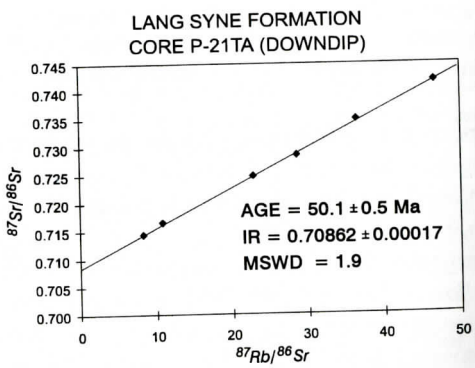

Figure 6. Rb-Sr errochron plot of $^{87}Rb/^{86}Sr$ versus $^{87}Sr/^{86}Sr$ of glauconitic mica from the downdip Lang Syne Formation (core hole P-21TA). Data points are significantly larger than analytical uncertainties.

Examination of model dates for each sample, calculated using a Thanetian seawater value of 0.70776 as the initial Sr isotopic ratio (Koep-

Table 1. Rb-Sr and K-Ar analytical data for glauconitic mica from the late Paleocene Lang Syne Formation, Savannah River Site, South Carolina. Note that downdip samples have a greater spread in age than the updip samples indicating that they are less radiogenic.

	Sample	Sand Size	Rb (ppm)	Sr (ppm)	$^{87}Rb/^{86}Sr$	$^{87}Sr/^{86}Sr$	Mean Wt. % K	$^{40}Ar^*$ (%)	$^{40}Ar^*$ (ppm)	Rb-Sr Model Date (Ma)	K-Ar Conventional Date (Ma)
UPDIP (P-14TA)											
	H8703-60	Fine, medium	302.40	8.20	107.55	0.78787				52.5 ± 0.8	
	H8703-70[1]	Coarse, fine	287.60	4.92	171.20	0.83523				52.4 ± 0.8	
	H8703-80	Fine	297.50	9.38	92.38	0.77598				52.0 ± 0.8	
	H8703-100	Fine, fine	294.00	5.32	161.71	0.82668				51.8 ± 0.6	
	H8703-120	Fine, fine	293.60	4.59	187.31	0.84336				51.0 ± 0.6	
	H8704-40	Medium	300.40	6.14	143.11	0.81670				53.6 ± 0.8	
	H8704-60	Fine, medium	303.40	11.53	76.54	0.76478	6.204	20.90	0.02170	52.5 ± 0.8	49.8 ± 1.9
	H8704-70	Coarse, fine	294.70	10.91	78.61	0.76713				53.2 ± 0.8	
	H8704-80	Fine	302.80	9.16	96.33	0.77819				51.5 ± 0.8	
	H8704-100[1]	Fine, fine	296.80	6.60	131.37	0.80343				51.3 ± 0.8	
	H8704-120	Fine, fine	291.90	3.15	273.39	0.90271				51.4 ± 1.8	
	H8704-140	Very fine	297.10	4.98	174.90	0.83241				50.2 ± 0.6	
DOWNDIP (P-21TA)											
	H8712-40[1]	Medium	283.70	99.40	8.26	0.71439				56.5 ± 3.6	
	H8712-70[1]	Coarse, fine	312.90	31.77	28.55	0.72854				51.3 ± 1.4	
	H8712-100[1]	Fine, fine	312.80	19.45	46.67	0.74179				51.3 ± 1.2	
	H8713-40[1]	Medium	300.50	80.42	10.82	0.71653				57.1 ± 2.8	
	H8713-70[1]	Coarse, fine	331.10	42.13	22.77	0.72484	6.190	55.00	0.02564	52.8 ± 1.6	58.8 ± 2.3
	H8713-100	Fine, fine	317.00	25.25	36.43	0.73489				52.4 ± 1.4	
DOWNDIP (P-18TB)											
	H8719-100	Fine, fine	323.50	15.62	60.19	0.75215	6.041	20.00	0.02014	51.9 ± 1.0	47.5 ± 1.8
	H8719-120	Fine, fine	326.20	14.49	65.45	0.75472				50.5 ± 1.0	

[1] Samples examined by microprobe.

*Radiogenic

Rb-Sr model dates for glauconitic micas calculated using initial 87Sr/86Sr from published Thanetian seawater value of 0.70776. Errors on Rb-Sr model dates and K-Ar conventional dates are one standard deviation.

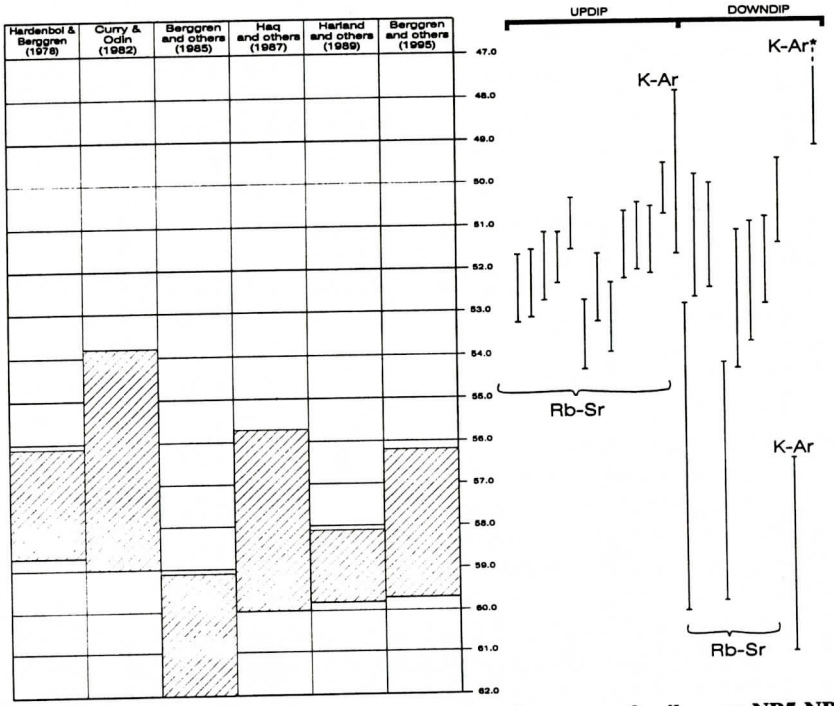

Figure 7. Comparison of the geochronometric limits placed on nannofossil zones NP5-NP8 (shaded areas) by several different geologic time scales to Rb-Sr model dates and K-Ar dates from the Lang Syne Formation. Model dates are plotted with one standard deviation errors. Eighteen model dates are younger than all estimates of the age limits placed on nannofossil zones. Two model dates agree with the suggested age limits, but these dates have large errors because of low $^{87}Sr/^{86}Sr$ ratios. One conventional K-Ar date also agrees with the biostratigraphic age; the other two are younger than the biostratigraphic age. *Error is ± 1.8 Ma and is not totally shown because of temporal scale.

nick and others, 1985), indicates that considerable variation occurs in the dates (Table 1). Updip samples (H8703, H8704) yield dates that range from 50.2 to 53.6 Ma whereas downdip samples (H8712, H8713, H8719-100 and H8719-120) yield dates that range from 50.5 to 57.1 Ma.

Two downdip samples (H8712-40 and H8713-40) yield Rb-Sr model dates (~57 Ma) that are considerably older than other model dates, and when the errors are considered the dates approximate the suggested time of deposition of the Lang Syne Formation. These samples have the lowest Rb/Sr ratios of any samples that were analyzed, and thus, they also have the lowest $^{87}Sr/^{86}Sr$ ratios (0.714 and 0.716). These low ratios mean that the model dates are highly dependent upon the value assumed for the initial $^{87}Sr/^{86}Sr$ ratio. If the initial ratio were only 0.0005 higher than the assumed value of 0.70776, the model dates would be 52.2 and 53.8 Ma. Thus, the calculated old dates for these samples could be apparent rather than real. These two downdip samples are from the coarsest size fractions of glauconitic mica (Table 1). This pattern of older dates being associated with the coarsest size fraction of glauconitic mica also may be seen in the updip samples; but here the age differences are small.

K-Ar

Three glauconitic mica splits, one updip sample (H8704-60) and two downdip samples (H8713-70 and H8719-100) yield conventional K-Ar dates of 49.8 ± 1.9 Ma, 58.8 ± 2.3 Ma, and 47.5 ± 1.8 Ma, respectively. The 49.8 Ma and 47.5 Ma dates are 5 and 9% younger than the Rb-Sr model dates determined from the same samples; the older date is about 12% greater

than the Rb-Sr model date determined from a sample split. The older K-Ar date (58.8 ± 2.3 Ma) approximates the suggested age of sedimentation for the Lang Syne Formation (Figure 7) and is in analytical agreement with the downdip Rb-Sr model dates from the two coarsest size fractions (Table 1).

Sr CONCENTRATIONS

Sr concentrations from updip samples (P-14TA) range from 3.15 ppm to 11.53 ppm (average 7.07 ppm) whereas Sr concentrations in downdip samples (P-21TA) range from 19.45 ppm to 99.40 ppm (average 49.74 ppm) (Table 1). As the two samples from core-hole P-18TB were acid-washed during sample preparation and the other samples were not, they are excluded from the discussion below.

ELECTRON MICROPROBE

Electron microprobe analysis of selected sample splits was undertaken to examine the spatial distribution and variations in concentration of Ca, Sr, K, Rb, Fe, Mg, Al, P and Si within the glauconitic micas (Table 1). It was assumed that the young dates could be explained by one or a combination of any of the following diagenetic reactions: 1) removal of ^{87}Sr from the samples after system closure, 2) Rb absorption by the samples after system closure, or 3) complete or partial isotopic homogenization of the glauconitic micas during a later geologic event. Ideally, we originally wanted to examine the spatial distribution of Rb, Sr, K and Ar in selected glauconitic micas; however, low concentrations of Rb, Sr and Ar generally made it impossible to map their distribution. In all glauconitic samples, the distribution and concentration of K and Ca were mapped and used as a proxies to suggest the distribution and concentration of Rb and Sr, respectively. It was assumed in both cases that because Rb and Sr have ionic radii only slightly different from that of K and Ca, they would follow these elements in the glauconitic micas. In addition, the concentration of P was also determined to assess if high Ca concentrations were the result of phosphate contamination. Rb distribution was mapped in a total of five grains from downdip samples H8712-70 and H8712-100 at magnifications from 500x to 1500x. Elemental mapping indicates a uniform distribution of Rb in these samples; however, no quantitative analyses were made. Sr mapping was also attempted on four grains from these same samples, and although Sr was detected, its concentration was at the lower limits of detectability. Therefore, Sr results are suspect and are not reported.

General electron microprobe observations are: 1) Sr concentrations were too low to be detected in all samples, 2) K concentrations generally were uniformly distributed throughout the grains in all samples, 3) P is somewhat variable and probably occurs only where apatite is present as impurities in samples, 4) Al is uniformly distributed within the grains in updip samples and generally exhibits higher concentrations on grain exteriors in downdip samples, 5) Ca is generally more highly concentrated in sites with high P content in downdip samples,

P-14TA-UPDIP

Element	Grain		Uniform Distribution [1]	Random Distribution [2]	Not Detected
	Exteriors	Interiors			
Ca			X		
Sr					X
K			X		
Rb			X		
Fe		X			
Mg*			X		
Al		X			
P			X		
Ti**			X		

P-21TA-DOWNDIP-YOUNG

Element	Grain		Uniform Distribution [1]	Random Distribution [2]	Not Detected
	Exteriors	Interiors			
Ca				X	
Sr					X
K		X			
Rb			X		
Fe		X			
Mg*			X		
Al	X				
P				X	
Ti**			X		

P-21TA-DOWNDIP-OLD

Element	Grain		Uniform Distribution [1]	Random Distribution [2]	Not Detected
	Exteriors	Interiors			
Ca		X		X	
Sr					
K			X		
Rb					
Fe			X		
Mg*					
Al	X				
P		X		X	
Ti**			X		

* Distribution based on grain mapping
** Lower limit of detectability
1 Uniform distribution indicates little variability in concentration from exterior to interior.
2 Random distribution indicates significant variability in concentration.

Table 2. Summary of the distribution of elements mapped by electron microprobe in updip and downdip glauconitic micas, Savannah River Site. X indicates areas of principal concentration.

Table 3. Average concentration of selected oxides from Lang Syne Formation glauconitic micas based on electron microprobe analysis.

		UPDIP YOUNG GLAUCONITIC MICAS	DOWNDIP OLD GLAUCONITIC MICAS	DOWNDIP YOUNG GLAUCONITIC MICAS
Al_2O_3 Wt. %	Grain Exterior	13.77	6.54	9.07
		11.16	5.46	8.45
		11.49	4.84	6.57
		10.46	4.27	6.55
		10.32	3.76	6.52
		9.84	4.08	5.71
		9.65	4.14	5.81
		10.96	4.57	4.80
		9.06	5.30	6.10
	Grain Interior	9.17	3.71	6.29
Fe_2O_3 Wt. %	Grain Exterior	18.21	13.54	19.23
		18.68	16.19	20.19
		19.97	16.86	20.61
		20.35	15.47	23.06
		20.69	14.41	22.75
		20.65	15.70	21.84
		20.87	15.74	20.81
		20.58	15.13	18.29
		19.96	15.49	22.74
	Grain Interior	21.05	14.82	24.41
K_2O Wt. %	Grain Exterior	6.24	5.16	6.86
		6.35	6.32	6.98
		6.72	5.99	6.98
		6.91	5.57	7.87
		7.08	5.04	7.55
		6.99	5.59	7.37
		7.08	5.72	7.14
		6.93	5.41	6.10
		6.53	5.43	7.55
	Grain Interior	7.09	5.41	7.72
Ti_2O Wt. %	Grain Exterior	0.05	0.04	0.04
		0.05	0.03	0.02
		0.04	0.03	0.02
		0.05	0.02	0.02
		0.10	0.03	0.02
		0.06	0.02	0.02
		0.05	0.02	0.02
		0.06	0.03	0.02
		0.04	0.01	0.04
	Grain Interior	0.04	0.04	0.06
P_2O_5 Wt. %	Grain Exterior	0.07	4.18	0.34
		0.06	5.27	0.29
		0.05	4.90	1.28
		0.07	7.81	0.53
		0.07	8.74	0.96
		0.05	6.77	0.75
		0.07	5.44	0.37
		0.07	6.46	0.36
		0.07	6.14	0.02
	Grain Interior	0.10	8.74	0.19
CaO Wt. %	Grain Exterior	0.18	7.77	0.84
		0.19	7.47	0.87
		0.21	8.55	3.90
		0.19	13.53	0.67
		0.21	15.99	2.20
		0.19	11.09	1.78
		0.19	12.79	1.67
		0.20	12.79	2.56
		0.16	11.17	2.10
	Grain Interior	0.22	16.77	0.09

and 6) Fe increases or stays constant toward the interior of grains. For discussion purposes, electron microprobe data are grouped below into young updip glauconitic micas, young downdip glauconitic micas and old downdip glauconitic micas. Table 2 summarizes electron microprobe observations; microprobe data are given in Table 3.

Table 4. Summary of major oxide composition in glauconites as determined by microprobe analysis (modified from Birch and others, 1976).

	IMMATURE	INTERMEDIATE	MATURE	OXIDIZED
SiO_2	48.03	50.10	50.97	28.08
Al_2O_3	5.74	4.43	4.29	4.00
Fe_2O_3	19.14	22.15	21.01	44.73
MgO	4.04	4.36	5.45	2.83
CaO	1.68	0.32	0.18	0.30
Na_2O	0.14	0.14	0.07	0.11
K_2O	5.22	7.35	9.01	3.40
P_2O_5	0.19	0.19	0.15	0.52

DISCUSSION AND CONCLUSIONS

Isotopic Dates

Rb-Sr Dates

Rb-Sr model and errorchron dates of glauconitic micas from the Lang Syne Formation are about 10 to 15% younger than the biostratigraphic age suggested by most recent time scales (Figures 4-6). In addition, the calculated initial $^{87}Sr/^{86}Sr$ ratios of 0.70968 ± 40, 0.70862 ± 17, and 0.70822 ± 10 from the errochrons are higher than the 0.70776 initial $^{87}Sr/^{86}Sr$ ratio that is suggested for Thanetian seawater by Koepnick and others (1985). The young dates, high initial Sr ratios, and moderate scatter of the Rb-Sr data points all indicate that the Rb-Sr systems of the samples have been altered since the mineral formed in Selandian/Thanetian seawater. The high MSWD values (in two cases) indicate that the scatter of the data points (Figures 4 and 5) exceeds expected analytical uncertainties, and thus the linear arrays of $^{87}Rb/^{86}Sr$ versus $^{87}Sr/^{86}Sr$ are termed errochrons.

Assuming that there was initial homogeneity of the samples, lower Sr contents of updip glauconitic micas (core hole P-14TA), and higher Sr contents in downdip glauconitic micas (core hole P-21TA) suggest that either Sr was removed updip or Sr was added downdip or some combination of both processes occurred. The overall agreement of the Rb-Sr dates argues against random events. The errochron representing all Lang Syne Formation glauconitic micas probably represents partial isotopic reequilibration of the samples during a widespread geologic event. As this area of the southeastern Atlantic Coastal Plain has probably never been buried deeply, some mechanism other than burial must be invoked to explain the general consistency of the Rb-Sr data.

Complete isotopic homogenization of glauconitic micas during later uplift (Laskowski and others, 1980), hydrothermal activity (Stein and Kish, 1985, 1991), and sea level change (Morton and Long, 1984) have been used to explain linear arrays on $^{87}Sr/^{86}Sr$ versus $^{87}Rb/^{86}Sr$ plots. Hydrothermal activity is not known to have occurred in this part of the Southeast Georgia Embayment during the Cenozoic. Either uplift or sea level change is the most likely candidate for explaining the young glauconitic mica dates for the Lang Syne Formation.

K-Ar Dates

Three K-Ar dates from Lang Syne Formation glauconitic micas are more difficult to explain. Two K-Ar dates (47.5 and 49.8 Ma) are less than 10% younger than corresponding Rb-Sr dates; the third K-Ar date (58.8 Ma) from the downdip core hole (H8713-70) is approximately 10% older than the Rb-Sr date of 52.8 ± 1.6 Ma for the same sample. Assuming that the 58.8 Ma K-Ar date is valid, it would appear that the Rb-Sr system of the sample was altered without significantly affecting the K-Ar system. The 58.8 Ma K-Ar date approximates the suggested biostratigraphic age of the unit, and is in analytical agreement with the two older Rb-Sr model dates discussed above.

Electron microprobe

Birch and others (1976), in an electron microprobe study of glauconies from the west coast of South Africa, recognized four stages of maturity based on petrographic criteria. For each stage, they determined the average composition of SiO_2, Al_2O_3, Fe_2O_3, MgO, CaO, Na_2O, K_2O and P_2O_5 as well as the concentrations of the same oxides in oxidized glaucony

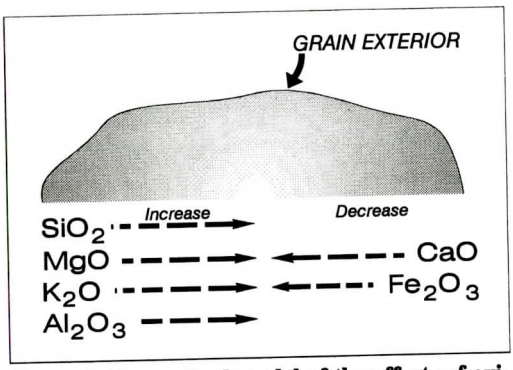

Figure 8. Generalized model of the affects of oxidation on certain elemental concentrations in evolved to highly evolved glauconitic micas.

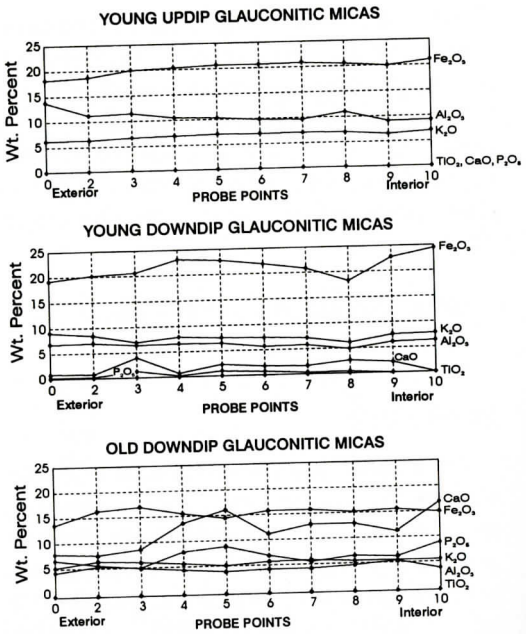

Figure 9. A comparison of selected oxides from updip young glauconitic micas, and downdip young and old glauconitic micas. Percentages were determined by electron microprobe analysis. Note that old downdip glauconitic micas have relatively low K_2O content.

pellets, foraminiferal infillings, and altered faecal pellets. Table 4 summarizes their results; Figure 8 illustrates the major points. Important observations from their work are that during maturation, wt.% SiO_2, K_2O, Fe_2O_3 and MgO increase, and Al_2O_3 and CaO decrease. Furthermore, during oxidation, glaucony pellets suffer significant reductions in wt.% SiO_2, MgO, and K_2O, a minor reduction in wt.% Al_2O_3, a significant increase in wt.% Fe_2O_3, and a minor increase in wt.% CaO. We used these results to evaluate the glauconitic micas from the Lang Syne Formation for effects of oxidation as ground water in the formation has a pH of about 5 (Thayer, 1997, personal communication). Based on the observations of Odin and Matter (1981), glauconitic micas show an increase in maturation from grain exterior to interior. Based on the spatial position of Lang Syne Formation samples, updip glauconitic micas (P-14TA) might have experienced a greater degree of oxidation than downdip glauconitic micas (P-21TA). Figure 9 summarizes the distribution of major oxides determined by electron microprobe for all samples.

The distribution of Al_2O_3, Fe_2O_3, and K_2O indicates that the young updip glauconitic micas have more mature interiors than exteriors (Table 3). Birch and others (1976) found that oxidized glauconies had lower wt.% Al_2O_3 than mature glauconies, but the difference between the two values was minor (Table 4). The point here is that mature and oxidized glauconitic micas have concentrations of Al_2O_3 that are lower than immature glauconitic micas. If the assumption is valid that grain exteriors should be more affected during oxidation than interiors, then exterior concentrations of Al_2O_3 should be less than interior concentrations. This is not the case with updip glauconitic micas. Although Lang Syne glauconies have a wt.% Al_2O_3 that is about two to three times that observed by Birch and others (1976), wt.% Al_2O_3 is less in interiors than exteriors and does not support oxidation of the samples. Birch and others (1976) also showed that wt.% Fe_2O_3 in oxidized grains was about twice that found in mature grains. This relationship is not observed on grain exteriors of Lang Syne glauconies, in fact they have lower wt.% Fe_2O_3 on exteriors than interiors. Although Birch and others (1976) observed a significant decrease in wt.% K_2O in mature samples upon oxidation, Lang Syne glauconies show only a slightly lower wt.% K_2O on grain exteriors (Table 3). Electron microprobe analysis of updip glauconitic mica grains also reveals no zoning of oxides, and essentially no CaO and

P_2O_5.

Concentration and distribution of major oxides (Al_2O_3, Fe_2O_3 and K_2O) in downdip glauconitic micas that have young dates also suggests that they have not been oxidized (Table 3). The distribution of Al_2O_3, Fe_2O_3 and K_2O in these samples is similar to the compositions formed during the maturation process suggested by Birch and others (1976). However, the CaO and P_2O_5 contents of these samples are significantly higher than the updip samples. Regression analysis between CaO and P_2O_5 yields a correlation coefficient of 0.64 which indicates that there is a moderate sympathetic relationship between the two oxides. However, several probe points in the interiors of these samples have high concentrations of CaO that are not accompanied by high concentrations of P_2O_5 (Table 3). The higher concentrations of CaO in these locations may suggest that these samples have been affected differently by ground water than the updip samples. As the interval assigned to the Lang Syne Formation in updip core-hole P-14TA is within the Crouch Branch aquifer, and the interval in downdip core-hole P-21TA the Crouch Branch confining unit (Aadland and others, 1995), samples would be expected to have been affected differently. Although based on X-ray analysis and K_2O content these samples are mature and should have low concentrations of CaO, the high CaO concentrations in sites with low P_2O_5 concentrations suggests that it has been added during diagenesis. It also follows, then, that Sr has been added to these samples.

Electron microprobe analysis of downdip glauconitic micas (H8712-40 and H8713-40) that have dates approximating the time of deposition of the Lang Syne Formation reveal significant differences in oxide concentrations from the other samples examined (Table 3). Wt.% Al_2O_3 and Fe_2O_3 generally follows the same trend of the updip and downdip samples that are younger than the time of sedimentation. However, the percent K_2O for the older samples shows no consistent direction of change from grain exterior to grain interior. In addition, these samples also show very high P_2O_5 and CaO concentrations (Table 3) which increase from grain exterior to interior. Regression analysis of the relationship between P_2O_5 and CaO yields a correlation coefficient of 0.91 indicating a significant sympathetic relationship between the compounds.

Birch and others (1976) found that immature glauconites have higher concentrations of CaO on grain exteriors than interiors, and that oxidized samples have higher P_2O_5 concentrations than non-oxidized samples. They also showed that CaO and P_2O_5 percentages were generally higher in foraminiferal infillings and altered fecal pellets than in pellets whose origin was undetermined. Downdip glauconitic micas from the Lang Syne Formation with dates that approximate the biostratigraphic age of the unit apparently have higher concentrations of impurities (apatite) resulting in higher concentrations of CaO and P_2O_5. Higher CaO is associated with higher concentrations of Sr (Table 1), and thus indicates common Sr also has probably been added to these samples during diagenesis.

MODEL FOR DATE RESETTING

Rb-Sr, K-Ar and electron microprobe analyses of glauconitic micas suggest the following scenario to explain the dates for samples from the Lang Syne Formation. The Lang Syne Formation was deposited during a single cycle of relative sea level (TA2.1). Haq and others (1988) suggest that the TA2.1 depositional sequence has boundary ages of 58.5 Ma and 55 Ma, respectively, and that the surface of maximum flooding within the condensed section has an age of 56.5 Ma. They also indicate that errors of ages ± 1.4 Ma "... can be ascribed to Early Tertiary stage boundaries." Assuming that these same errors can be applied to sequence boundary ages as well as the surface of maximum flooding, the TA2.1 sequence spans a maximum time interval of 59.4 Ma to 53.6 Ma, and the surface of maximum flooding an interval of 57.9 Ma to 55.1 Ma. Glauconitic micas dated in this study were collected from the transgressive systems tract of the TA2.1 depositional sequence, i.e., from between the lower sequence boundary (unconformity) and the surface of

maximum flooding. This limits the suggested depositional age of the transgressive part of the Lang Syne Formation to the interval 59.4 Ma and 55.1 Ma. Therefore, dates based on Rb-Sr errochrons (Figures 4-6), 18 of the Rb-Sr model dates and two of the K-Ar dates (Table 1) are 10-15% younger than the time suggested for deposition of the transgressive part of the TA2.1 sequence (Figure 7).

The low Sr concentrations in glauconitic micas updip indicate that all samples have probably experienced Sr removal during diagenesis, resulting in an increase in the Rb/Sr ratios and a lowering of the model dates. Based on the general consistency of the Rb concentrations in the samples, Rb was probably not affected during diagenesis. Sr removal during diagenesis probably occurred through interaction of the glauconitic micas with acidic ground water which is typical of ground water systems within siliciclastic sediments in the subtropical southeastern U.S. today at the SRS site (Cummins and others, 1990). The increase in Rb/Sr ratio with decreasing sample size indicates that more Sr was removed from the finer glauconitic micas than the coarser glauconitic micas. The smaller diameter, finer samples would be more conducive to alteration because they have more surface area per mass unit than do the larger grains. Electron microprobe analysis of updip glauconitic micas reveals the total lack of zoning of oxides in the samples which supports total or near total sample re-equilibration at some time after deposition. The young K-Ar dates support this total or near total re-equilibration of the glauconitic micas.

Downdip glauconitic micas form two distinct groups based on their major element concentration. One of these compositional groups yields dates that are younger than the biostratigraphic age and the other group yields dates that are older (Tables 1, 2 and 3). Downdip glauconitic micas that are young have higher concentrations of Sr and CaO than updip glauconitic micas (Tables 1 and 3). As there is only a moderate sympathetic relationship between P_2O_5 and CaO in the young downdip samples (correlation coefficient = 0.64), some Ca and Sr may have been added during diagenesis. The higher concentration of Ca (Table 3) and by inference Sr supports this process. If the Sr that was added had a lower $^{87}Sr/^{86}Sr$ ratio than did the Sr initially incorporated into the sample, this would lower the date and thus result in dates consistent with the updip samples. The addition of Sr to these samples suggests that the chemistry of the ground water must have changed from a lower pH to a higher pH in order for the alkaline metals to be adsorbed.

Downdip glauconitic micas that yield Rb-Sr dates that are close to the suggested biostratigraphic age of the Lang Syne Formation (Tables 1 and 6) have the lowest $^{87}Sr/^{86}Sr$ ratios, the highest quantities of Sr and are derived from the coarsest samples (Table 1). Electron microprobe analyses of these glauconitic micas indicates that they have high concentrations of P_2O_5 and CaO which based on the high correlation coefficient (0.91) is sympathetic. This is consistent with the high Sr concentrations. Diagenetic alteration through ground water has probably also affected these samples, but because of their coarser grain size, the effect has not been as great as the effect on the finer size fractions. However, the higher Sr content of these samples maybe be related to a change in the redox potential of the ground water, so that Sr has also been absorbed into these samples as well as the other downdip samples. However, if this is the case, it is unclear why some downdip glauconitic micas have had their dates reduced whereas others have retained their original depositional age.

The young, approximately 51 Ma dates possibly represent a time of sea level fall. Haq and others (1987) suggested that during the latest Paleocene and earliest Eocene nine global changes in sea level occurred. Based upon their data, the largest fall occurred at 51.5 Ma. It is suggested that re-equilibration of the smaller glauconitic micas occurred during this major fall in sea level.

SUMMARY

This paper presents Rb-Sr and K-Ar dates on samples of the upper Paleocene Lang Syne Formation from the Savannah River Site, Southeast Georgia Embayment which are interpreted to

have re-equilibrated with ground water during a global fall of sea level in the early Eocene. The following summarizes the main points of this paper.

(1)A 20 point Rb-Sr glauconitic mica errochron of 51.5 ± 0.1 Ma and conventional K-Ar glauconitic mica dates of 49.8 ± 1.9 Ma and 47.5 ± 1.8 Ma from three core holes representing the transgressive part of the TA2.1 sequence of Lang Syne Formation, are 10-15% younger than the time of suggested deposition of the unit.

(2)Rb-Sr model dates of the samples, assuming the Thanetian $^{87}Sr/^{86}Sr$ ratio suggested by Koepnick and others (1985), indicates 18 dates younger than the biostratigraphic age (50.2-53.6 Ma) and two approximating the biostratigraphic age (56.5, 57.1 Ma).

(3)A conventional K-Ar date of 58.8 ± 2.3 Ma from a single downdip sample approximates the time of deposition for the unit.

(4)Updip glauconitic micas reacted with ground water during a major fall in sea level with Sr being removed from the samples resulting in an increase in their Rb/Sr ratios and a lowering of the dates and $^{87}Sr/^{86}Sr$ ratios.

(5)Downdip glauconitic micas interacted with ground water also during this same major fall in sea level. However, these samples absorbed lower $^{87}Sr/^{86}Sr$, resulting in decreases in Rb/Sr and $^{87}Sr/^{86}Sr$ ratios. Nevertheless, two samples with large grain sizes did not have their Rb-Sr dates significantly changed from the biostratigraphic age of the unit.

ACKNOWLEDGEMENTS

The authors thank Van Price and E. I. DuPont Company, former operator of the Savannah River Site, and Westinghouse Savannah River Company for financial funding for the radiometric dates (Contracts #AX0721024 and #AX0853015). In addition, Westinghouse Savannah River Company is gratefully acknowledged for providing access to the electron microprobe. The Faculty Research and Development Committee of the University of North Carolina at Wilmington provided partial funding for the electron microprobe analyses, the Center of Marine Science Research, the University of North Carolina at Wilmington, provided release-time from teaching, and former Dean Carolyn Simmons of the College of Arts and Sciences provided partial financial support for this research. Each of these sources is thanked. In addition, Van Price and Roy Odom who reviewed the manuscript, are thanked for their rhetorical questions about glauconite and their constructive comments that improved the manuscript. This is contribution #160 from the Center for Marine Science Research, the University of North Carolina at Wilmington.

REFERENCES CITED

Aadland, R.K., Gellici, J.A. and Thayer, P.A., 1995, Hydrogeologic framework of west-central South Carolina: Water Resources Division, Report 5, South Carolina Department of Natural Resources, 200 p.

Berggren, W.A., Kent, D.V., Swisher, C.C. and Aubrey, M-P., 1995, A revised Cenozoic geochronology and chronostratigraphy; *in* Berggren, W.A., Kent, D.V., Aubrey, M-P. and Hardenbol, J., eds., Geochronology, time scales and global stratigraphic correlation: Society for Sedimentary Geology, Special Publication 54, p. 129-212.

Birch, G.F., Willis, J.P., and Rickard, R.S., 1976, An electron microprobe study of glauconites from the continental margin off the west coast of South Africa: Marine Geology, v. 22, p. 271-283.

Conrad, M., Kreuzer, H., and Odin, G.S., 1982, Potassium-argon dating to tectonized glauconies; *in* Odin, G.S., ed, Numerical dating in stratigraphy, part 1: Chichester, John Wiley and Sons, p. 321-332.

Cummins, C.L., Martin, D.K. and Todd, J.L., 1990, Savannah River Site Environmental Report: Westinghouse Environmental Monitoring Section, WSRC-IM-91-28, vol. I, 167 p.

Edwards, L.E., 1992, Dinocysts from the lower Tertiary units in the Savannah River area, South Carolina and Georgia, *in* Zullo, V.A., Harris, W.B., and Price, V., *eds.*, Savannah River region: transition between the Gulf and Atlantic Coastal Plains: Second Bald Head Island Conference, U. S. Department of Energy, Westinghouse Savannah River Company, p. 97-99.

Fallaw, W.C., and Price, V., 1992, Outline of stratigraphy at the Savannah River Site; *in* Fallaw, W.C., and Price, V., eds., Geological investigations of the central Savannah River area, South Carolina and Georgia: Carolina Geological Society, Field Trip Guidebook, p. CGS-92-B-II-1 to CGS-92-B-II-33.

Fallaw, W.C. and Price, V., 1995, Stratigraphy of the Savannah River Site and vicinity: Southeastern Geology, v. 35, p. 21-58.

Grant, N.K., Laskowski, T.E., and Foland, K.A., 1984, Rb-

Sr and K-Ar ages of Paleozoic glauconites from Ohio-Indiana and Missouri, USA: Isotope Geoscience, v. 2, p. 217-239.

Haq, B.U., Hardenbol, J., and Vail, P.R., 1987, Chronology of fluctuating sea levels since the Triassic: Science, v. 235, p. 1156-1167.

Haq, B.U., Hardenbol, J., and Vail, P.R., 1988, Mesozoic and Cenozoic chronostratigraphy and cycles of sea-level change; *in* Wilgus, C.K., Hastings, B.S., Kendall, C.G.C., Posamentier, H.W., Ross, C.A., and Van Wagoner, J.C., eds., Sea-level changes: an integrated approach: Society of Economic Paleontologists and Mineralogists, Special Publication, 42, p. 71-108.

Harris, W.B., and Fullagar, P.D., 1989, Comparison of Rb-Sr and K-Ar dates of middle Eocene bentonite and glauconite, southeastern Atlantic Coastal Plain: Geological Society of America Bulletin, v. 101, p. 573-577.

Harris, W.B., and Zullo, V.A., 1992, Sequence stratigraphy of Paleocene and Eocene deposits in the Savannah River region; *in* Zullo, V.A., Harris, W.B., and Price, V., *eds.*, Savannah River region: transition between the Gulf and Atlantic Coastal Plains: Second Bald Head Island Conference, U. S. Department of Energy, Westinghouse Savannah River Company, p. 134-142.

Harris, W.B., Zullo, V.A., and Laws, R.A., 1993, Coastal onlap stratigraphy of the onshore Paleogene, southeastern Atlantic Coastal Plain, U. S. A.; *in* Posamentier, H.W., Summerhayes, C.P., Haq, B.U. and Allen, G.P., eds., Sequence stratigraphy and facies associations: International Association of Sedimentologists, Special Publication 18, p. 537-561.

Koepnick, R.B., Burke, W.H., Denison, R.E., Hetherington, E.A., Nelson, H.F., Otto, J.B., and Waite, L.E., 1985, Construction of the seawater $^{87}Sr/^{86}Sr$ curve for the Cenozoic and Cretaceous: Support data: Chemical Geology, Isotope Geoscience Section, v. 58, p. 55-81.

Laskowski, T.E., Fluegeman, R.H., and Grant, N.K., 1980, Rb-Sr glauconite systematics and the uplift of the Cincinnati arch: Geology, v. 8, p. 368-370.

Martini, E., 1971, Standard Tertiary and Quaternary calcareous nannoplankton zonation; *in* Frainacci, A., ed., Proceedings of the Second Planktonic Conference: Rome, Italy, Edizonioni Technoscienza, p. 739-785.

Morton, J.P., and Long, L.E., 1980, Rb-Sr dating of Paleozoic glauconite from the Llano region, central Texas: Geochimica et Cosmochimica Acta, v. 44, p. 663-672.

Morton, J.P., and Long, L.E., 1984, Rb-Sr ages of glauconite recrystallization: Dating times of regional emergences above sea level: Journal of Sedimentary Petrology, v. 54, p. 495-506.

Obradovich, J.D., 1988, A different perspective on glauconite as a chronometer for geologic time scale studies: Paleoceanography, v. 3, p. 757-770.

Odin, G.S., 1982, Numerical dating in stratigraphy, part 1: Chichester, John Wiley and Sons, 630 p.

Prowell, D.C., Edwards, L.E., and Frederiksen, N.O., 1985, The Ellenton Formation in South Carolina--a revised age designation from Cretaceous to Paleocene: U. S. Geological Survey Bulletin 1605-A, p. A63-A69.

Seidemann, D.E., 1992, The significance of Rb-Sr glauconite ages, Bonneterre Formation, Missouri: late Devonian-early Mississippian brine migration in the mid-continent: a discussion: Journal of Geology, v. 100, p. 639-641.

Siple, G.E., 1967, Geology and groundwater of the Savannah River Plant and vicinity, South Carolina: U. S. Geological Survey Water Supply Paper 1841, 133 p.

Smalley, P.C., Forsberg, A., and Raeheim, A., 1987, Rb-Sr dating of fluid migration in hydrocarbon source rocks: Chemical Geology, Isotope Geoscience Section, v. 65, p. 223-233.

Stein, H.J. and Kish, S.A., 1985, The timing of ore formation in southeast Missouri: Rb-Sr glauconite dating at the Magmont Mine, Viburnum Trend: Economic Geology, v. 80, p. 739-753.

Stein, H.J. and Kish, S.A., 1992, The significance of Rb-Sr glauconite ages, Bonneterre Formation, Missouri; Late Devonian-Early Mississippian brine migration in the Midcontinent: Journal of Geology, v. 99, p. 468-481.

Zullo, V.A., Willoughby, R.H., and Nystrom, P.G., Jr., 1982, A late Oligocene or early Miocene age for the Dry Branch Formation and Tobacco Road Sand in Aiken County, South Carolina; *in* Nystrom, P.G., and Willoughby, R.H., eds., Geological investigations related to the stratigraphy in the kaolin mining district, Aiken County, South Carolina: Carolina Geological Society, 1982, Field Trip Guidebook, p. 34-45.

APPENDIX 1. SAMPLE PREPARATION AND ANALYTICAL PROCEDURES

Radiometric Dating

Five glaucony-rich samples that weighed less than a kilogram each were collected from three conventional core holes drilled on the Savannah River Site:

Samples	Core	Location*		Depth
		North (Lat.)	West (Long.)	(MSL)**
H8703	P-14TA	33.3107	81.6062	-3.1'
H8704	P-14TA	33.3107	81.6062	-5.1'
H8712	P-21TA	33.1468	81.6075	-200.5'
H8713	P-21TA	33.1468	81.6075	-203.5'
H8719	P-18TB	33.2530	81.6726	-37.7'

* Locations shown in Figure 1; **Depth to mean sea level

Glaucony-rich samples were hand-crushed and screened into different size fractions; in Table 1 the samples are identified by U. S. Standard Testing Screen Number as well as sand-size. Each size fraction consisted of mammillated, lobate, or earthy glaucony. Earthy is used here to describe grains that are angular and po-

rous, which appear to represent broken mammillated grains. All samples were washed with distilled or demineralized water, dried with reagent-grade acetone and separated on the basis of magnetic susceptibility with a Frantz magnetic separator. Each separated fraction, with the exception of samples H8719-100 and H8719-120, was washed in de-mineralized water in an ultrasonic bath for 30 seconds to dislodge any loose, surface contamination, acetone-dried, and hand-picked of impurities. All but two samples were not acid-washed. Samples H8719-100 and H8719-120 were washed for 60 seconds in 0.1 N HC1, rinsed in de-mineralized water, and then washed for 60 seconds in de-mineralized water in an ultrasonic bath. Based upon microscopic examination, samples showing evidence of reworking, alteration, or mineral impurities were discarded. Each hand-picked sample consisted of 100% glaucony.

All samples were studied by X-ray diffractometry following the technique described by Odin (1982) in order to determine glaucony type. Based on this analysis, all samples are evolved to highly-evolved glauconitic mica as they contain greater than 6% K_2O.

All glauconitic-mica fractions were analyzed for Rb, Sr, and Sr isotopic composition by standard mass spectrometic techniques. All $^{87}Sr/^{86}Sr$ values are reported relative to a value of 0.70800 for the Eimer and Amend Sr isotopic standard. Thirteen analyses in our laboratory during this study gave an average $^{87}Sr/^{86}Sr$ ratio of 0.70801 ± 0.00003 (one standard deviation). NBS K-feldspar standards 70a and 607 have been analyzed 21 times in our laboratory and give an average date of 1377 ± 6 Ma (one standard deviation) using $\lambda = 1.42 \times 10^{-11} yr^{-1}$ as the ^{87}Rb decay constant, and assuming an initial $^{87}Sr/^{86}Sr$ ratio of 0.710. All $^{87}Rb/^{86}Sr$ values have been determined by isotope dilution analyses. Rb-Sr and K-Ar analytical data, along with model dates are given in Table 1. Model dates were calculated using an initial $^{87}Sr/^{86}Sr$ value of 0.70776 which is the ratio reported for Thanetian seawater by Koepnick and others (1985). Analytical uncertainties (one standard deviation) for the isochrons were calculated using the method of York (1969) with errors of 0.5% and 0.025% for the $^{87}Rb/^{86}Sr$ and $^{87}Sr/^{86}Sr$ ratios, respectively. Figures 5-7 give Rb-Sr errochron dates for glauconitic micas reported in this study. Three glauconitic-mica splits were dated by the K-Ar conventional technique by Krueger Enterprises, Cambridge, Massachusetts. Decay constants used were $\lambda\beta = 4.962 \times 10^{-10} yr^{-1}$ and $\lambda\epsilon = 0.581 \times 10^{-10} yr^{-1}$.

Electron microprobe

Splits of glauconitic micas from core hole P-14TA (H8703-60, H8703-70, H8704-60, H8704-80, H8704-100, H8704-120) and core hole P-21TA (H8712-40, H8712-70, H8712-100, H8713-40, H8713-70, H8713-100) were prepared for electron microprobe analysis by D. M. Organist Petrographic Laboratory (Table 2). In addition, GLO was also prepared for analysis and selected as a standard because detailed studies of this sample have indicated that it provides accurate and precise radiometric dates. Glauconite samples consisted of purified sand-size splits mounted in epoxy on 1" diameter thin-section glass with one surface polished. Polished samples were coated with C under vacuum and mounted on 1" diameter aluminum stubs for placement in the electron microprobe.

Glauconitic samples were analyzed for Fe (iron), Al (aluminum), Mg (magnesium), Ca (calcium), Sr (strontium), Rb (rubidium), K (potassium), P (phosphorous), and in some cases Ti (titanium) using an ARL SEMQ electron microprobe interfaced with a Tracor Northern (now Noran Instruments) TN5600 programmable automatic controller and TN5500 energy dispersive X-ray analyzer in the Savannah River Technology Center, Savannah River Site, South Carolina. These elements were chosen for detection as they either provide documentation of the developmental process of glauconitization, or they provide evidence for analysis of the dating technique systematics. Kα lines for Fe, Ti, K, Ca, P, Al, and Mg, and Lα lines for Rb and Sr were measured at 20keV with a total beam current of approximately 100 nanoamps. X-ray lines were measured using the following analyzing crystals: PET for Rb, Sr, P, and Ca; LIF

for K, Fe, and Ti; and TAP for Al and Mg using gas proportional detectors. Elemental distributions were mapped for five to six grains in samples H8712-70, H8712-100, and H8713-70. Each map was a 256x256 pixel image with a dwell time of 0.05 seconds per pixel. Map magnifications varied from 500x to 1500x. In addition, distributions of Fe, Al, Mg, Ca, Rb, K, and P were mapped in glauconite standard GLO.

Quantitative measurements were made by performing linescans of the following seven samples: H8703-70, H8704-100, H8712-40, H8712-100, H8713-40, and H8713-70. A linescan consisted of measuring 10 spots from grain exterior to interior; seven to 10 grains were analyzed for each of the seven samples. A Charles M. Taylor multi-element standard #202 which contained Fe, Ti, Al, and orthoclase (K) and an ARL alignment specimen #12107-1 which contained CaP were used for the quantitative measurements. The raw data were corrected and reduced using the Tracor Northern ZAF program. The standards were analyzed as unknowns before and after each linescan to verify instrument stability and reproducibility. The measured concentrations of the standards were within 10% of the reported values.

SOUTHEASTERN GEOLOGY
V. 37, No. 2, October 1997, p. 73-90

BIVALVE FAUNA OF A PLIO-PLEISTOCENE CORAL BIOSTROME IN EASTERN NORTH CAROLINA: PALEOECOLOGIC STABILITY, CHANGE, AND SCALING

WILLIAM MILLER, III

Geology Department
Humboldt State University
Arcata, California 95521

ABSTRACT

Overburden stripping at the Lee Creek phosphate mine in the late 1980's exposed an extremely fossiliferous unit probably within the lower James City Formation. The unit was located on the northern edge of a large channel cut into the Pliocene Yorktown Formation and near the top of the associated Plio-Pleistocene channel-fill sequence, in what was then the southern part of the mine. Enclosed in this shallow-shelf, shelly sand unit was a bed containing the coral *Septastrea crassa*, similar to other *Septastrea* biostromes reported from the Chowan River and Yorktown Formations of the mid-Atlantic Coastal Plain.

Samples of the rich bivalve fauna collected from within and from immediately below the Lee Creek *Septastrea* biostrome contained apparently conflicting ecologic "signals". Although some taxa showed changes in relative abundance with appearance of the biostrome, most showed no such trend in abundance. Taxonomic composition remained unchanged among the most abundant bivalves. Two seemingly plausible interpretations for this pattern are possible: one would emphasize the minor changes in abundance of bivalves and identify this as subtle evidence of local community replacement; the other would stress compositional stasis notwithstanding development of a coral thicket at the site. The apparent faunal stability and change have to be reconciled in some way, and faunal condensation and time-averaging in a shallow-shelf depositional environment also have to be considered. A more ecologically realistic interpretation takes into account the kinds of ecologic system likely to be preserved in this setting (biotope or regional ecosystems, as opposed to more ephemeral local ecosystems or communities), the time-averaged record, and the disturbance regime and temporal heterogeneity of shallow shelves (dominated in this case by storms in the short term and spread of the coral thicket in the long term). In this view, the compositional stability of the bivalves, with some changes in relative abundance, appears to have resulted from a stable regional ecosystem that essentially swamped the record of local ecologic processes. This type of paleoecologic pattern is probably typical for time-averaged shelly deposits of shallow continental shelves and seaways.

INTRODUCTION

Scaling considerations are factors in the accurate interpretation of all biologic systems, whether fossil or modern. In the simplest terms, these involve getting the right time and space scales associated with evolutionary or ecologic processes under investigation (Schneider, 1994), but may also involve the correct identification of hierarchical properties (e.g., relationship of entities to larger, more inclusive systems as well as to their component systems [Miller, 1991]). In paleontology, there is the related consideration of *correspondence*, or the identification of the original living systems recorded in fossil data sets (Miller, 1993). The two perennial questions of paleoecology are sensitive to these issues: Did ancient ecologic systems change through time (and what were the causes

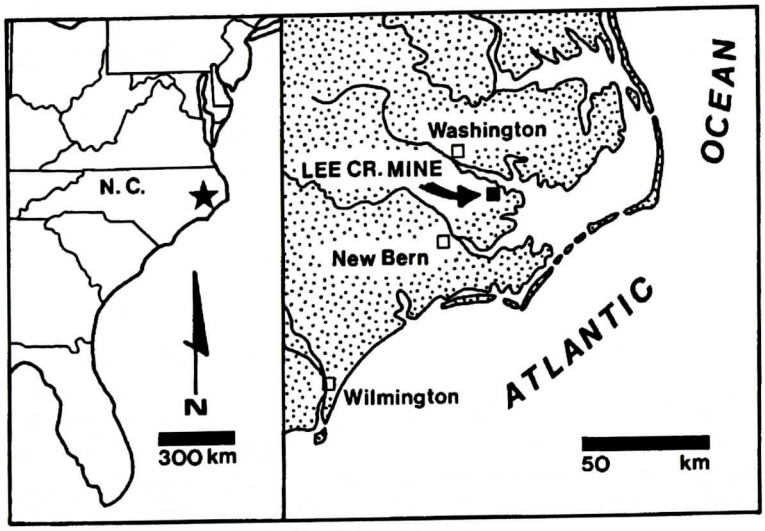

Figure 1. Location of study site in eastern North Carolina.

of change), or did the systems of interest to us have a kind of stasis or stability (and how did that come about) (cf. Gould, 1977)?

Richard H. Bailey and his coworkers have described in detail two Pliocene coral thickets in the Atlantic Coastal Plain (Bailey and Tedesco, 1986; Bailey and Blow, 1996). These studies are significant because they document a kind of ecologic system on the shallow shelf that has no close modern counterpart. The studies also are models of thoroughness and correct scaling in multispecies paleoecology. They document overall development of *Septastrea* coral thickets preserved in the Chowan River and Yorktown Formations, as well as smaller-scale dynamics recorded in the establishment and growth pattern of individual *Septastrea* coralla. My study is intended as both documentation of a younger *Septastrea* thicket, preserved in Plio-Pleistocene beds at the Lee Creek phosphate mine, and as an evaluation of the importance of scale in paleoecologic interpretations.

The original intention was to use the well-preserved bivalve fauna to track the development of the Lee Creek coral thicket, and then to attempt to identify environmental or biotic processes controlling the transition, as in previous studies of "community replacement" (Miller, 1986; Miller and DuBar, 1988). During the processing of samples, however, I made a perplexing discovery. If I asked the perennial question, of whether the fossil record of the Lee Creek *Septastrea* biostrome reflected ecologic change or stasis, the answer was going to be "yes". Either aspect of the record could be legitimately and plausibly emphasized. If I sought for changes through time in species-abundance distribution patterns in the bivalve fauna, I found them; if I tried to detect stability as persistence of the dominant bivalve species, I found that, too. The aspects of faunal transition and of stability are equally significant, but the correct interpretation of scaling and correspondence is just as important for the interpretation of a very fossiliferous, open shelf, time-averaged deposit like the one containing the Lee Creek coral thicket.

LOCALITY AND GEOLOGIC CONTEXT

The bulk samples used in this study were collected in 1989 from exposures in the Lee Creek mine (operated at that time by Texasgulf Inc.), located 7 km north of Aurora and 30 km southeast of Washington (Fig. 1), in southeastern Beaufort County. The study site was in mining block 18 (Gilmore, 1985, fig. 2), 1200 m west of North Carolina Highway 306 and approximately 5400 m south of the Pamlico River, in what was then the southern area of active mining. Samples were collected from a unit that the miners referred to as the "shell bed" exposed in

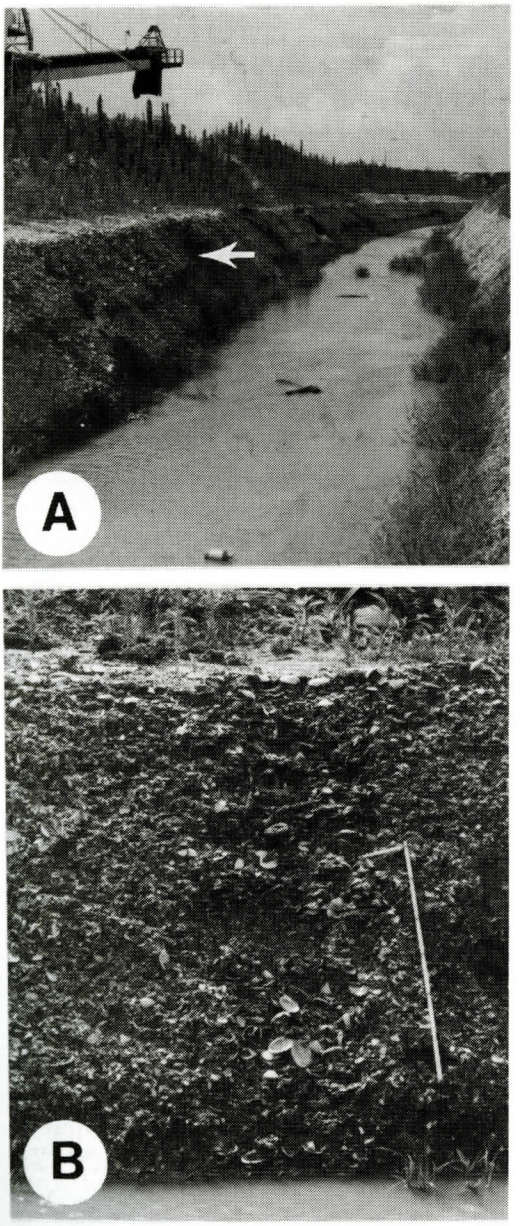

Figure 2. Study site in the southern area of the Lee Creek phosphate mine as it appeared in July, 1989. A, Large drainage ditch cut into the "25′ bench" (arrow points to *Septastrea* bed in ditch bank). B, Ditch-bank exposure (ruler is 1 m long).

the wall of a large drainage ditch that had been cut into the "25' bench" (Figs. 2, 4), the level (25 ft or 7.6 m below sea level) to which overburden was initially removed by a bucket-wheel excavator and where heavy digging machinery was later located for stripping away the remaining overburden. As a part of the ongoing mining operation, the study site was stripped sometime between late 1989 and 1991. My attention was drawn to the "shell bed" in this part of the mine because of the presence of abundant coral associated with a rich molluscan fauna.

The stratigraphy of post-Miocene units exposed in the Lee Creek mine and immediate vicinity has been investigated repeatedly over the last two decades (DuBar and others, 1974; Mixon and Pilkey, 1976; Daniels and others, 1977; Blackwelder, 1981a, b; Belt and others, 1983; Gibson 1983, 1987; Hazel, 1983; Snyder and others, 1983; Wheeler and others, 1983; Miller, 1985; Ward and Blackwelder, 1987). Recent summaries and interpretations include those by Blackwelder (1981b), Johnson and Peebles (1986), Ward and others (1991), and Lyons (1991). Notwithstanding the concentrated interest, the Pliocene and Pleistocene units are in need of restudy and reevaluation, especially in light of the new exposures created continuously by expansion of the mine, new fossil discoveries and interpretations, and the new possibilities for more accurate age determinations and correlations.

In the mid-1980's, overburden stripping in the southern portion of the Lee Creek mine had begun to expose an intriguing complication in local stratigraphy: the Yorktown Formation had been deeply incised by an east-west trending channel containing a relatively thick sequence of post-Yorktown sediments. The "channel structure", as the miners referred to it, and its sedimentary fill, are described in an unpublished company report (Gilmore, 1985) containing many detailed cross sections and lithologic descriptions. The outcrops used in my study are exposures of very shelly sand located near the top of the sedimentary fill and on the northern flank of the "channel structure" (Fig. 3). The company report shows that the channel-fill sequence near my study site was up to 15 - 20 m thick, and consisted of vertically and laterally variable fossiliferous mud and sand beds. In the report (Gilmore, 1985, p. 5), S. W. Snyder of East Carolina University is said to have determined "... that the age of the entire channel se-

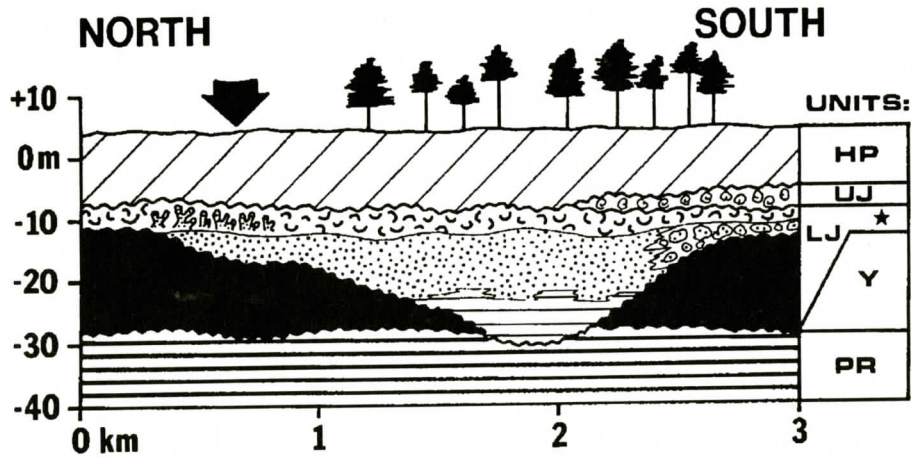

Figure 3. Interpretation of stratigraphy in the vicinity of the "channel structure" based largely on Gilmore (1985). Arrow indicates approximate position of study site. Stratigraphic units include: PR, Miocene Pungo River Formation; Y, Pliocene Yorktown Formation; LJ, Plio-Pleistocene(?) lower phase of the James City Formation, which may completely fill the channel and includes the sample interval; UJ, early or mid-Pleistocene upper James City Formation; and HP, middle to late Pleistocene and Holocene deposits undifferentiated. The lower part of the channel-fill sequence may consist of estuarine deposits; the "boulder bed" described in the literature on the Lee Creek mine is interpreted to be in the flank of the channel in this area. The uppermost beds in the channel-fill sequence include the extremely fossiliferous bedding unit known at the mine as the "shell bed".

quence was Pleistocene due to the types of faunas, especially forams...". No list of taxa was given and there is no indication of whether Snyder was using 1.8 or 1.6 Ma as the Pliocene-Pleistocene boundary age.

The discovery of the "channel structure" at the Lee Creek mine, and of similar features elsewhere in the Atlantic Coastal Plain, has several important implications. We are accustomed to thinking of the geometry of formations as being broadly wedge shaped and thickening toward the ocean, or more recently as blanket-shaped deposits having local thickness variations associated with lateral facies transitions. We think of the units, at least within specific regions, as stacked one on top of the other, bounded by unconformities, with the major lithologic and faunal changes occurring interregionally. Now we must adjust our mental picture of these units to include local channels containing sequences that are up to ten times thicker than those observed in the more typical exposures and consisting of a wider variety of facies than one normally encounters in coastal outcrops. There were hints of these complications in the description of the "Small Sequence" in the Pamlico-Neuse divide by Daniels and others (1972), which is also a complex, relatively thick Plio-Pleistocene deposit probably equivalent to the James City Formation of DuBar and Solliday (1963). Another implication is that the "channel structure" is comparable to the "estuarine valley-fill sequences" familiar to stratigraphers working in the Cretaceous of the western interior of North America (e.g., Pattison, 1992, and references therein). These Cretaceous valley-fills contain successions of paralic and shallow marine deposits comprising a complex facies architecture. The Lee Creek channel and similar Coastal Plain features are likely to contain more complete records of eustatic flooding and regression cycles than the thinner correlative deposits on intervalley platforms.

The deposits sampled in this study were located near the top of the channel-fill sequence and on the northern side of the channel axis (Fig. 3). The exposure consisted of a lower medium to coarse quartz sand containing mostly small (<1 cm in largest dimension) shell and coral fragments; overlain by a shell bed that was 20 - 30 cm thick having many large (> 1 cm) bivalve shells and relatively little sand matrix in a

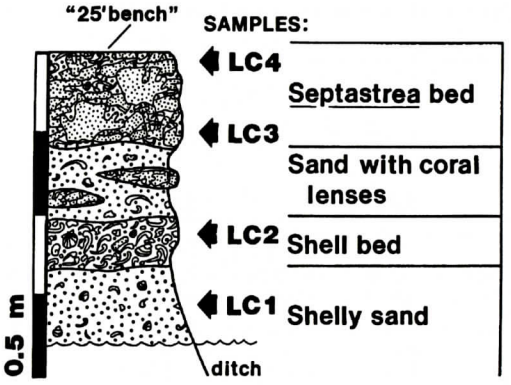

Figure 4. Bedding units in ditch-bank exposure (Fig. 2) showing levels where the bulk samples were collected.

bioclast-supported fabric; which was in turn overlain by a 40-cm-thick medium to coarse sand containing lenses of coral fragments; grading upward into a thick bed containing large coral bioclasts and a few more or less intact coralla of *Septastrea crassa* in a shelly sand matrix (Figs. 2, 4). The beds vary in thickness along the ditch bank by 10's-of-cm's, are medium gray to light olive gray in color (N5 - 5Y6/1), and have obscure lenticular stratification controlled by the ratio of bioclasts to sand and by the size distribution of the bioclasts. The same succession of bedding units (shelly sand —> shell bed —> *Septastrea* bed) was observed along the north-south-trending ditch-bank exposure over a lateral distance of approximately 240 m. The *Septastrea* bed grades laterally into shelly sands and shell beds just like those located beneath it at the study site (Fig. 4). The succession of beds records development of a *Septastrea* coral thicket on the sandy shallow shelf. Whether the channel was still influencing local hydrographic properties of this area is unknown. Composition and richness of the molluscan fauna suggest a subtropical, shallow marine setting for the thicket. The inferred environment as well as the abundance and varied preservation of skeletal material point to condensation and time-averaging of the fossil assemblages, as discussed below.

Based on stratigraphic position and the molluscan fauna, these bedding units are probably within the "lower phase" of the James City Formation (see the recent discussion of two depositional phases within this unit in Ward and others, 1991, p. 281, 288-289), and may be equivalent to beds C or D of Ward and Blackwelder (1987, fig. 3). That the channel-fill sequence contains fossils no older than Pleistocene needs to be confirmed. If true, the entire sequence, along with the beds I sampled, could be within the lower James City, representing an early Pleistocene highstand of sea level that inundated a coastal valley, resulting in the deposition of paralic and marine facies, and culminating in the deposition of the extremely fossiliferous beds exposed beneath the "25' bench". The James City Formation (and its southern equivalent, the Waccamaw Formation) is considered to be early Pleistocene in most of the recent stratigraphic summaries (Blackwelder, 1981a, b, c; McCartan and others, 1982; Wehmiller and Belknap, 1982; Carter, 1983; Jordan and Smith, 1983; Cronin and others, 1984; Ward and Blackwelder, 1987; Rossbach and Carter, 1989; Ward and others, 1991). Lyons (1991, p. 147-149), however, has questioned the early Pleistocene age for the oldest beds within the James City-Waccamaw based on the presence of gastropods that apparently did not survive the end of the Pliocene. These taxa include *Diodora nucula* and *Cymatosyrinx lunata*, which were uncommon in my samples (Appendix). There is the added complication created when some authors use 1.8 Ma for the Plio-Pleistocene boundary while others use 1.6 Ma. Considering all these complications, it will suffice here to regard the beds I sampled as Plio-Pleistocene.

METHODS

Four bulk samples (2.0 - 2.5 liters each) were collected from within and immediately below the *Septastrea* bed (Fig. 4). Samples were processed by soaking them in a 10% solution of sodium hexametaphosphate for 24 - 48 hr, then wet sieving them on screens having 2 and 4 mm openings. Shelly concentrates were picked several times to recover all identifiable fossils. A total of 21,708 identifiable mollusk specimens were separated from matrix and counted. The

Table 1. The abundant bivalve mollusks in the Lee Creek mine samples. Sample levels are shown in Figure 4.

Bivalve taxa[1]	Feeding behavior[2]	Relative abundance[3] LC1	LC2	LC3	LC4	Ubiquity[4]
Nucula proxima	SDF	2.7%	8.0%	2.4%	1.9%	1.0
Nuculana acuta	SDF	4.0	19.1	4.1	2.1	1.0
Anadara aequicostata	SSF	1.2	0.3	0.5	0.6	1.0
Noetia limula	SSF	0.2	----	----	----	0.25
Glycymeris americana	SSF	1.1	0.4	0.6	0.9	1.0
G. arata	SSF	1.4	3.3	1.2	0.8	1.0
G. sloani	SSF	3.6	3.0	2.8	2.1	1.0
Crenella decussata	ESF	0.3	----	----	----	0.25
Carolinapecten eboreus	ESF	1.1	0.6	0.9	1.2	1.0
Plicatula marginata	ESF	7.5	2.3	11.7	11.1	1.0
Conradostrea lawrencei	ESF	3.7	3.1	12.8	8.9	1.0
Cavilinga trisulcata	DSF	0.5	0.6	0.3	0.2	1.0
Diplodonta spp.	SSF	0.4	----	0.9	1.1	0.75
Bornia triangula	ESF?	----	0.6	----	0.2	0.5
Anisodonta carolina	?	----	----	----	0.3	0.25
Ensitellops elongata	SSF?	----	0.4	----	----	0.25
Carditamera arata	SSF	----	0.4	----	----	0.25
Pleuromeris auroraensis	SSF	1.5	1.0	0.5	0.8	1.0
P. decemcostata	SSF	2.1	3.6	1.4	0.6	1.0
Pteromeris perplana	SSF	0.4	0.9	----	----	0.5
Cyclocardia granulata	SSF	12.8	13.2	9.5	8.6	1.0
Astarte concentrica	SSF	6.9	12.7	8.0	9.7	1.0
Astarte sp. aff. *A. castanea*	SSF	2.2	1.3	0.5	0.3	1.0
Crassinella spp.	SSF	4.4	3.3	2.1	2.7	1.0
Laevicardium sublineatum	SSF	----	----	----	0.2	0.25
Spisula spp.	SSF	10.0	3.8	8.2	10.9	1.0
Ensis directus	DSF	3.8	1.6	2.7	3.1	1.0
Tellina agilis	SDF	6.4	3.1	7.9	9.0	1.0
Donax fossor	SSF	----	----	0.3	0.2	0.5
Semele bellastriata	SSF	0.7	----	0.3	0.7	0.75
Abra aequalis	SDF	0.4	0.7	0.7	0.6	1.0
Cumingia tellinoides	DDF	0.4	1.2	0.6	0.3	1.0
Gouldia metastriatum	SSF	5.0	1.8	3.2	2.9	1.0
Transennella stimpsoni	SSF	3.1	2.3	2.5	3.1	1.0
Macrocallista greeni	SSF	0.6	0.3	0.5	0.9	1.0
Mercenaria permagna	SSF	1.2	4.2	1.0	0.4	1.0
Sphenia sp.	SSF	----	0.2	----	----	0.25
Caryocorbula spp.	SSF	9.6	1.9	10.3	12.2	1.0
Gastrochaena hians	BSF	----	----	0.9	0.5	0.5
Hiatella arctica	SSF	----	----	----	0.2	0.25
Pandora sp. cf. *P tuomeyi*	SSF	0.5	0.6	0.4	0.4	1.0
Cochlodesma emmonsii	?	0.2	0.3	----	----	0.5

1 -- Taxa represented in samples by ≥ 10 valves or ≥ 5 articulated shells (i.e., by roughly 5 or more individuals).

2 -- SSF = shallow-burrowing suspension feeder; SDF = shallow-burrowing deposit or detritus feeder; BSF = boring suspension feeder; DSF = deep-burrowing suspension feeder; DDF = deep-burrowing deposit feeder; ESF = epibenthic suspension feeder; ? = unknown.

3 -- Relative abundance among species having ≥ 10 valves or ≥ 5 shells.

4 -- Proportion of samples in which species is represented by ≥ 10 valves or ≥ 5 shells.

Table 2. Characteristics of the bivalve fauna.

Sample	S_b [1]	Abundant S_b [2]	H´ [3]	Holdover S_b [4]
LC4	64	35 (54.7%)	2.85	31 (88.6%)
LC3	65	31 (47.7)	2.96	27 (87.1)
LC2	58	33 (56.9)	2.84	30 (90.9)
LC1	61	33 (54.1)	3.01	----------

1 -- Total bivalve species richness.
2 -- Bivalves represented by ≥ 10 valves or ≥ 5 articulated shells (Table 1).
3 -- Diversity of the abundant bivalves, $H' = -\Sigma\, p_i \ln p_i$ (where $p_i = n/N$ for each species).
4 -- Proportion of the abundant bivalve taxa that persist from the subjacent sample level.

resulting census is given in the Appendix. All specimens have been deposited in the Invertebrate Paleontology Collection, Virginia Museum of Natural History (accession no. VMNH 1997-119; lot no.s 93.001 [= sample LC1], 93.002 [= LC2], 93.003 [= LC3] and 93.004 [= LC4]).

The majority of specimens were bivalves and gastropods, and most of the identifications were made using the comprehensive monograph of Plio-Pleistocene mollusks from the Lee Creek mine by Ward and Blackwelder (1987). The samples also contained abundant barnacle plates, decapod appendage fragments, bryozoans, and the plates and spines of echinoids. Tooth and bone fragments were rare. Foraminiferids and ostracodes were present in the samples, but no attempt was made to recover them. Of all these organisms, the bivalves were most abundant and are probably the most reliable records of ecologic processes. The abundant bivalves are listed in Table 1.

I rely on the abundant bivalve taxa to trace ecologic history for several reasons. Autecologic properties are known for most of the species or can be inferred from closely related taxa. The bivalves, especially larger species, have relatively complete fossil records (Valentine, 1989; Kidwell and Bosence, 1991; Kidwell and Flessa, 1995), although their durability makes them especially prone to time-averaging (Kowalewski, 1997). Gastropod shells were abundant but most were small, epibenthic species; the few larger specimens may have had their distributions affected by hermit-crab occupation (Walker, 1988, 1989). By eliminating the rare bivalve species from consideration the effects of sample size in densely fossiliferous deposits is somewhat minimized (CoBabe and Allmon, 1994). Roughly half of the bivalve taxa (approximately 42 of 78 species) were represented in samples by either ≥ 10 valves or ≥ 5 articulated shells, and these were considered reliable for ecologic analysis (Table 2). Of these, the twelve taxa represented by ≥ 200 valves or ≥ 100 articulated shells in at least one sample probably record ecologic patterns with the greatest reliability (Table 3), and will be referred to here as the "core" fauna.

SEPTASTREA BIOSTROME

The coral bed formed a ledge visible in the upper part of the ditch-bank exposure over a lateral distance of 224 m (Fig. 2 A). The bed varied in thickness from 0.4 to > 1.0 m and contained thin, shelly sand lenses that gave the internal stratification a "webby" appearance (Fig. 2B). The coral species is *Septastrea crassa*[1], represented by fragments ranging from

1. Lauck W. Ward points out in his review of this paper that the Plio-Pleistocene coral identified with *Septastrea crassa* is in need of restudy and revision. He suggested that Conrad's name *S. bella (Proceedings of the Academy of Natural Sciences of Philadelphia*, 1841, v. 1, no. 3, p. 33) based on specimens probably from the James City Formation near New Bern, N.C., may be more appropriate for the Lee Creek mine species. He also suggests the possibility that *S. crassa* may belong to another genus, based on comparison with the type species, *S. marylandica*. I continue to use the name *S. crassa* as an expedient: this is the name traditionally used for the Plio-Pleistocene species and taxonomic revision is beyond the scope of my report. The Lee Creek species is illustrated in Figure 5, and specimens are stored in the Virginia Museum of Natural History awaiting the attention of a coral expert.

Table 3. Distribution of the twelve most abundant bivalve taxa (the "core" fauna of the sample interval). Typical examples are illustrated in Figure 6. These taxa occur in all of the samples.

Taxa [1]	Samples [2] LC 1	LC 2	LC 3	LC 4	$\bar{x}$ [3]	sd [4]	Times in top 10	top 5
Nucula proxima	66 (11)	228 (4)	44 (10)	49 (11)	96.8 (9)	88.0	2	1
Nuculana acuta	99 (9)	543 (1)	76 (8)	53 (10)	192.8 (5)	243.3	4	1
Plicatula marginata	185 (4)	66 (10)	219 (2)	280 (2)	187.5 (6)	90.0	4	3
Conradostrea lawrencei	91 (10)	88 (8)	239 (1)	224 (6)	160.5 (7)	82.2	4	1
Cyclocardia granulata	318 (1)	375 (2)	178 (4)	215 (7)	271.5 (1)	90.9	4	3
Astarte concentrica	170 (5)	360 (3)	150 (6)	245 (4)	231.3 (2)	95.1	4	3
Crassinella spp.	110 (8)	93 (7)	39 (11)	70 (9)	78.0 (10)	30.7	3	0
Spisula spp.	247 (2)	107 (6)	153 (5)	275 (3)	195.5 (4)	78.8	4	3
Tellina agilis	159 (6)	87 (9)	148 (7)	226 (5)	155.0 (8)	57.0	4	1
Gouldia metastriatum	123 (7)	51 (12)	60 (9)	72 (8)	76.5 (11)	32.2	3	0
Mercenaria permagna	29 (12)	120 (5)	19 (12)	9 (12)	44.3 (12)	51.2	1	1
Caryocorbula spp.	238 (3)	55 (11)	193 (3)	306 (1)	198.0 (3)	106.0	3	3

1 -- Bivalves represented in at least one of the samples by ≥100 individuals.
2 -- Number of individuals; rank abundance (in this list) in parentheses.
3 -- Average among samples; average rank in parentheses.
4 -- Standard deviation.

pebble-size bioclasts to large cylindrical to palmate branches several cm's in thickness and 10's-of-cm's in longest dimension (Figs. 5 B, C). The "25' bench", cut into the top of the *Septastrea* biostrome, exposed occasional in situ coralla, the largest being approximately 0.7 m in diameter, having low radiating branches and thick central stumps (Fig. 5A). Smaller coralla were more common. Most of the coral fragments were encrusted with barnacles, bryozoans, and the clams *Plicatula marginata* (Fig. 6F) and *Conradostrea lawrencei* (Figs. 6H, 7A). Clionid sponge borings were common everywhere in the biostrome; clam borings produced by *Lithophaga yorkensis* and *Gastrochaena hians* were less common and more localized. Fracture surfaces in some of the large coral fragments revealed greenish-gray sandy mud filling open spaces, contrasting with the coarse shelly sand surrounding the fragments (Fig. 5D).

Size, shape, and faunal composition of the Lee Creek biostrome are generally similar to the *Septastrea* buildups described by Bailey and coworkers (Bailey and Tedesco, 1986; Bailey and Blow, 1996). This indicates that shallow marine biotopes characterized by aggregations of *Septastrea* colonies and their associated fauna persisted as a distinctive kind of ecologic system through the Pliocene, and possibly into the earliest Pleistocene, along the mid-Atlantic shelf. There are, however, some important differences between the older buildups and the Lee Creek biostrome. Differences in species-level composition and relative abundance of the mollusks are the most obvious ones, and are the result of Pliocene extinctions and evolutionary replacements discussed by Ward and others, 1991). In addition, depositional environments were not exactly the same. Bailey's thickets are enclosed in muddy or silty sands, suggesting slightly deeper or more protected settings, compared to the coarse shelly sand associated with the Lee Creek thicket. The similarities are nonetheless notable. This type of fossil assemblage recurrence, involving the same ecologic structure but different composition and context with each incarnation, has been called *structural continuity* (Miller, 1996). Structural continuity of *Septastrea* biotopes spanned at least 2.5 million years in this region.

Located on the shallow shelf, the Lee Creek thicket would have been exposed to winter storms and hurricanes. Physical disturbance resulting from increased turbidity, strong bottom currents and wave agitation causing scour and collision of colony fragments, lowered salinity, and temperature excursions would have been regular events in this environment. Assisted by the erosion produced by boring and burrowing

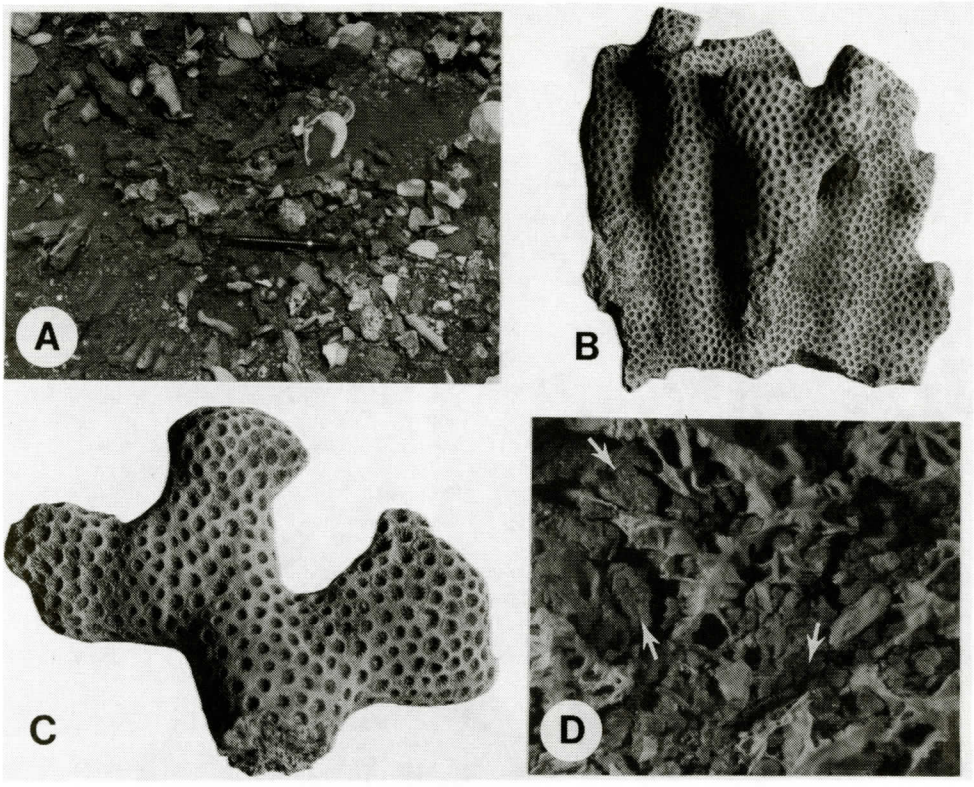

Figure 5. ***Septastrea crassa*** **from the Lee Creek mine. A, Surface of the "25′ bench" cut in the top of the** ***Septastrea*** **biostrome revealing an** ***in situ*** **corallum having many radiating, cylindrical branches (pen is 15 cm long). B, Palmate corallum fragment formed by lateral fusion of several cylindrical branches (sample LC4; specimen is 11.9 cm in width). C, Branching, terminal fragment displaying flaring, club-shaped extremities probably indicating an interval of rapid colony growth (LC3; 8.7 cm width). D, Fracture surface in corallum showing sandy mud filling open spaces (arrows) (LC4; field of view is approximately 12 mm wide).**

organisms, storm-related disturbance probably accounts for most of the damaged coralla, broken branches, and smaller coral fragments in the *Septastrea* bed. During "normal" background intervals, the thicket may have covered 1 to 4 x 10^4 m^2 of seafloor, and contained zones of living coral colonies interspersed with rubbly areas resulting from the large storms. Along the outcrop, appearance of abundant *Septastrea* is preceded by a shell bed (Fig. 4), which may indicate that an extensive shelly pavement was a prerequisite for establishment and spread of the coral thicket. Shelly sand lenses within the biostrome were deposited in small channels or other open spaces within the thicket.

Such "snapshot" reconstructions can be rather misleading, but are useful in marine paleoecology for developing a tentative reconstruction of the original living association of organisms and their environmental context. The concentration of skeletal material, bioerosion and encrustation, variable preservation of coralla, mud matrix within some of the coral fragments, and the shallow shelf setting together point to significant time averaging and mixing of fossils. The *Septastrea* biostrome, then, must be a record of some more inclusive, durable system than a *single* local ecosystem or community.

BIVALVE FAUNA

Of the 78 species of bivalves, 42 were judged to be abundant enough to use as reliable "pale-

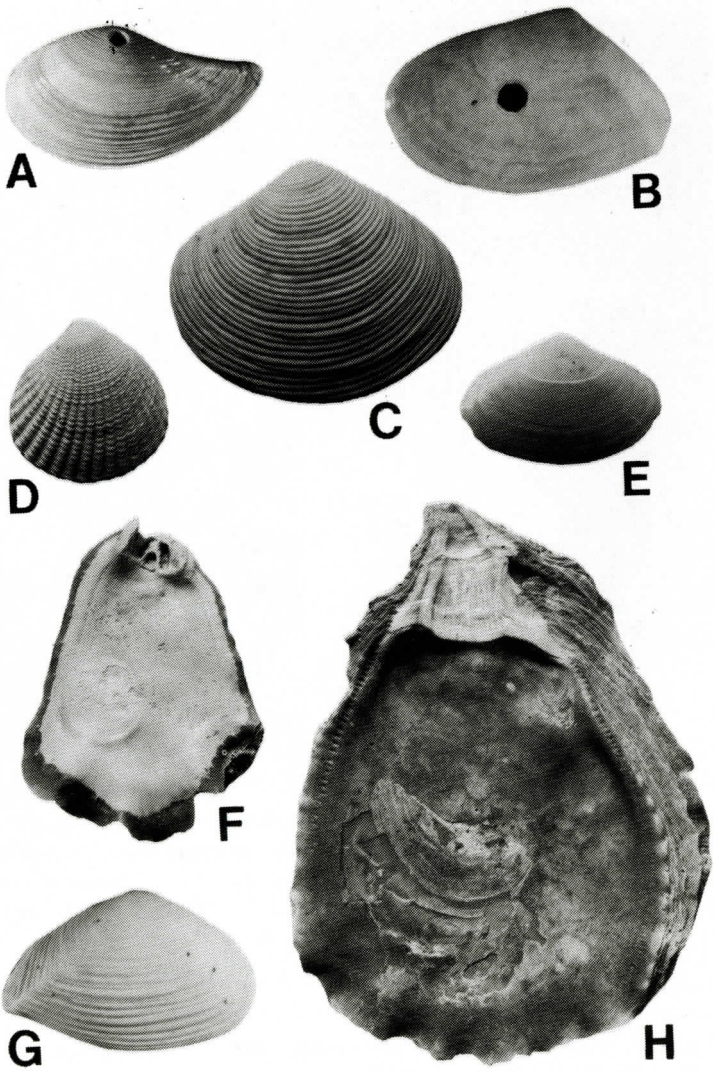

Figure 6. Typical bivalves from the sample interval. A, *Nuculana acuta* (sample LC2; valve is 9 mm in width). B, *Tellina agilis* (LC4; 10 mm width). C, *Astarte concentrica* (LC4; 23 mm width). D, *Cyclocardia granulata* (LC2; 15 mm width). E, *Spisula* sp. (LC3; 17 mm width). F, *Plicatula marginata* (LC3; 18 mm greatest width). G, *Caryocorbula* sp. (LC3; 8.5 mm width). H, *Conradostrea lawrencei* (LC4; 52 mm greatest width).

oecologic tracers" (Table 1). Distribution in the samples is summarized in Table 2, and some of the typical taxa are illustrated in Figure 6. Properties of the 12 most abundant taxa are listed in Table 3. Bivalve diversity of broadly similar coral-related modern assemblages is reviewed in Reed and Mikkelsen (1987).

The bivalves are dominated by endobenthic suspension feeders (30 of the 42 abundant species). Epibenthic suspension feeders (5 species) and endobenthic deposit feeders (5 species) are represented by a few taxa; two species have unknown feeding behavior. The Shannon diversity index for the abundant bivalves was uniformly high (range = 2.84 - 3.01, average = 2.93), and there is little turnover in species composition between samples (Table 2).

Most of the abundant bivalves have variable relative abundance among samples, but only a few taxa show a trend of any kind. For example,

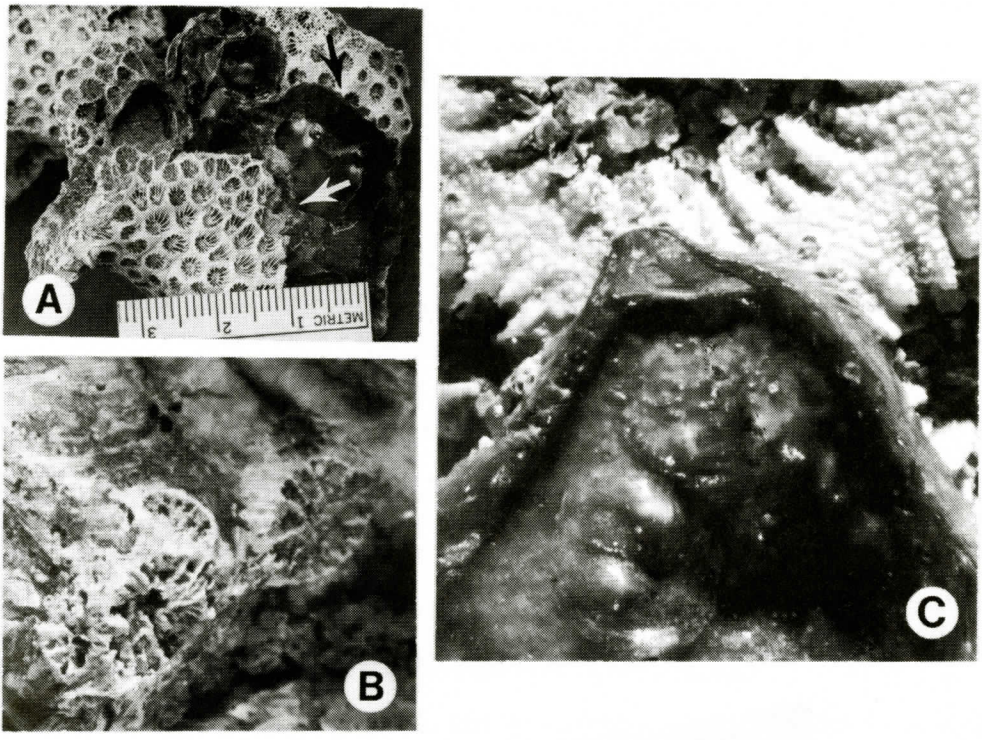

Figure 7. Evidence of interaction of *Septastrea crassa* and *Conradostrea lawrencei* in the coral thicket. A, *Conradostrea* overgrowing *Septastrea* (black arrow), and *Septastrea* overgrowing *Conradostrea* (white arrow) (field photograph; ruler marked in mm's and cm's). B, Nascent *Septastrea* colonies on the surface of a *Conradostrea* valve (LC3; field of view approximately 2.5 mm wide). C, *Conradostrea* spat attached to surface of a *Septastrea* corallum (LC3; field of view 2 mm wide).

the deposit feeders *Nucula proxima* and *Nuculana acuta* range through the sample interval, but are more abundant before the appearance of the *Septastrea* bed. In contrast, *Plicatula marginata* and especially *Conradostrea lawrencei*, both epilithic species, become more common after establishment of the thicket. Other abundant species like *Cyclocardia granulata, Astarte concentrica, Glycymeris sloani,* and *Transennella stimpsoni*, all shallow endobenthic suspension feeders that may have preferred shelly substrate, range through the interval and show rather independent oscillation in relative abundance (Table 1).

To emphasize change in the sample interval, one could focus attention on species such as *Conradostrea lawrencei*, a large marine oyster whose fortunes were intertwined with those of *Septastrea* (Fig. 7A). The oyster is uncommon below the biostrome, but is more abundant within the coral bed (Table 3) and has larger shell size (Fig. 6H). Some of the large coral fragments are overgrown by *Conradostrea* (Fig. 7C), and it appears that *Septastrea* may have used oyster shells as stable or protected habitat for nascent colonies (Fig. 7B). Although the exact ecologic interaction is not clear, a kind of cyclic facilitation appears to be recorded here (see Stephens and Bertness, 1991). Physical disturbance and die-back of the coral could have resulted in provision of abundant, stable attachment sites for the oyster and other epilithic organisms; oyster shells would have provided pavement for coral patches and stable, protected substrates for new colonies.

To emphasize faunal stability, one could consider distribution of bivalves represented by ≥ 100 individuals (Table 3). These taxa occur in all of the samples. Although their relative abundances vary, and a few taxa show directional

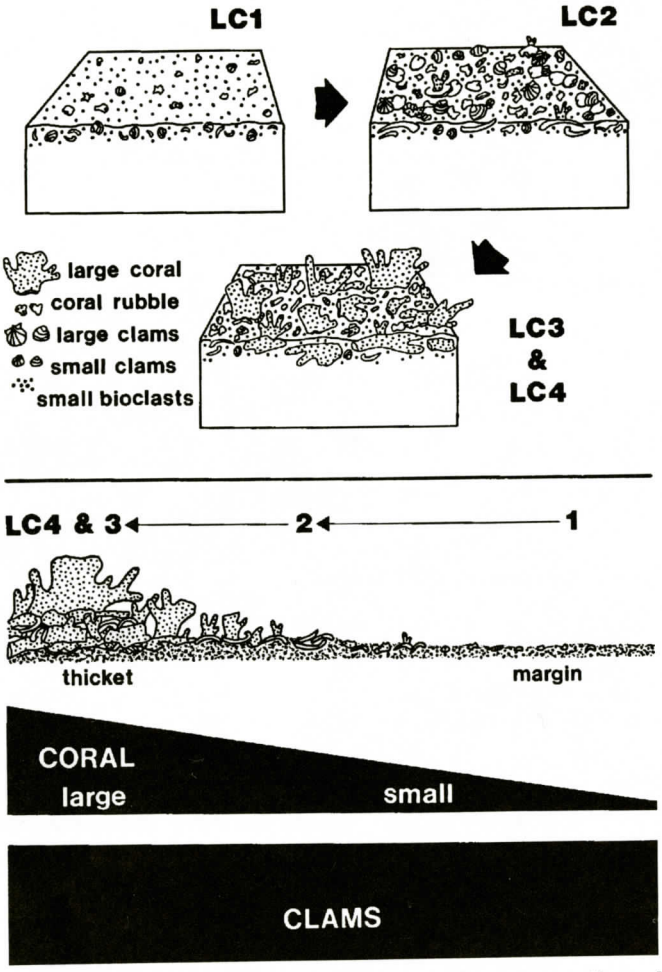

Figure 8. Two possible interpretations of the sample interval. Top, community replacement sequence coinciding with appearance of the coral thicket, emphasizing subtle changes in bivalve relative abundance. Bottom, reconstruction of the thicket and adjacent seafloor, emphasizing overall compositional stability of the bivalve fauna with appearance of the coral thicket. Both interpretations are partly correct, but neither is sensitive to ecologic scaling.

change, there is no remarkable overall change in the core fauna. Each sample of bivalves, sorted and arranged in a cabinet drawer, looks like the others. The strongest impression one derives from hundreds of person-hours of sample processing is that all the samples could represent a single "paleocommunity".

As was the case with the coral, bivalve specimens were variably preserved, from pristine shells having the original color pattern to small, heavily bioeroded valve fragments. Shells were extremely abundant in places, often exceeding the relative volume of sand matrix and forming bioclast-supported fabrics (Fig. 2B). The abundance of deposit feeders in the shell bed (Fig. 4) suggests short-term variation in the environment and temporary establishment of a local ecosystem that was possibly not overwhelmingly dominated by suspension feeders. These properties, and the shallow shelf setting, again indicate that faunal condensation and time-averaging are significant properties of these assemblages. In the terminology proposed by Kidwell and Bosence (1991), each sample represents a *within-habitat time-averaged assemblage* consisting of the skeletal residue of

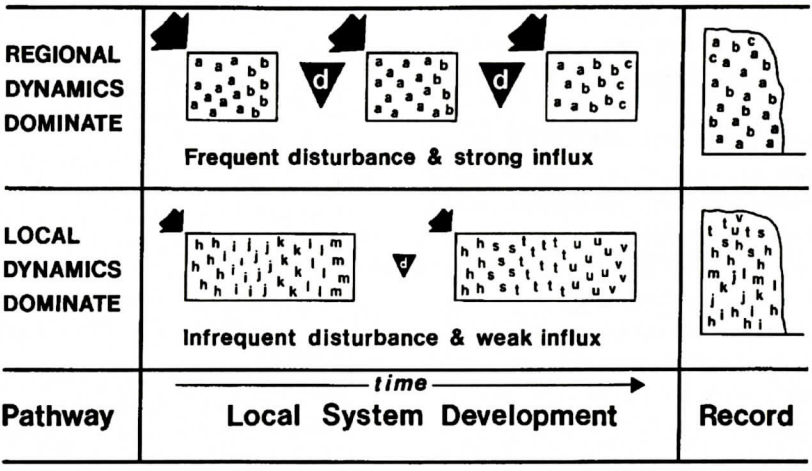

Figure 9. A more ecologically realistic model to explain the record of both stability and minor change in the time-averaged bivalve fauna. The development pathway involving frequent disturbance (d's in black triangles) and strong connection to the regional fauna best explains the succession of generally similar assemblages of bivalves even with establishment of the *Septastrea* thicket. In other words, the record of a stable regional ecosystem apparently swamped that of a series of local systems, at this particular site. The view that such patterns in the marine fossil record result from interaction of regional and local ecologic processes is based on Palmer and others (1996).

several local ecosystems or communities. The problem of paleoecologic interpretation of the sample interval, then, becomes one of reconciling general faunal stability, limited internal changes, and the scale of resolution.

DISCUSSION

Figure 8 presents two interpretive models based on distribution of bivalves in the sample interval at the Lee Creek mine. One model emphasizes change at a particular site on the seafloor (Fig. 8, top), while the other uses the concept of gradient but stresses faunal stability (bottom). Both are plausible interpretations, in general terms, if and only if the units or gradient segments are considered to be equivalent to local ecosystems, patches, or communities in the same sense that a neoecologist would use these terms. In the top diagram development of the coral thicket is shown to coincide with community replacement (sensu Bailey and Tedesco, 1986; Miller, 1986) or possibly a series of community states (e.g., Gray, 1981). The bottom diagram casts the same transition in terms of continuous addition of coralla and coral debris to the seafloor with bivalves hardly reacting at all. Both interpretations contain an element of truth, but both are ecologically naive because they ignore scaling and correspondence, and because there is no reconciliation between the indications of faunal change and stability.

Samples appear to have contained condensed assemblages that record ecologic systems that were more inclusive and more durable than local ecosystems or communities. As within-habitat time-averaged assemblages, each sample is a record of "...both short- and long-term changes in the local physical environment, whether driven by external forces, by the community itself..., or by live/dead interactions..." (Kidwell and Bosence, 1991, p. 178). The Lee Creek beds must reflect development of a series of biotope systems consisting of several short-lived local ecosystems, or possibly even more durable regional ecosystems (Miller, 1991). These are the kinds of system recorded in many cases in shelly deposits of open shelves and seaways, as opposed to more ephemeral local systems, but are largely unrecognized in paleoecologic studies and unexploited as sources of information on the interaction of local and

regional ecologic processes (see Ricklefs, 1987; Ricklefs and Schluter, 1993; Miller, 1996; Palmer and others, 1996; Caley and Schluter, 1997).

A more realistic interpretation of the sample interval takes into account nature of the ecologic systems, the time-averaged record, and the kind of disturbance regime of this environment (Fig. 9). Although a few of the bivalves showed directional changes in abundance, most ranged through the interval seemingly insensitive to the appearance of the *Septastrea* thicket. There is the indication, therefore, that local processes were essentially swamped by a more stable regional ecologic signal (Palmer and others, 1996). Owing to frequent disturbance on the shallow shelf and strong influx of recruits from the regional fauna, the overall record is one of stability with some compositional variation. If disturbance had been less significant and connection to the regional fauna more limited, the record of local ecologic change would have dominated and a pattern resembling community replacement would have been detected in the fossil assemblages. Sediment winnowing and concentration of skeletons during storms (the sedimentologic "defining events" described by Sadler, 1993) ensured that the succession of assemblages at this site would record regional over local ecologic processes.

ACKNOWLEDGMENTS

My sincere thanks go to Ralph Chamness and Tex Gilmore, Texasgulf Inc. geologists, for their time, help and advice at the Lee Creek mine, and especially for allowing access to Gilmore's unpublished report. Nancy Walters sorted the fossils with unwavering dedication, and Rosemary Hawkins typed the manuscript in record time. John Wells identified the coral and offered encouragement to investigate the paleoecology of *Septastrea*. Richard H. Bailey and Lauck W. Ward provided useful reviews of the manuscript. This project was supported by grants from the Humboldt State University Foundation.

REFERENCES CITED

Bailey, R. H. and Blow, W. C., 1996, Paleoecology and taphonomy of a Pliocene coral thicket from the Yorktown Formation of Virginia: Paleontological Society Special Publication 8, p. 19.

Bailey, R. H. and Tedesco, S. A., 1986, Paleoecology of a Pliocene coral thicket from North Carolina: an example of temporal change in community structure and function: Journal of Paleontology, v. 60, p. 1159-1176.

Belt, E. S., Frey, R. W. and Welch, J. S., 1983, Pleistocene coastal marine and estuarine sequences, Lee Creek mine: Smithsonian Contributions to Paleobiology, no. 53, p. 229-263.

Blackwelder, B. W., 1981a, Stratigraphy of upper Pliocene and lower Pleistocene marine and estuarine deposits of northeastern North Carolina and southeastern Virginia: U.S. Geological Survey Bulletin 1502-B, 19 p.

Blackwelder, B. W., 1981b, Late Cenozoic stages and molluscan zones of the U. S. middle Atlantic Coastal Plain: Paleontological Society Memoir 12, 34 p.

Blackwelder, B. W., 1981c, Late Cenozoic marine deposition in the United States Atlantic Coastal Plain related to tectonism and global climate: Palaeogeography, Palaeoclimatology, Palaeoecology, v. 34, p. 87-114.

Caley, M. J. and Schluter, D. 1997, The relationship between local and regional diversity: Ecology, v. 78, p. 70-80.

Carter, J. G., 1983, Biostratigraphy Newsletter, Gulf and Atlantic Coasts of North America, no. 1: Chapel Hill, N. C., 118 p. and chart.

CoBabe, E. A. and Allmon, W. D., 1994, Effects of sampling on paleoecologic and taphonomic analysis in high-diversity fossil accumulations: an example from the Eocene Gosport Sand, Alabama: Lethaia, v. 27, p. 167-178.

Cronin, T. M., Bybell, L. M., Poore, R. Z., Blackwelder, B. W., Liddicoat, J. C., and Hazel, J. E., 1984, Age and correlation of emerged Pliocene and Pleistocene deposits, U. S. Atlantic Coastal Plain: Palaeogeography, Palaeoclimatology, Palaeoecology, v. 47, p. 21-51.

Daniels, R. B., Gamble, E. E., Wheeler, W. H. and Holzhey, C. S., 1972, Field Trip Guidebook: Carolina Geological Society and Atlantic Coastal Plain Geological Association, Raleigh, 68 p.

Daniels, R. B., Gamble, E. E., Wheeler, W. H. and Holzhey, C. S., 1977, The Arapahoe Ridge -- a Pleistocene storm beach: Southeastern Geology, v. 18, p. 231-247.

DuBar, J. R. and Solliday, J. R., 1963, Stratigraphy of the Neogene deposits, lower Neuse estuary, North Carolina: Southeastern Geology, v. 4, p. 213-233.

DuBar, J. R., Solliday, J. R. and Howard, J. F., 1974, Stratigraphy and morphology of Neogene deposits, Neuse River estuary, North Carolina, *in* Oakes, R. Q., Jr. and DuBar, J. R., eds., Post-Miocene Stratigraphy, Central and Southern Atlantic Coastal Plain: Utah State Univ. Press, Logan, Utah, p. 102-122.

Gibson, T. G., 1983, Key Foraminifera from upper Oligocene to lower Pleistocene strata of the Central Atlantic Coastal Plain: Smithsonian Contributions to

Paleobiology, no. 53, p. 355-453.

Gibson, T. G., 1987, Miocene and Pliocene Pectinidae (Bivalvia) from the Lee Creek mine and adjacent areas: Smithsonian Contributions to Paleobiology, no. 61, p. 31-112.

Gilmore, I. K., 1985, Preliminary Findings on the Channel Structure in the Yorktown Clay: unpublished report, Texasgulf, Inc., Aurora, N.C., 7 p. and 23 figs.

Gould, S. J., 1977, Eternal metaphors of palaeontology, *in* Hallam, A., ed., Patterns of Evolution, As Illustrated by the Fossil Record: Elsevier, Amsterdam, p. 1-26.

Gray, J. S., 1981, The Ecology of Marine Sediments: Cambridge Univ. Press, Cambridge, 185 p.

Hazel, J. E., 1983, Age and correlation of the Yorktown (Pliocene) and Croatan (Pliocene and Pleistocene) Formations at the Lee Creek mine: Smithsonian Contributions to Paleobiology, no. 53, p. 81-199.

Johnson, G. H. and Peebles, P. C., 1986, Quaternary geologic map of the Hatteras 4° x 6° quadrangle, United States: U. S. Geological Survey Map I-1420 (NI-18), 1 sheet.

Jordan, R. R. and Smith, R. V., coordinators, 1983, Atlantic Coastal Plain: Correlation of Stratigraphic Units of North America Project: A.A.P.G., Tulsa, 1 chart.

Kidwell, S. M. and Bosence, D. W. J., 1991, Taphonomy and time-averaging of marine shelly faunas, *in* Allison, P. A. and Briggs, D. E. G., eds. Taphonomy: Releasing the Data Locked in the Fossil Record: Plenum, New York, p. 115-209.

Kidwell, S. M. and Flessa, K. W., 1995, The quality of the fossil record: populations, species, and communities: Annual Review of Ecology and Systematics, v. 26, p. 269-299.

Kowalewski, M., 1997, The reciprocal taphonomic model: Lethaia, v. 30, p. 86-88.

Lyons, W. G., 1991, Post-Miocene species of *Latirus* Montfort, 1810 (Mollusca: Fasciolariidae) of southern Florida, with a review of regional marine biostratigraphy: Bulletin of the Florida Museum of Natural History, Biological Sciences, v. 35, p. 131-208.

McCartan, L., Owens, J. P., Blackwelder, B. W., Szabo, B. J., Belknap, D. F., Kriausakul, N., Mitterer, R. M. and Wehmiller, J. F., 1982, Comparison of amino acid racemization geochronometry with lithostratigraphy, biostratigraphy, uranium-series coral dating, and magnetostratigraphy in the Atlantic Coastal Plain of the southeastern United States: Quaternary Research, v. 18, p. 337-359.

Miller, W., III, 1985, The Flanner Beach Formation (middle Pleistocene) in eastern North Carolina: Tulane Studies in Geology and Paleontology, v. 18, p. 93-122.

Miller, W., III, 1986, Paleoecology of benthic community replacement: Lethaia, v. 19, p. 225-231.

Miller, W., III, 1991, Hierarchical concept of reef development: Neues Jahrbuch für Geologie und Paläontologie Abhandlungen, v. 182, p. 21-35.

Miller, W., III, 1993, Models of recurrent fossil assemblages: Lethaia, v. 26, p. 182-183.

Miller, W., III, 1996, Ecology of coordinated stasis: Palaeogeography, Palaeoclimatology, Palaeoecology, v. 127, p. 177-190.

Miller, W., III and DuBar, J. R., 1988, Community replacement of a Pleistocene *Crepidula* biostrome: Lethaia, v. 21, p. 67-78.

Mixon, R. B. and Pilkey, O. H., 1976, Reconnaissance geology of the submerged and emerged Coastal Plain province, Cape Lookout area, North Carolina: U.S. Geological Survey Professional Paper 859, 45 p. and 2 charts.

Palmer, M. A., Allan, J. D. and Butman, C. A., 1996, Dispersal as a regional process affecting the local dynamics of marine and stream benthic invertebrates: Trends in Ecology and Evolution, v. 11, p. 322-326.

Pattison, S. A. J., 1992, Recognition and interpretation of estuarine mudstones (central basin mudstones) in the tripartite valley-fill deposits of the Viking Formation, central Alberta, *in* Pemberton, S. G., ed., Applications of Ichnology to Petroleum Exploration, S.E.P.M. Core Workshop 17, p. 223-249.

Reed, J. K. and Mikkelsen, P. M, 1987, The molluscan community associated with the scleractinian coral *Oculina varicosa*: Bulletin of Marine Science, v. 40, p. 99-131.

Ricklefs, R. E., 1987, Community diversity: relative roles of local and regional processes: Science, v. 235, p. 167-171.

Ricklefs, R. E. and Schluter, D., 1993, Species diversity: regional and historical influences, *in* Ricklefs, R. E. and Schluter, D., eds., Species Diversity in Ecological Communities: Univ. Chicago Press, Chicago, p. 350-363.

Rossbach, T. J. and Carter, J. G., 1989, Biostratigraphy Newsletter, Gulf and Atlantic Coasts of North America, no. 3: Chapel Hill, N.C., 48 p. and chart.

Sadler, P. M., 1993, Models of time-averaging as a maturation process: How soon do sedimentary sections escape reworking?: Paleontological Society Short Course 6, p. 188-209.

Schneider, D. C., 1994, Quantitative Ecology: Spatial and Temporal Scaling: Academic Press, San Diego, 395 p.

Snyder, S. W., Mauger, L. L. and Akers, W. H., 1983, Planktonic Foraminifera and biostratigraphy of the Yorktown Formation, Lee Creek mine: Smithsonian Contributions to Paleobiology, no. 53, p. 455-481.

Stephens, E. G. and Bertness, M. D., 1991, Mussel facilitation of barnacle survival in a sheltered bay habitat: Journal of Experimental Marine Biology and Ecology, v. 145, p. 33-48.

Valentine, J. W., 1989, How good was the fossil record? Clues from the Californian Pleistocene: Paleobiology, v. 15, p. 83-94.

Walker, S. E., 1988, Taphonomic significance of hermit crabs (Anomura: Paguridea): epifaunal hermit crab-infaunal gastropod example: Palaeogeography, Palaeoclimatology, Palaeoecology, v. 63, p. 45-71.

Walker, S. E., 1989, Hermit crabs as taphonomic agents: Palaios, v. 4, p. 439-452.

Ward, L. W. and Blackwelder, B. W., 1987, Late Pliocene

and early Pleistocene Mollusca from the James City and Chowan River Formations at the Lee Creek mine: Smithsonian Contributions to Paleobiology, no. 61, p. 113-283.

Ward, L. W., Bailey, R. H. and Carter, J. G., 1991, Pliocene and early Pleistocene stratigraphy, depositional history, and molluscan paleobiogeography of the Coastal Plain, *in* Horton, J. W., Jr. and Zullo, V. A., eds., The Geology of the Carolinas: Univ. of Tennessee Press, Knoxville, p. 274-289.

Wheeler, W. H., Daniels, R. B. and Gamble, E. E., 1983, The post-Yorktown stratigraphy and geomorphology of the Neuse-Pamlico area, North Carolina: Smithsonian Contributions to Paleobiology, no. 53, p. 201-218.

Wehmiller, J. F. and Belknap, D. F., 1982, Amino acid age estimates, Quaternary Atlantic Coastal Plain: comparison with U-series dates, biostratigraphy, and paleomagnetic control: Quaternary Research, v. 18, p. 311-336.

APPENDIX

Inventory of mollusks from the bulk samples (Figure 4), Lee Creek mine, North Carolina

Taxa	Samples [9] LC1	LC2	LC3	LC4
Bivalvia				
Nucula proxima	132v	451v, 2s	88v	97v
N. taphria	___	2v, 2s	1v	___
Nuculana acuta	177v, 10s	900v, 93s	144v, 4s	100v, 3s
Anadara aequicostata	60v	15v	18v	27v
Quadrilatera sp. cf *Q. adamsi*	___	___	___	1v
Noetia limula	10v	9v	4v	3v
Glycymeris americana	56v	20v	24v	45v
G. arata	70v	189v	44v, 1s	41v
G. sloani	177v, 1s	166v, 2s	102v, 2s	104v, 1s
Crenella decussata	14v	5v	6v	4v
Modiolus sp.	6v	3v	4v	6v
Lithophaga yorkensis	___	___	6v[10]	9v[10]
Amusium sp.	___	___	___	1v
Leptopecten? *auroraensis*	___	___	1v	___
Carolinapecten eboreus	56v	33v	32v	57v
?*Propeamussium* sp.	___	___	1v	___
Plicatula marginata	256v, 57s	100v, 16s	348v, 45s	425v, 67s
Anomia simplex	3v	1v	2v	4v
Conradostrea lawrencei	181v	173v, 1s	477v	446v, 1s
Parvilucina multilineata	2v	2v	___	5v
Bellucina waccamawensis	___	___	___	1v
Cavilinga trisulcata	26v	31v	12v	11v
Callucina keenae	___	___	2v	___
Diplodonta spp.[1]	21v	6v	32v	55v
?*Phlyctiderma* sp.	___	___	1v	___
Chama gardnerae	1v	___	___	1v
Aligena striata	4v	2v	2v	5v
Bornia triangula	9v	34v	8v	11v
Mysella beaufortensis	___	1v	1v?	2v
Anisodonta carolina	5v	2v	5v	13v
?*Sportella* sp.	___	___	1v	___
Ensitellops elongata 4v	21v	3v	___	
Carditamera arata	6v	23v	5v	6v
Pleuromeris auroraensis	72v, 1s	55v	19v	39v
P. decemcostata	101v	203v	51v	31v
Pteromeris perplana	22v	50v	8v	9v
Cyclocardia granulata[2]	631v, 2s	746v, 2s	356v	430v
Astarte concentrica	340v	719v	299v	490v
Astarte sp. cf. *A. undulata*	2v	___	6v	5v
Astarte sp. aff. *A. castanea*[3]	105v, 1s	72v, 1s	18v	13v

Marvacrassatella kauffmani	1v	4v	4v	___
Crassinella spp.[4]	220v	184v, 1s	78v	137v
Laevicardium sublineatum	___	___	6v	12v
Mulinia lateralis	2v	5v	8v	7v
Spisula spp.[5]	494v	213v	305v	550v
Raeta plicatella	6v	6v	4v	4v
Ensis directus	190v	90v	99v	157v
Strigilla sp.	1v	___	___	___
Tellina agilis	317v	173v	295v	451v
Tellina sp.	___	5v	___	1v
Macoma holmesii	1v	1v?	___	1v
Donax fossor	8v	2v	12v	10v
Semele bellastriata	34v	2v	12v	36v
S. nuculoides	___	___	3v	___
Abra aequalis	17v	42v	26v	31v
Cumingia tellinoides	21v	65v	23v	16v
Gouldia metastriatum	245v	101v	120v	143v
Transennella stimpsoni	154v	127v	92v	158v
Pitar sp.	3v?	7v	5v?	9v?
Macrocallista greeni	30v	15v	20v	44v
Gemma magna[6]	5v	1v	1v	2v
Chione grus	2v	___	2v	1v
C. cribraria	3v	___	___	___
Mercenaria permagna	57v	238v, 1s	37v	17v
Petricola pectorosa	2v	9v	2v	5v
P. pholadiformis	4v	8v	2v	3v
?*Mya* sp.	1v	___	___	___
Paramya subovata	1v	3v	___	___
Sphenia sp.	3v	10v	4v	3v
Caryocorbula spp.[7]	468v, 4s	110v	386v	612v
Gastrochaena hians	___	___	32f	2v, 12f
Hiatella arctica	4v	1v?	8v	11v
?*Panopea* sp.	___	___	___	1v
?*Cyrtopleura* sp.	___	1v	___	___
Pandora sp. cf. *P. tuomeyi*	25v	33v	16v	18v
Cochlodesma emmonsii	10v	17v	4v	5v
Thracia brioni	1v	2v	2v	5v
Verticordia lockei	2v	___	4v	4v
Scaphopoda				
Cadulus quadridentatus	___	___	2s	2s
Amphineura				
?*Chaetopleura* sp.	4v	6v	9v	___
Gastropoda				
Diodora nucula	12s	1s	5s	3s
Diodora sp.	2s	___	___	___
Calliostoma sp.	2s	___	2s	3s
Arene pergemma	19s	5s	13s	7s
Cyclostremiscus obliquestriatus	___	1s	___	___
Didianema carolinae	___	1s	___	___
?*Solariorbis* sp.	___	___	1s	___
Caecum pulchellum	4s	1s	2s	1s
C. imbricatum	2s	2s	10s	1s
Caecum sp. cf. *C. flemingi*	___	1s	2s	___
Turritella perexilis	15s	6s	10s	13s
Vermicularia sp.	3s	___	4s	1s
Serpulorbis granifera	9s	14s	5s	4s
Seila adamsii	5s	10s	5s	3s
Triphora sp.	___	1s	___	___
Epitonium leai	1s	2s	___	1s

E. sohli	___	1s	1s	2s
Epitonium sp. cf. *E. carolinae*	1s	3s	___	___
Strombiformis bartschi	1s	2s	1s?	1s?
S. dalli	___	1s	___	2s
Crucibulum sp. cf. *C. lawrencei*	12s	3s	3s	3s
Calyptraea centralis	6s	1s	___	6s
Crepidula aculeata	16s	62s	11s	20s
C. fornicata	26s	15s	9s	14s
C. convexa	13s	12s	6s	10s
C. plana	7s	2s	1s	3s
Trivia floridana	___	1s	___	___
Polinices duplicata	2s	___	6s	___
Lunatia heros	___	___	___	2s
Tectonatica pusilla	18s	5s	12s	18s
?Murexiella sp.	1s	1s	___	___
Urosalpinx perrugata	2s	7s	3s	6s
?Pterorhytis sp.	___	___	1s	___
?Eupleura sp.	2s	3s	___	___
Mitrella gardnerae	3s	1s	9s	1s?
Anachis milleri	16s	23s	16s	15s
Aesopus gardnerae	___	___	1s	___
A. ithitoma	2s	___	1s	1s
A. stearnsii	5s	___	2s	___
Nassarius chowanensis	14s	5s	12s	26s
N. cornelliana	9s	4s	2s	1s
N. fargoi	2s	___	4s	4s
N. schizopyrga?	___	1s	___	___
Busycon sp.	1s	2s	1s?	5s
?Fasciolaria sp.	___	___	___	2s
?Fusinus sp.	1s	___	___	___
Oliva carolinensis	1s	___	1s	___
Olivella mutica	107s	53s	102s	93s
Vexillum wandoense	3s	2s	3s	3s
Scaphella sp.	1s?	___	___	1s
?Cancellaria sp.	1s	___	1s	1s
Granulina ovuliformis	15s	5s	5s	9s
Prunum limatulum	82s	25s	46s	86s
Dentimargo polyspira	7s	6s	___	2s
Dentimargo sp.	___	___	7s	4s
Volvarina sp.	24s	22s	12s	20s
Conus sp.	___	___	3s	___
Strioterebrum sp.	2s	2s	5s	3s
Cymatosyrinx lunata	1s?	___	___	5s
Sedilia sp.	___	4s	1s	2s
?Glabrocythara sp.	___	2s	___	___
Brachycythara reidenbachi	___	3s	___	1s
Odostomia sp.	1s	___	___	1s
Pyrgiscus spp.[8]	3s	2s	1s	2s
Turbonilla abrupta	1s	6s	4s	2s
Turbonilla sp.	___	3s	2s	___
Acteocina candei	___	___	4s	___

1 - - *Diplodonta acclinis* and *D. berryi*, undifferentiated owing to mostly poor preservation.
2 - - Identified as *Cyclocardia* sp. cf. *C. granulata* by Ward and Blackwelder (1987).
3 - - *Astarte* resembling the modern *A. castanea*, possibly an undescribed new species.
4 - - Mostly *Crassinella lunata,* but probably includes some *C. dupliniana* and *C. johnsoni* as described by Ward and Blackwelder (1987).
5 - - *Spisula solidissima* and *S. similis*, undifferentiated.
6 - - Ward and Blackwelder (1987) recognize the subspecies *Gemma magna majorina.*
7 - - *Caryocorbula contracta* and a few *C. auroraensis*, undifferentiated.
8 - - At least two species.
9 - - Symbols for specimens: v = valve, s = shell (articulated shells in the bivalves), f = flask of *Gastrochaena hians.*
10 - -Only free valves counted, not borings.

SOUTHEASTERN GEOLOGY
V. 37, No. 2, October 1997, p. 91-107

PETROLOGY, MINERALOGY, AND GEOCHEMISTRY OF THE ROLESVILLE GRANITIC BATHOLITH, EASTERN PIEDMONT, NORTH CAROLINA

JOANNA KOSECKI AND R.V. FODOR

Department of Marine, Earth, and Atmospheric Sciences
North Carolina State University
Raleigh, NC 27695 USA

ABSTRACT

The Rolesville granitic batholith in eastern Piedmont, North Carolina, is one of many plutons emplaced ~300 Ma during the Alleghanian orogeny. We studied twenty samples from two quarries for petrography and whole-rock, mineral, and Sr- and O-isotopic compositions. Our objectives were to determine compositional variations in localized areas to help establish how various granitoid types are related by igneous processes, and to determine how trace-element and isotopic compositions can contribute to understanding source materials for the batholith. We identified foliated biotite-rich granitoid, nonfoliated granite, and late-stage granitic dikes that are largely peraluminous and collectively demonstrate trends of, for example, increasing SiO_2 (66-76 wt.%) and decreasing CaO (2.5 to 0.8 wt.%), FeO (4 to 0.27 wt.%), and rare-earth element (La 70 to 7 ppm) abundances. Low Nb (5-18 ppm) manifests as negative anomalies. Plagioclase is An_{22-14} and K-feldspar is Or_{88-92}. Initial $^{87}Sr/^{86}Sr$ ratios are 0.70305 to 0.70419, and $\delta^{18}O$ values are ~4.6 to 5.6 for feldspar and ~6.5 to 6.7 for quartz.

Rb, Ba, and Sr, the trace elements characteristic of the granitoid silicate phases, do not correlate well with major elements but correlate well among themselves. In particular, increasing Rb attends decreasing Sr and Ba -- relationships that are consistent with vapor-absent dehydration melting of a muscovite-bearing source. Our interpretation is that the Rolesville batholith represents multiple magma batches produced from varying percentages of melting of a source nearly uniform in composition. The Nb anomalies and $^{87}Sr/^{86}Sr$ ratios are consistent with the source proposed for other Piedmont Alleghanian plutons — namely, ~600 Ma metamorphosed crust (e.g., Carolina terrane) that represents oceanic subduction/volcanic environments. However, high Sr contents (~200-700 ppm) in Rolesville granitoids preclude identifying their specific parentage in any examples of metamorphosed crust for which trace-element compositions are available (e.g., Sr 250-300 ppm).

INTRODUCTION

Deformation and metamorphism in the eastern North Carolina Piedmont during Alleghanian time was attended by emplacement of at least a dozen granitoid plutons between about 315 and 285 Ma (Farrar, 1985; Russell and others, 1985; Speer and others, 1994; Coler and others, 1997). Ages of some Piedmont plutons have long been established (e.g., Fullagar and Butler, 1979) and accordingly applied to unraveling the tectonic history of the southern Appalachians (e.g., Russell and others, 1985). Also, pluton emplacement mechanisms have been assessed (Speer and others, 1994), and most recently, the whole-rock and Sr-, Nd-, and Pb-isotopic compositions of Alleghanian plutons have been addressed (e.g., Samson and others, 1995; Coler and others, 1997). On the other hand, mineral compositional data are unavailable, nor is there information for geochemical variations within plutons to help establish petrologic relationships among different rock types comprising particular plutons and relationships among various plutons.

The purpose of this work, therefore, is to apply a smaller scale, more concentrated approach to establishing geochemical aspects of

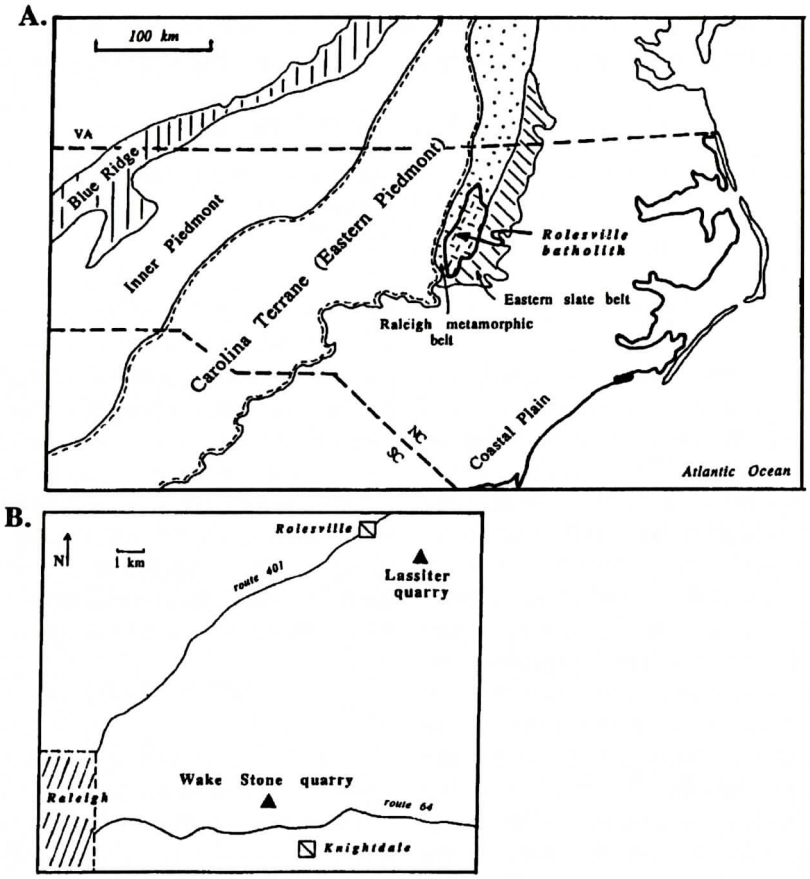

Figure 1. (A) Map of North Carolina showing the location of the Rolesville batholith and the neighboring Carolina terrane, Raleigh metamorphic belt, and Eastern slate belt. (B) Detail map showing the sampling locations, Lassiter quarry and Wake Stone quarry, relative to Raleigh, NC.

Alleghanian plutons. We sampled one of the largest exposed eastern Piedmont plutons, the Rolesville batholith near Raleigh, North Carolina, to examine its petrographically distinct aspects in compositional detail. In particular, we sampled two rock quarries within the Rolesville batholith, believing that the varieties of granitoid exposed sufficiently represent the batholith for this first attempt to evaluate igneous processes responsible for compositional ranges within the batholith and to establish characteristics about its source material. Our study of twenty samples includes determining their mineral, whole-rock major- and trace-element, and Sr and O isotopic compositions.

GEOLOGIC SETTING, BACKGROUND, AND SAMPLE LOCATIONS

The Rolesville granitoid batholith originated during the Alleghanian orogeny of the southern Appalachians (e.g., Farrar, 1985; Speer, 1994; Speer and others, 1994). It intruded the amphibolite-grade felsic gneisses and schists of the Raleigh metamorphic belt (Figure 1), and presently has a ~24 x 80 km northeast-trending exposure in eastern North Carolina (Figure 1). The batholith is bounded on the west by the Carolina terrane, one of the largest terranes of the Appalachian orogen, and on the east by the Eastern slate belt, the easternmost metamorphic belt of the southern Appalachians (Figure 1).

Understanding the nature of these three neighboring geologic provinces is pertinent to establishing the origin of the Rolesville batholith. The west-bounding Carolina terrane represents Neoproterozoic accreted crust comprised of volcanic and volcaniclastic material metamorphosed to amphibolite and greenschist facies grades. It is isotopically 'juvenile' crust derived from the mantle in an oceanic setting ~600 Ma (Samson and others, 1995). The Eastern slate belt is also comprised of ~600 Ma volcanic and volcaniclastic material, but metamorphosed only to greenschist grade. It correlates with the Carolina terrane (Stoddard and others, 1991). Similarly, the Raleigh metamorphic belt, host province for the Rolesville batholith, probably also correlates with the Carolina terrane (Coler and others, 1997).

Early studies of the Rolesville batholith include Parker's (1968) field evaluation of the batholith, and petrographic studies by Bowman (1970) and Becker and Farrar (1977). The batholith composition has been identified on the basis of IUGS classification as largely granite (e.g., Coler and others, 1997). Additionally, the batholith is recognized as having both foliated and nonfoliated components that are cut by leucogranitic dikes (Parker, 1979), and being comprised of sheeted plutons representing multiple magma pulses in active shear zones (Speer, 1994). Major-element compositions of the Rolesville batholith were first presented by Becker and Farrar (1977), and trace-element and Sr- and Nd-isotopic compositions for eight samples are in Coler and others (1997).

Our samples are from Lassiter quarry near Rolesville, and from Wake Stone quarry near Knightdale (Figure 1). The two localities are about 14 km apart.

PETROGRAPHY

The main minerals of the Rolesville batholith are plagioclase, quartz, K-feldspar, biotite, and Fe-Ti oxides. Minor minerals include chlorite, white mica, and apatite. Chlorite occurs as a biotite replacement. The irregular outlines of white mica grains and their occurrence largely within or adjacent plagioclase grains suggest a secondary origin (e.g., Miller and others, 1981); white mica is more common in Wake Stone samples (often 1-2 vol%; Table 1) than in Lassiter samples. Accessory minerals are monazite, most common in Wake Stone samples, allanite, mostly in Lassiter samples, and zircon.

Textures are largely anhedral granular but with subhedral granular and equigranular mosaic aspects to some samples. Plagioclase is subhedral to anhedral, and quartz and K-feldspar, chiefly microcline, occur as anhedral grains interstitial to plagioclase. The K-feldspar commonly contains inclusions of plagioclase and quartz. Some plagioclase is myrmekitic. Samples with relatively large amounts of biotite (e.g., >5 vol%; Table 1) have foliation owed to biotite orientation. Foliation in Rolesville granitoids, as well as in other Alleghanian plutons, is believed due to regional tectonism concomitant with magma emplacement and cooling (e.g., Russell and others, 1985).

Based on modal percentages of quartz and feldspars (Table 1), the majority of quarry samples studied are granite, two are granodiorite, two are quartz monzonite, and one is quartz monzodiorite (Figure 2a). Granitoid types at each quarry are gradational with respect to modal mineral components, and for the purpose of coordinating broad variations in modal mineralogy with whole-rock and mineral compositions, we categorized the samples into three groups: foliated biotite-rich granitoid, nonfoliated granite, and late-stage granitic dikes.

Foliated Biotite-rich Granitoid

Foliated biotite-rich (6 to 20 vol%) granitoid appears to be the most abundant type at Lassiter quarry and occurs as granite, quartz monzodiorite, and granodiorite compositions (Figure 2a). Foliated biotite-rich rock at Wake Stone quarry is represented by granite and granodiorite. Grain sizes of major modal minerals are mainly 0.5 to 3 mm at both sample sites.

Nonfoliated Granite

Lassiter quarry granite occurs as tabular

Table 1. Whole-rock-major- and trace-element compositions and modal compositions for Roles granitoids from Lassiter (L) and Wake Stone (WS) quarries, Wake County, North Carolina (in order of decreasing FeO for each quarry).

	Lassiter											Wake Stone								
	qmd	g	g	gd	g	g	g	g	g	qm	g	gd	g	g	g	g	qm	g	g	g
group	fol	fol	fol	fol	gran	gran	gran	gran	gran	dike	dike	fol	fol	fol	gran	gran	dike	gran	dike	dike
sample	L6a	L2	RV3	L7a	L4b	L3b	L5	L7b	L6b	L4a	L1	WS3	WS8a	WS9	RV2	WS2	WS5	WS1c	WS4	WS8b
SiO_2	65.67	68.06	68.33	68.83	72.74	73.23	72.78	70.25	73.58	70.90	73.50	66.73	69.70	71.86	73.03	75.71	68.63	71.99	73.94	73.38
TiO_2	0.78	0.56	0.53	0.50	0.23	0.22	0.16	0.19	0.13	0.10	0.04	0.47	0.42	0.39	0.22	0.18	0.12	0.14	0.09	0.07
Al_2O_3	17.22	16.13	15.95	16.58	14.97	14.34	14.70	17.07	16.39	16.84	15.75	17.29	16.19	14.72	15.54	13.38	16.87	17.18	14.45	14.50
FeO	3.89	2.40	2.34	2.22	1.16	0.95	0.89	0.85	0.68	0.48	0.27	2.44	1.97	1.90	1.18	1.04	0.75	0.73	0.71	0.46
MnO	0.05	0.02	0.01	0.02	0.01		0.01					0.05	0.03	0.01	0.01	0.02	0.01	0.01	0.01	
MgO	1.50	0.91	0.97	0.85	0.41	0.26	0.30	0.20	0.40	0.09	0.02	0.87	0.62	0.61	0.17	0.28	0.46	0.23	0.27	0.30
CaO	2.54	2.05	2.20	2.07	1.68	1.55	1.54	1.50	1.60	1.07	1.09	2.56	2.01	1.84	1.14	1.18	1.48	1.31	1.31	0.84
Na_2O	3.80	4.30	4.40	4.46	4.55	3.27	4.38	4.10	2.27	1.64	4.32	5.43	4.91	4.21	3.36	3.92	4.52	4.50	4.31	2.88
K_2O	3.46	4.63	4.24	4.17	4.16	4.40	4.54	5.74	4.45	7.64	5.20	3.18	3.97	4.28	5.42	4.56	6.86	4.28	4.59	7.14
P_2O_5	0.20	0.14	0.16	0.14	0.07	0.04	0.05	0.07	0.05	0.03	0.01	0.18	0.13	0.10	0.08	0.04	0.12	0.02	0.02	0.02
Total	99.11	99.2	99.13	99.84	99.98	98.26	99.35	99.97	99.55	98.79	100.20	99.20	99.95	99.92	100.15	100.31	99.82	100.40	99.70	99.59
Mg#	43.3	42.9	45.1	43.1	41.2	35.2	40	31.8	53.8	27.1	12.8	41.4	38.4	38.9	22.2	34.8	54.9	38.4	43	56.4
LOI				0.04			0.19		0.16										1.15	
Rb ppm	173	156	124	157	146	132	162	166	138	236	189	199	172	145	184	201	290	188	205	241
Sr	503	580	674	644	396	531	388	628	488	463	263	316	713	410	394	225	350	149	158	536
Ba	880	1482	1608	1524	750	1045	726	1640	1021	1910	129	521	1239	885	1169	398	847	194	222	1284
Zr	328	291	290	278	126	38	88	105	85	62	22	206	211	213	142	100	31	107	123	11
Hf	9.9	-	7.07	-	-	3.4	-	-	3.1	-	0.6	6.1	5.2	-	4.22	3.3	0.9	-	4	0.5
Nb	13	7	5	10	6	11	7	8	7	8	7	18	8	10	18	16	10	11	9	8
Y	21	16	13	18	14	10	12	14	12	12	14	28	16	11	14	17	26	20	25	22
Cu	143	89	15	26	14	8	24	12	7	17	89	26	186	70	6	3	18	29	24	9
Zn	108	73	62	62	27	30	4	28	16	11	2	95	49	53	41	36	27	10	23	9
Sc	6.1	-	3.3	-	-	1.7	-	-	1.1	-	0.8	6.9	2.9	-	1.8	2.2	1.7	-	1.6	1
Th	22	-	20.3	-	-	12.7	-	-	14.1	-	9.8	24.5	17.5	-	25.5	24	5.1	-	22	4
La	69.8	-	61.6	-	-	28.5	-	-	22.7	-	9	37	40.6	-	31.6	28.9	7.9	-	6.6	7.1
Ce	156.9	-	104	-	-	61.9	-	-	53.2	-	24.3	84.4	90.8	-	55	69.2	17.8	-	15.9	16.5
Nd	44.7	-	32	-	-	23.9	-	-	12.8	-	5.2	18.9	22	-	18	21.5		-		
Sm	6.52	-	4.9	-	-	2.6	-	-	2.7	-	1.7	5.77	3.6	-	3.5	3.98	1.86	-	2.68	1.21
Eu	1.03	-	1.11	-	-	0.76	-	-	0.71	-	0.55	0.8	0.89	-	0.72	0.59	0.69	-	0.43	0.51
Tb	0.7	-	0.38	-	-	0.18	-	-		-		0.66	0.25	-	0.29	0.31	0.23	-	0.38	0.21
Yb	1.53	-	0.54	-	-	0.92	-	-	0.52	-	0.76	1.62	1.12	-	0.51	1.17	0.82	-	1.76	1.43
Lu	0.23	-	0.17	-	-		-	-		-	0.21	0.37		-	0.16			-	0.33	0.33
Mode vol%																				
sample	L6a	L2	RV3	L7a	L4b	L3b	L5	L7b	L6b	L4a	L1	WS3	WS8a	WS9	RV2	WS2	WS5	WS1c	WS4	WS8b
quartz	9.5	24	27.7	24.7	28.7	27.9	32.9	28.7	32.3	18	41.8	24.9	24.2	29.9	35.6	34.5	12.1	31.3	41	36.2
K-feld	13.2	27.3	23.7	17.7	32.9	34.6	26.2	29.7	36.3	45.8	29.4	17	25.9	22.9	22.6	26.3	35.7	26.1	21.4	48.9
plag	55.4	39.2	38.6	49.2	34.7	32.7	38.4	38.9	27.6	33.8	26	44.2	39.9	36.6	29.5	31.6	48.5	37.9	30.3	14.1
biotite	19.5	8.2	7.4	6.3	2.3	3.6	2	1.6	2.9	0.5	1.5	8.5	7.6	6.9	1.6	0.8	2	0.6	0.1	< 0.1
musc	< 0.1	0.1	<0.1	0.1	0.1	0.2	0.2	0.2	< 0.1	0.6	0.3	1.3	0.9	0.4	0.2	2.1	0.3	2.6	3.7	0.2
chlorite	< 0.1	0.1	0.2	0.1	0.2	0.2	0	< 0.1	0.1	0.3	0.1	0.3	0.1	0.6	0.5	1	0.4	0.7	0.7	< 0.1
opaques	0.7	0.4	0.7	0.9	0.4	0.3	0.1	0.3	0.3	0.3	0.8	0.6	0.5	0.8	0.4	0.4	< 0.1	0.2	0.1	0.1
zircon	< 0.1	0.1	0.1	0.1	tr	<0.1	tr	< 0.1	0.1	tr	tr	< 0.1	tr	< 0.1	0	tr	tr	tr	tr	tr
allanite	0.4	0.2	0.3	0.1	0.1	0.1	0	0	0	0	0	0	0	0.4	0	0	0	0	0	0
apatite	0.8	0.2	0.7	0.3	0.2	0.1	< 0.1	0.2	< 0.1	< 0.1	0	0.4	0.2	0.4	0	< 0.1	0.2	0	0	0.1
monazite	0	0	0	0	0	0	0	0	0	0	tr	tr	0	0	0	tr	0	tr	0	0
alteration	0.1	< 0.1	0.3	0.3	0.3	< 0.1	< 0.1	0.2	0.1	0.6	< 0.1	2.6	0.7	1	9.6	3.1	0.7	0.5	2.6	0.1

Major elements reported wt.% volatile-free, after 1000°C ignition..
Rock types: g = granite; gd = granodiorite; qm = quartz monzonite; qmd = quartz monzodiorite
Group: fol = foliated biotite-rich granitoid; gran = nonfoliated granite; dike = late-stage dike
LOI = loss on ignition; values represent volatile loss (wt.%) without taking into account any weight gains due to Fe oxidation; where no values are reported, weight gains were observed during ignition.

bodies of various thicknesses that are both parallel to the foliation in the biotite-rich granitoids and cross-cut it. Grain sizes for granites are also generally 0.5 to 3 mm, but are up to ~7 mm, particularly at Wake Stone quarry.

Late-stage Dikes

Late-stage, generally leucogranitic, dikes can be as thin as 2 to 3 cm or up to about 10 cm. They penetrate both foliated and nonfoliated granitoids. Compositionally, they are granite and quartz monzonite (Figure 2a). Grain sizes reach 8-10 mm, or are aplitic and with 1-mm sized grains.

ANALYTICAL TECHNIQUES

We determined whole-rock major- and trace-element compositions by x-ray fluorescence spectrometry (Philips 1410) at North Carolina State University. We prepared glass disks for major elements, except Na and K, and powder pellets for Na, K, and trace elements Rb, Sr, Ba, Zr, Nb, Y, Cu, and Zn. Our trace-element matrix corrections included the overlapping of Rb and Sr $K\beta$ peaks on, respectively, the Y and Zr $K\alpha$ peaks. Neutron activation instru-

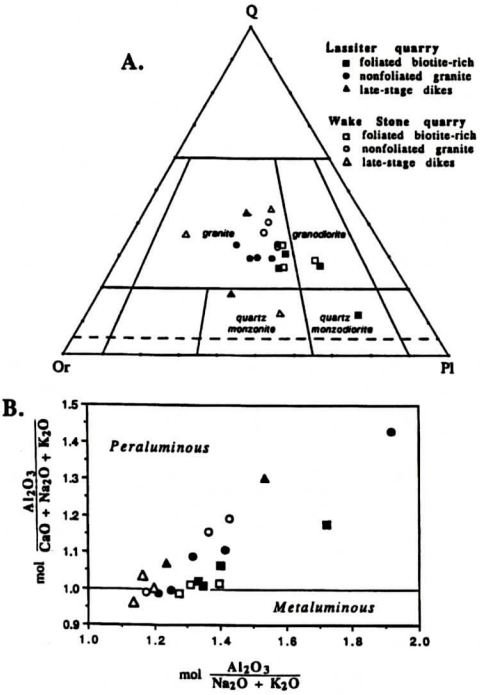

2 (a) IUGS ternary diagram for the compositions of the Rolesville batholith samples studied. (b) Most Rolesville batholith granitoid samples have peraluminous compositions.

mentation at Oregon State University radiation center was used for rare-earth elements (REE), Hf, Th, and Sc.

We acquired mineral compositions using an ARL-EMX electron microprobe at North Carolina State University (15 keV; 0.015 μA) and applied Bence-Albee matrix corrections. Strontium isotope compositions were determined at the University of North Carolina-Chapel Hill isotope laboratory using a Nuclide single collector spectrometer, and oxygen isotope analyses were determined (by JK) at the University of Georgia isotope laboratory using a Finnigan MAT spectrometer.

ANALYTICAL RESULTS

Whole-rock Compositions

Whole-rock compositions are in Table 1 and are represented in SiO_2 variation diagrams in Figure 3. Relatively low amounts of whole-rock volatile components, namely H_2O expressed as loss-on-ignition, suggest that weathering and/or secondary alteration did not severely hydrate these rocks to affect their compositions. On the other hand, the occurrence of white mica and chlorite (e.g., alteration products of plagioclase and biotite, respectively) indicate that the Rolesville was affected at least by some secondary processes.

Most Lassiter and Wake Stone samples are peraluminous, consistent with earlier observations for Rolesville batholith compositions (Becker and Ferrar, 1977), but some are transitional to metaluminous (Figure 2b). Collectively, Lassiter and Wake Stone samples have a ~66 to 76 wt.% SiO_2 range, and major elements FeO, TiO_2, CaO, MgO, Al_2O_3, and P_2O_5 decrease with increasing SiO_2 (Figure 3). On the other hand, K_2O weakly increases with increasing SiO_2 and is highest in some late-stage dikes. The compositional trends for the collective samples correspond, in a general way, to the overall change in rock type from foliated biotite-rich granitoid, to nonfoliated granite, to late-stage dikes. There are, however, some foliated biotite-rich granitoids and some nonfoliat-

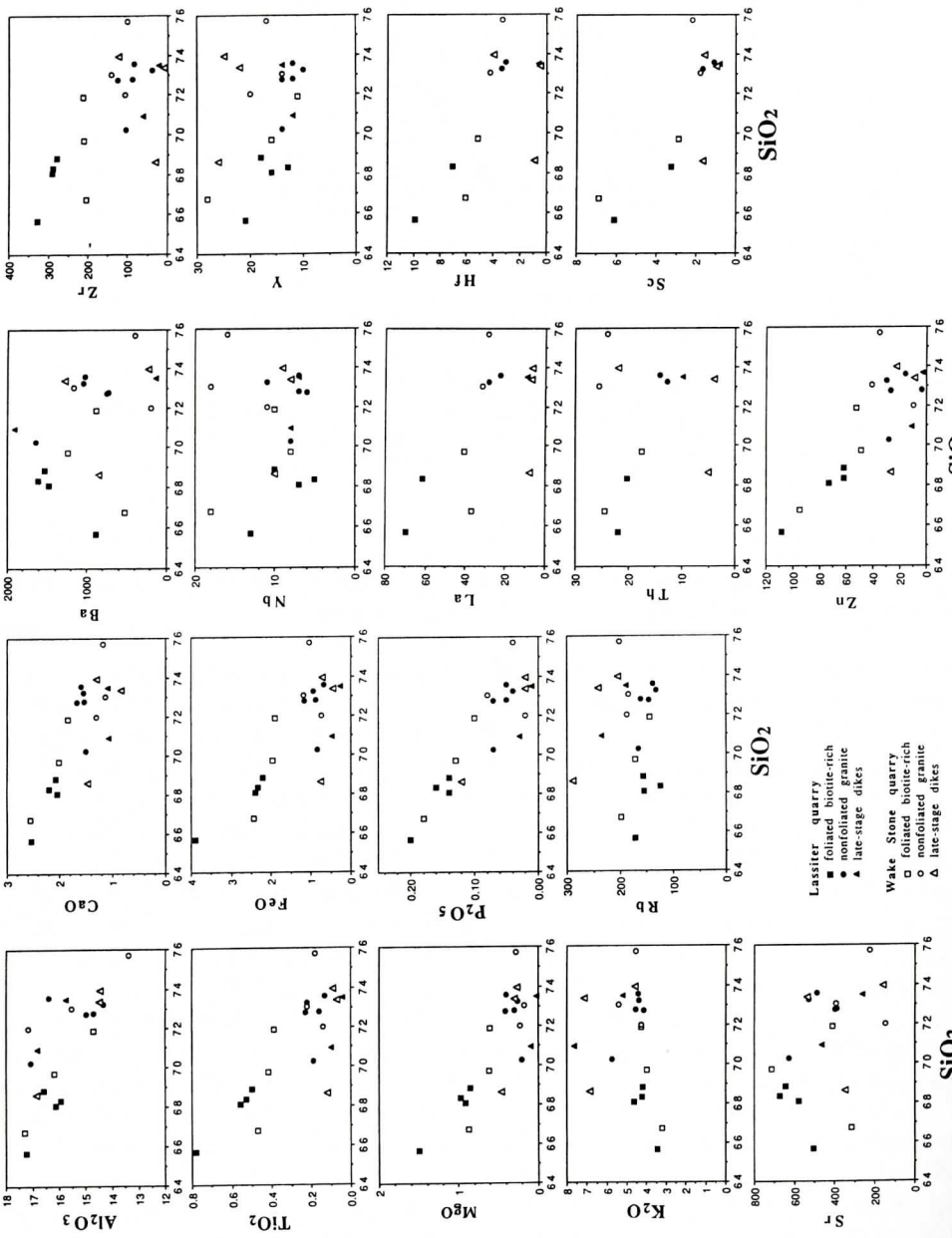

Figure 3. SiO_2 variations diagrams for major- and trace-element abundances in Rolesville batholith granitoid samples.

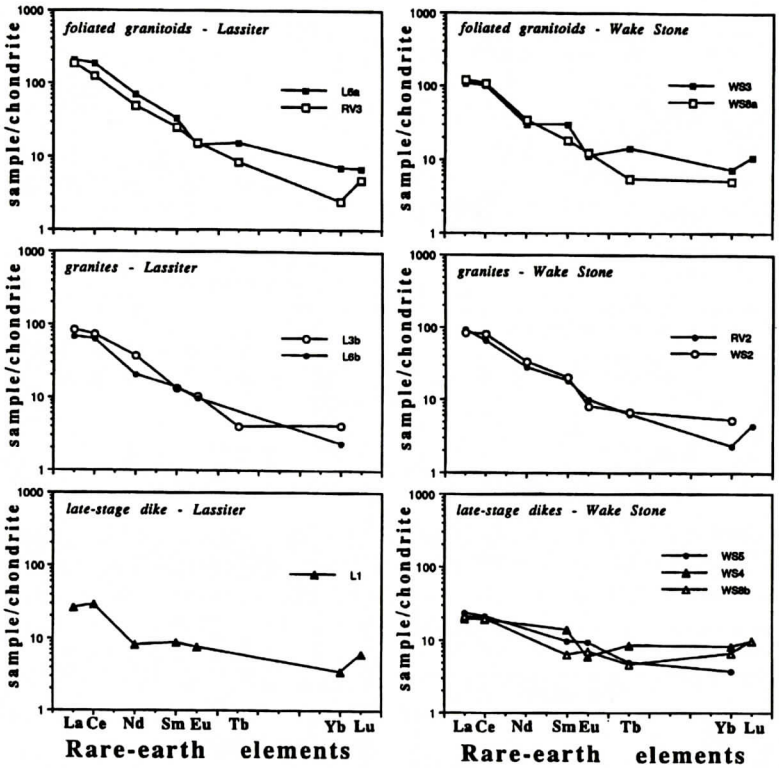

Figure 4. Chondrite-normalized rare-earth element patterns for representative Rolesville batholith granitoids. Sample numbers refer to Table 1.

ed granites that are compositionally more evolved (e.g., higher SiO_2; lower FeO, MgO, CaO) than some late-stage dikes (Figure 3). Overall, major-element compositions of samples from the two quarries overlap, but Lassiter quarry provided the most 'primitive' granitoid, containing 3.9 wt.% FeO and 1.5 wt.% MgO (Figure 3).

Among trace elements (Figure 3), Zr, Hf, La, Sc, and Zn have negative correlations with SiO_2. On the other hand, Rb has an overall flat trend and, like K, is highest in some late-stage dikes. Sr, Ba, Th, Y, and Nb do not correlate with SiO_2. Wake Stone samples have the highest Y values.

Chondrite-normalized REE patterns for twelve granitoids are in Figure 4. All samples are light-REE (LREE) enriched, although variably, as there are gradually decreasing light- and middle-REE abundances and decreasing La/Sm ratios over the change from foliated biotite-rich granitoids, to nonfoliated granites, to late-stage dikes for rock suites from both quarries. Because the preponderance of REE abundances in granitoids are hosted in accessory minerals (e.g., Gromet and Silver, 1983), the highest LREE concentrations (Figure 4) are in the more 'primitive' (e.g., highest FeO, lowest SiO_2) samples (Table 1) at each quarry -- namely the foliated granitoids -- due to their relatively high modal abundances of the LREE-enriched accessory minerals, monazite and allanite (Table 1). Negative Eu anomalies are observed among all granitoid types. However, two late-stage dikes that are K_2O (and Rb)-rich (~7 wt.%) and have abundant K-feldspar (36-49 vol%; Table 1) have positive Eu anomalies (Figure 4).

Normalizations to primitive-mantle abundances (Figure 5) show that all granitoid types share similar trace-element pattern shapes, with exception of those influenced by the REE, Zr, and Hf relative depletions in the dikes. Also notable is that all samples have negative Nb anom-

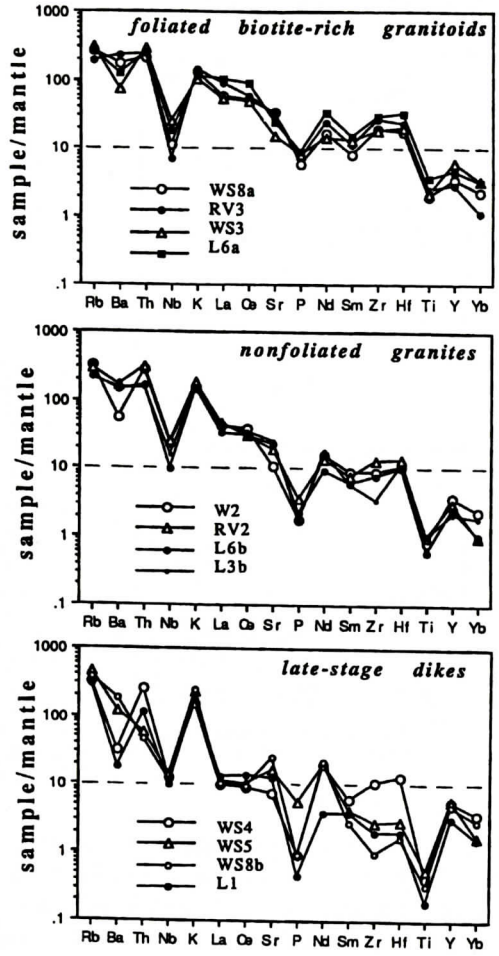

Figure 5. Primitive-mantle normalized patterns for representative samples of the Rolesville batholith according to foliated, nonfoliated, and dike occurrences. WS and L sample codes denote Wake Stone and Lassiter quarries, respectively; sample numbers refer to Table 1. Normalization values from Sun and McDonough (1989). Dashed line at '10 x' is for visual reference.

alies (Figure 5).

Mineral Compositions

Plagioclase

Average compositions for representative plagioclase grains in Rolesville granitoids (Table 2) range from about An_{22} to An_{14}, or oligoclase compositions. The plots for individual

Table 2. Representative plagioclase and K-feldspar compositions in Rolesville batholith granitoids, Wake County, NC.

	Plagioclase						K-feldspar					
	Lassiter			Wake Stone			Lassiter			Wake Stone		
	fol	*gran*	*dike*	*fol*	*gran*	*dike*	*fol*	*gran*	*dike*	*fol*	*gran*	*dike*
	L6a	L6b	L4a	WS8a	RV2	WS8b	L6a	L6b	L4a	WS8a	RV2	WS8b
SiO_2	64.0	63.9	64.0	64.1	62.6	64.1	64.3	64.8	64.5	64.6	63.6	64.7
Al_2O_3	23.8	24.0	22.3	23.1	23.5	22.7	19.3	19.3	19.4	19.0	19.3	19.3
CaO	4.3	4.0	4.0	3.8	4.2	3.6	0.04	0.04	0.01	0.05	0.01	0.05
Na_2O	8.7	8.3	9.5	8.3	8.8	8.7	1.1	1.1	1.0	0.97	1.1	1.1
K_2O	0.31	0.26	0.26	0.27	0.26	0.27	15.6	15.3	14.9	14.9	14.8	15.1
SrO	0.06	0.06		0.1		0.06	0.08	0.07		0.10		0.09
BaO	-	0.01		-		-	0.50	0.45		0.46		0.29
Total	101.17	101.53	100.06	99.67	99.36	99.43	100.92	101.06	99.81	100.08	98.81	100.63
An	21.1	20.7	18.6	19.9	20.6	18.3	0.19	0.20	0.05	0.26	0.05	0.25
Or	1.8	1.6	1.4	1.7	1.5	1.6	90.2	90.0	90.7	90.8	89.8	89.8

Each column is the average composition acquired from 8-12 point-analyses on one grain.
fol = foliated biotite-rich granitoid; *gran* = nonfoliated granite; *dike* = late-stage dike.

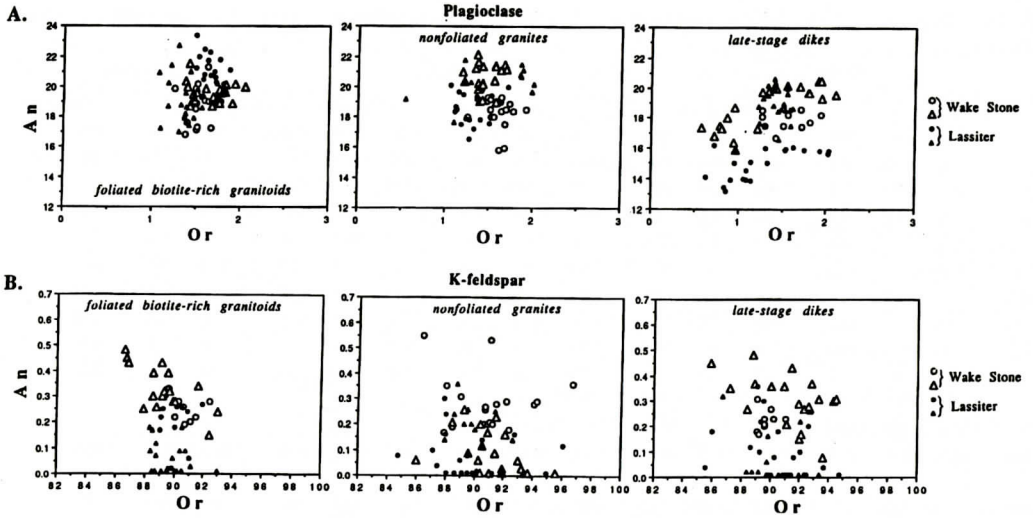

Figure 6. Compilation of point-analyses of plagioclase (a) and K-feldspar (b) expressed as An and Or molecular endmembers. Each symbol represents the compositional variation observed for a particular sample of foliated granitoid, nonfoliated granite, and late-stage dike for which feldspar was analyzed point-by-point. Full representative compositions are in Table 2.

point-analyses on grains from twelve samples show that compositional zoning is ~3 to 6 mol% An (Figure 6a). Foliated and nonfoliated granitoids have overlapping An compositions, whereas late-stage dikes, on the whole, have lower An contents (Figure 6a). Plagioclase grains in the dikes also have a wide range in Or, up to ~1.5 mol%, relative to ~0.5 to 1 mol% Or for the other samples (Figure 6a). We analyzed some grains for Sr and Ba and noted that they contain detectable amounts of SrO (e.g., 0.02 to 0.09 wt.%) but no detectable BaO (Table 2).

K-feldspar

K-feldspar in twelve samples have average compositions that range from Or_{88} to Or_{92} and have only ~$An_{0.2}$ (Table 2). Single-point analyses (Figure 6b) show that K-feldspar grains among foliated granitoid, nonfoliated granite, and late-stage dikes are, on the whole, identical in composition and span the range $Or_{85\text{-}97}$. Individual grains can be zoned extensively enough to represent the entire range. One small distinction between sample sites is that Lassiter rocks, on average, have K-feldspar with lower An contents than Wake Stone rocks (Figure 6b). The SrO contents in K-feldspar are about the same as in plagioclase, 0.04 to 0.10 wt.%, but BaO abundances are relatively high, ~0.3 to 0.5 wt.% (Table 2).

Micas

Compositions of biotites (Table 3) among the various rocks from both quarries have a range in Mg#s, ~39 to 46 [Mg# = mol MgO/(MgO/FeO) * 100], but there is no systematic variation with the Mg#s of the granitoids (Figure 7a). Across this biotite-Mg# range, biotite TiO_2 is between ~2 and 3 wt.%, but also without correlation to whole-rock Mg#s (Figure 7a). Biotite in samples of both quarries have both F and Cl <0.02 wt.%, amounts just above detection. In terms of FeO, MgO, and Al_2O_3, the biotites are consistent with the 'orogenic', or calc-alkalic, categorization for granites proposed by Abdel-Rahman (1994).

White micas have Mg#s from ~26 to 42 and TiO_2 contents 0.16 to 1.1 wt.% (Table 3), neither of which correlate with whole-rock Mg#s (Figure 7b). There are minor distinctions in white mica compositions between the two quarry sites, where Lassiter granitoids have lower TiO_2 (Figure 7b), but detectable amounts of F and Cl. White micas in Wake Stone samples, on the other hand, do not have detectable F and Cl (Table 3).

Table 3. Representative biotite, white mica, and chlorite compositions in Rolesville batholith samples, Wake County, NC

	Biotite						White Mica						Chlorite			
	Lassiter			Wake Stone			Lassiter			Wake Stone			Lassiter		Wake Stone	
	fol	gran	dike	fol	gran	dike	fol	gran	dike	fol	gran	dike	gran	dike	gran	dike
	L6a	L3b	L1	WS3	WS2	WS5	RV3a	L3b	L1	WS3	WS2	WS5	L3b	L4a	WS2	WS5
SiO_2	36.2	37.4	37.2	36.9	35.7	36.2	47	46.5	47.2	46	45.7	46.3	26.8	25.8	26	25.3
TiO_2	2.64	2.7	2.8	2.7	2.4	2.3	0.41	0.4	0.16	0.95	0.77	0.44	0.12	0.12	0.05	0.46
Al_2O_3	16.1	16.9	17.1	17.7	17.1	16.8	29	29.7	29.8	30.4	30.7	30	21.1	20.5	19.3	19.8
FeO	21.8	22	22.2	22.1	23	23.2	4.7	6.2	6.3	5.5	5.5	5.9	29.5	33.9	30.8	29.5
MgO	9.6	9.6	9.1	8.7	9.1	8.8	1.9	1.9	1.8	1.3	1.5	1.7	15	12.5	13.5	11.9
CaO	0.04	0.04	0.06	0.03	0.05	0.05	0.13	0.02	0.01	0.03	0.04	0.04	0.05	0.06	0.06	0.31
Na_2O	0.09	0.77	0.55	0.06	0.64	0.44	1.1	1.8	0.88	0.19	2.1	1.5	0.05	0.26	0.09	
K_2O	10.3	9.6	9.8	9.7	9.5	9.4	10.3	10.5	10.8	10.9	10.5	10.6	0.02	0.05	0.06	1.3
F			0.01	0.01	0.02	0.02		0.01						0.01		
Cl	0.01	0.04	0.01	0.02				0.04	0.06				0.01	0.01		
Total	96.78	99.05	98.83	97.92	97.51	97.21	94.54	97.07	97.01	0 95.27	96.81	96.48	92.65	93.21	89.86	88.57
Mg#	44	44.8	42.2	41.2	41.4	40.3	41.9	35.3	33.8	29.7	32.7	33.9	47.6	39.7	43.9	41.8

Each column is the average composition acquired from 8-10 point analyses on one grain.
fol = foliated biotite-rich granitoid; gran = nonfoliated granite; dike = late-stage dike.
Mg# = mol Mg/(Mg+Fe) x 100

Chlorite

Chlorite, which appears to be an alteration product of biotite, has Mg#s that range from ~40 to 48, comparable to those for biotites (Table 3). The amounts of FeO and MgO observed among different chlorite grains, however, range substantially -- namely, FeO from 11 to 30 wt.%, and MgO from 6 to 15 wt.%, while biotite has rather constant 'mid-range' values of FeO 21 to 25 wt.% and MgO ~9 wt.% (Table 3). The F and Cl contents in chlorite are at detection limits.

Fe-Ti oxides and Apatite

Titaniferous magnetite grains examined in three samples have consistent compositions of

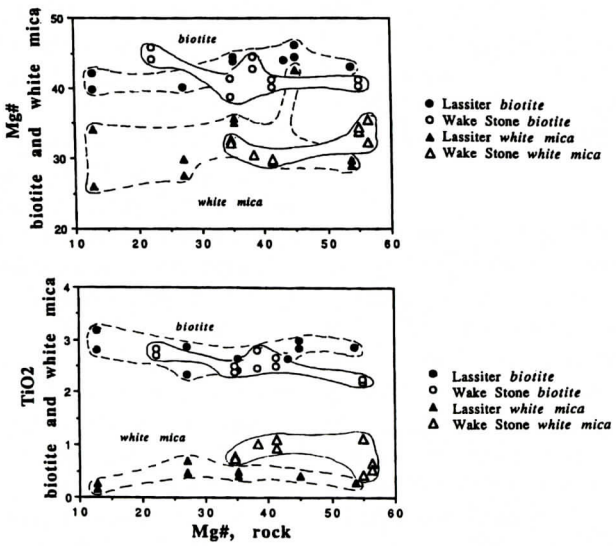

Figure 7. Average compositions of biotite and white mica (determined from compilations of 8-10 points per grain) expressed as Mg#s and TiO_2 wt.% compared to host rock Mg#s of Lassiter and Wake Stone quarry samples. Each data point represents an average values for one rock sample; full representative compositions are in Table 3. Mg# = mol MgO/(MgO+FeO) x 100.

Table 4. Representative Fe-Ti oxide and apatite compositions in Rolesville batholith samples, Wake County, NC

	Ti-magnetite		Ilmenite	
	L6a	WS3	L6a	L6b
TiO_2	16.2	15.8	50.0	49.7
Al_2O_3	0.19	0.18	0.32	0.16
FeO	81.6	82.2	50.2	51.3
sum	*97.99*	*98.18*	*100.52*	*101.16*
recalc.*				
FeO	46.7	46.4	44.9	44.7
Fe_2O_3	38.8	39.7	5.8	7.3
Total	101.89	102.08	101.02	101.86

	Apatite		
	RV3a	L3b	WS5
CaO	55.1	53.3	55.2
P_2O_5	41.5	42.2	42.5
F	3.6	3.7	3.8
Cl	0.02	0.02	0.02
Total	100.02	99.22	101.52

Each column is the average composition acquired from 6-8 point-analyses on one grain.

* = stoichiometric recalculation for Fe^{+2} and Fe^{+3}

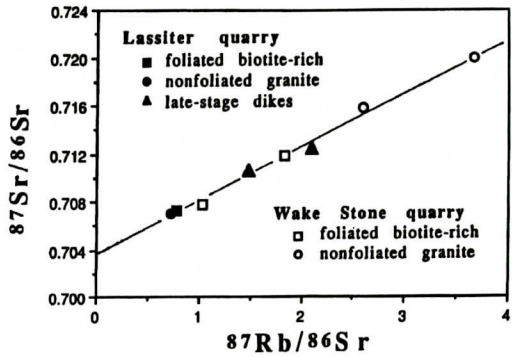

Figure 8. Isochron calculated for Rolesville batholith intitial Sr isotope ratios (see Table 5).

~16 wt.% TiO_2 and ~83 wt.% FeO (Table 4). Ilmenite grains in two of the same samples are comprised of about half FeO and half TiO_2 (Table 4).

Apatite grains in four samples have ~42.5 wt.% P_2O_5 (Table 4). Cl is essentially absent from the apatites, but they have ~3.7 wt.% F.

Isotopic Compositions

Strontium Isotopes

Strontium isotopic data for eight samples representing both quarries are in Table 5. All samples plot on an isochron (Figure 8) corresponding to ~316 ± 28 Ma. This agrees with the ~300 Ma ages reported for other Alleghanian plutons in the eastern portion of the Piedmont (e.g., Fullagar and Butler, 1979; Samson and others, 1995) and with other attempts to date the Rolesville batholith (Horton and Stern, 1994).

Calculated initial $^{87}Sr/^{86}Sr$ ratios for the eight samples range from 0.70305 to 0.70419 (Table 5), with an average of 0.70362 ± 0.00035. Our range for initial ratios is smaller and lower than that calculated for five samples of Rolesville batholith by Coler and others (1997), 0.70334-0.70733. Nonetheless, all of our ratios are low and characteristic of other syntectonic granitic plutons of the eastern Piedmont (e.g., Fullagar and Butler, 1979; Coler and others, 1997).

Table 5. Strontium isotopic compositions for selected Rolesville batholith granitoids from Lassiter (L) and Wake Stone (WS) quarries

	group	Rb ppm	Sr ppm	Rb/Sr	$^{87}Rb/^{86}Sr$	$^{87}Sr/^{86}Sr$ measured	±2σ error	$^{87}Sr/^{86}Sr$ initial
L2	*fol*	156	580	0.269	0.780	0.7072164	±0.00002	0.703720
L3b	*gran*	132	531	0.249	0.721	0.7069652	±0.00004	0.703729
L1	*dike*	189	263	0.719	2.084	0.7123900	±0.00037	0.703045
L4a	*dike*	236	463	0.510	1.478	0.7105400	±0.00036	0.703911
WS3	*fol*	199	316	0.630	1.826	0.7118515	±0.00010	0.703663
WS9	*fol*	145	410	0.354	1.026	0.7077800	±0.00076	0.703179
WS2	*gran*	201	225	0.893	2.591	0.7157946	±0.00080	0.704188
WS1c	*gran*	188	149	1.262	3.659	0.7199300	±0.00030	0.703528

Group: fol = foliated biotite-rich granitoid; gran = nonfoliated granite; dike = late-stage dike
Initial ratios calculated using 316 Ma

Table 6. Oxygen isotopic compositions for quartz and feldspar grains separated from selected Rolesville granitoids from Lassiter (L) and Wake Stone (WS) quarries

sample	*group*	quartz $\delta^{18}O$ per mil	feldspar $\delta^{18}O$ per mil	Δ qtz-feld
L2	*fol*	6.67	4.66	2.01
L3b	*gran*	6.58	4.66	1.92
L1	*dike*	6.52	4.69	1.83
L4a	*dike*	6.51		
WS3	*fol*	6.63	5.44	1.19
WS9	*fol*	6.46	5.65	0.81
WS1c	*gran*	6.50	5.31	1.19
WS2	*gran*	6.56	5.48	1.08
WS5	*dike*	7.44	5.41	2.03

group: fol = foliated biotite-rich granitoid; *gran* = granite; *dike* = late-stage dike

Oxygen Isotopes

We determined oxygen isotope ratios for coexisting quartz and feldspar (Table 6). Quartz separates from eight samples have nearly identical $\delta^{18}O$ values, within 6.46 to 6.67, but one additional sample has a higher $\delta^{18}O$ of 7.44. Isotopic ratios for feldspar in these samples are lower than for coexisting quartz, 4.66 to 5.65, and within this range, those from Lassiter quarry are the lowest (4.66-4.69). Accordingly, the $\Delta_{quartz\text{-}feldspar}$ values are smaller for Wake Stone granitoids than for Lassiter, ~1.07 vs. 1.92, with one exception for a Wake Stone sample with Δ–value 2.03 (Table 6).

DISCUSSION

Compositional Relationships Among the Various Rolesville Granitoids

The compositional trends for major- and trace-element abundances among the Lassiter and Wake Stone granitoid rocks and some similar oxygen and initial Sr isotopic compositions (within 2σ errors for Sr-isotope measurements) suggest that they are magmatically related. The covariations between most elements and SiO_2 (Figure 3) suggest that the granitoids are related by crystal fractionation or by progressive melting of a common source. To contrast, the absence of straight-line correlations among the elements plotted in SiO_2 variation diagrams and the absence of Ca-rich plagioclase cores (Figure 6) discount these rock compositions as being related by restite unmixing (e.g., Chappel and others, 1987).

The trends for decreasing CaO, P_2O_5, FeO, TiO_2, MgO, Zn, and Sc with increasing SiO_2 (Figure 3) are consistent with crystallization and segregation of plagioclase, apatite, biotite, and Fe-Ti oxides. Subtle decreasing of An contents over the change in rock type from foliated biotite-rich granitoid to late-stage dike (Figure 6a) -- or, from low-SiO_2, high-FeO rocks to high-SiO_2, low-FeO rocks -- also corresponds to a history of fractional crystallization of plagioclase among these samples. On the other hand, fractionation of plagioclase from silicic magmas is impeded by little density contrast and the relatively high viscosity of silicic melts; on that basis, fractionation processes may have been insignificant.

Trace elements Rb, Ba, and Sr are the only ones that reliably test granitoids for fractionation histories because most other trace elements that are characteristically modeled for mafic rocks, such as REE, are strongly influenced in granitic magmas by accessory mineral crystallization (e.g., Harris and Inger, 1992). Plotted against one another (Figure 9a), Rb, Ba, and Sr correlate well among all samples except three Rb- and K-enriched dikes. To evaluate the roles of Rb-, Ba-, and Sr-bearing phases on this correlation, we plotted vectors for paths of liquid compositions yielded by plagioclase, K-feldspar, and biotite crystallization. These vector directions are only approximations, however, because partitioning coefficients for Rb, Ba, and Sr in these phases are not well constrained (e.g., Inger and Harris, 1992; McDermott and others, 1996). Nonetheless, the correlated samples in Figure 9a collectively suggest trends owed to varying proportions of plagioclase, K-feldspar, and biotite crystallizing from 'mafic' representatives of Rolesville batholith.

However, SiO_2 (and other major elements) correlates poorly with Rb, Sr, and Ba (Figure 3).

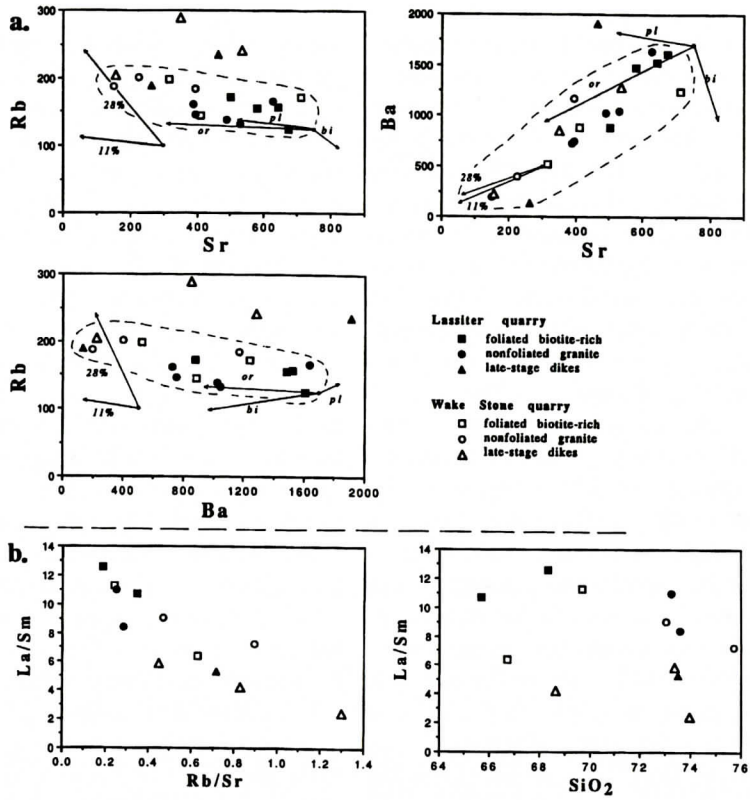

Figure 9. (a) Rb, Ba, and Sr variation diagrams to illustrate the trends formed by the majority of Rolesville samples (within dashed-line field); three late-stage dikes plot outside the field in the Rb diagrams. The trends are compared with liquid fractionation trends established by vectors for 10% crystallization of plagioclase, orthoclase, and biotite. Also compared are vapor-absent dehydration melting vectors for source material where muscovite only has melted out (11%) and where muscovite and biotite have melted out (28%). Partitioning coefficients are from Nash and Crecraft (1985). (b) La/Sm variation diagrams to demonstrate that REE abundances in the granitoids are more closely allied to Rb and Sr (and Ba) than SiO_2, to suggest that they were controlled more by partial melting of the source than by fractional crystallization.

In particular, these trace elements are not "keyed" to major-element abundances (Figure 3) in a way such that the most "primitive" granitoids (lowest SiO_2, highest FeO and CaO) consistently have highest Sr and Ba and lowest Rb (Figure 9a). Also, K-feldspar unlikely participated in crystal segregation processes because it is not a liquidus phase; it largely occurs interstitially in these granitoids. Moreover, K_2O increases with increasing SiO_2 contents (Figure 3). Any fractional crystallization relationships among Rolesville samples, then, are not supported well by Rb, Sr, and Ba abundances, and the suite as a whole, therefore, does not simply represent a line of descent between compositionally most primitive and most evolved samples.

Alternatively, there were several "parental" magma batches that had varying Rb, Sr, and Ba contents, depending on the characteristics and partial melting percentages of the sources that provided parental magmas. To expand this concept, the trend of increasing Rb with decreasing Sr and Ba (Figure 9a) requires evaluation. Muscovite-bearing source material can account for this compositional variation because vapor-absent muscovite dehydration melting yields Rb and complementary K-feldspar restite that, according to partitioning coefficients, would retain Sr and Ba (e.g., Harris and

Inger, 1992; Inger and Harris, 1993). Compositional vectors for melts produced from muscovite-bearing source material are shown in Figure 9a for 11% melting, a reasonable approximation for the exhaustion of even large amounts of muscovite (e.g., 20 modal percent) during melting of a crustal source under vapor-absent conditions (e.g., Harris and Inger, 1992). The observed Rb, Sr, and Ba trends (Figure 9a), then, we believe to be related to restites containing different proportions of feldspar after the incongruent melting of muscovite. The negative Eu anomalies (Figure 4) in the Rb-Ba-Sr correlated samples (Figure 9a) probably reflect the restitic feldspar after partial melting.

The three Rb- and K-enriched late-stage dikes (Figure 9a) may represent parental magma produced by dehydration melting of both muscovite and biotite; namely, biotite contributes notably to Rb concentrations in melts without significantly affecting Sr and Ba contents. In this case, however, fluids may have been present to deplete the source of feldspars (e.g., Harris and Inger, 1992) because these three Rb- and K-enriched late-stage dikes have moderate to high Sr and Ba contents (Figure 9a) and positive Eu anomalies (Figure 4).

The "rotation" of REE patterns from high La/Sm to low La/Sm ratios across the change in rock types from "mafic" to most evolved (Figures 4, 9b) conforms reasonably well with the Rb, Sr, and Ba correlations (Figure 9b). This suggests that either equilibrium melting of major silicate phases controlled the REE abundances in the granitic magmas or incorporation of REE-bearing phases in the source material added LREE proportionally with varying percentages of melting. In either case, partitioning coefficients for REE-bearing accessories are not well constrained nor is the knowledge of whether source accessory phases occurring as inclusions would actually equilibrate with anatectic melts (e.g., Harris and Inger, 1992). The alternative interpretation for decreasing La/Sm ratios and REE abundances is that fractional crystallization of REE-bearing accessory minerals, largely monazite and allanite, played a role. However, because there is poor correlation between La/Sm ratios and SiO_2 (Figure 9b), segregation of accessory minerals was probably not a significant process in establishing the REE abundances of Rolesville batholith samples.

In summary, based on correlations among major and trace-elements (mainly Rb, Sr, and Ba), the Rolesville batholith compositional variations are due largely to varying percentages of melting of a common source nearly uniform in composition -- probably with small variations in Rb, Ba, and Sr abundances and $^{87}Sr/^{86}Sr$ -- to yield multiple batches of granitoid magma. Multiple magmas are consistent with the field interpretations of Speer (1994), who envisions the Rolesville batholith as a composite of magma pulses that created an overall sheeted pluton. The general compositional trends can also be reconciled with fractionation of plagioclase and biotite, but the highly silicic compositions (i.e., relatively low density; high viscosity) make crystal segregation unlikely to have been a significant process. Similarly, while fractionation of REE-bearing accessories can account for the REE abundances in the granitoids, the Rb/Sr vs. La/Sm relationships favor partial melting percentages as an explanation for relative REE abundances among the Rolesville samples.

Source Material Relative to the Two Sample Sites

Because the whole-rock major- and trace-element and isotopic compositions of Lassiter and Wake Stone quarry samples are similar and in many cases overlap (Tables 1, 5, 6; Figures 3, 9a), their protolith sources were likely to have been the same or very similar. We observe some small compositional differences between the two sample sites, such as higher $\delta^{18}O$ in Wake Stone feldspar, higher TiO_2 and no F and Cl in Wake Stone white micas, slightly more Y in some Wake Stone samples, and slightly higher LREE in Lassiter foliated samples (Figures 3, 4, 7; Table 6). Additionally, one Wake Stone late-stage dike has anomalously high $\delta^{18}O$ for quartz (e.g., 7.4 vs. ~6.5 for all other quartz).

The $\delta^{18}O$ distinctions may reflect some source-area heterogenieties, but we cannot discount that the higher values in Wake Stone feld-

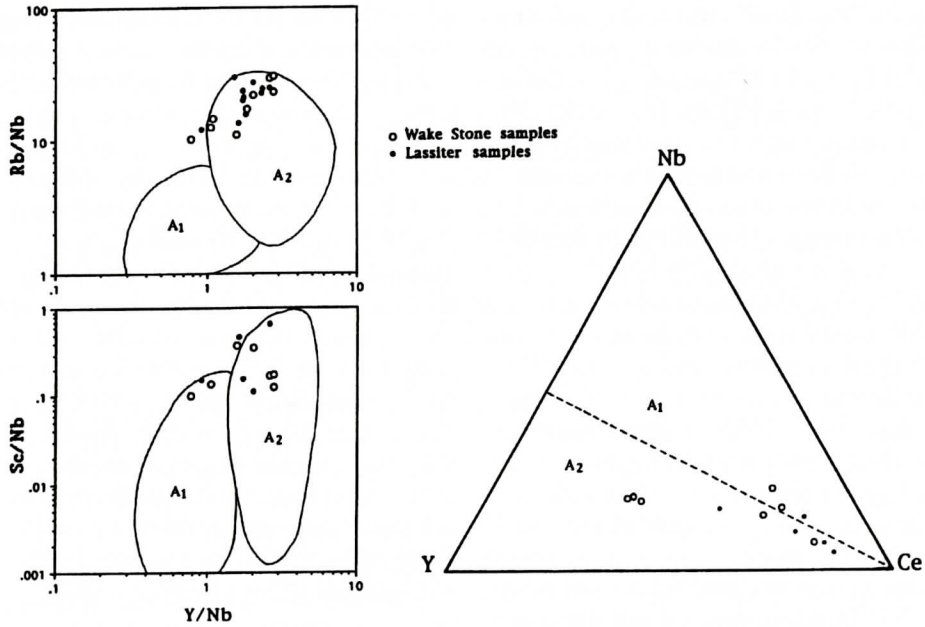

Figure 10. Evaluation of Rolesville samples in terms of A-type granitoids, according to Eby (1992). Most samples are subtype A_2, implying collisional or island arc histories.

spars (and one example of quartz) are possibly owed to alteration and/or weathering. Differences among white mica compositions are likely due to their secondary origin, and the larger modal amounts in Wake Stone samples (Table 1) may reflect relatively prolific secondary processes to form white mica. The higher LREE abundances in Lassiter samples largely reflect the more primitive whole-rock compositions represented. The slightly higher Y contents observed for Wake Stone granitoids (Figure 3) can be explained by the more common occurrence of monazite in samples analyzed from that quarry. In summary, then, source materials for Rolesville batholith as represented in both Lassiter and Wake Stone quarries had essentially identical compositions.

Source Material With Respect to Batholith Origin

The low $^{87}Sr/^{86}Sr$ initial ratios of the quarry samples, averaging 0.70362 ± 0.00035, are consistent with non-sedimentary source material. The Sr isotopic compositions in conjunction with the peraluminous characterization of the bulk of the Rolesville samples (Figure 2b) affords them A-type (anorogenic) categorization, even though the batholith is syntectonic with respect to eastern Carolina Piedmont deformation. Nonetheless, A-type categorization has a wide interpretation with regard to tectonic settings and can include source material with continental crust and island-arc basalt characteristics and with various tectonic histories (e.g., Eby, 1992). In particular, trace-element discriminations, such as those based on Nb, Y, Rb, and Ce abundances (e.g., Pearce and others, 1984), place the Rolesville batholith into the A_2 subcategory (Eby, 1992) of granitoids with sources in crust that had experienced subduction zone or continent-continent collisional histories (Figure 10). This identification of source material is further borne out by the negative Nb anomalies in Rolesville granitoids (Figure 5), a feature characteristic of melts produced in subduction zone environments. In accordance, the $\delta^{18}O$ values are within the range known for oceanic and continental-margin subduction zone magmatism (e.g., Harmon and Hoefs, 1995).

According to the isotopic studies of Sam-

son and others (1995) and Coler and others (1997), the particular subduction zone environment for Piedmont Alleghanian granitoid plutons was an oceanic volcanic province(s) that is now represented as the metamorphic crust surrounding the Rolesville batholith -- namely, the regions identified as the Carolina terrane and the Raleigh metamorphic and Eastern slate belts (Figure 1). As required in our model for vapor-absent melting of muscovite-bearing source material, crustal rocks comprising these provinces include muscovite-bearing metasedimentary, metavolcanic, and hydrothermally altered rocks (e.g., Feiss, 1982; Stoddard and others, 1991). On the other hand, reconciling the relatively high Sr abundances of the Rolesville samples (~200-700 ppm; Figure 9) with Carolina terrane is problematic. The few samples of Carolina terrane analyzed (Coler and others, 1997; E.F. Stoddard, personal communication, 1997) are too low (<300 ppm) to represent source material for the majority of Rolesville batholith granitoid samples. The source must have been notably richer in Sr, particularly in light of the negative Eu anomalies in the most mafic granitoids (Figure 4) which suggest that substantial feldspar remained as a restite phase.

In summary, the Rolesville batholith meets, on the whole, the criterion for A_2 granitoids -- which, in the evaluation of Eby (1992), is appropriately a subtype of I-granitoids (i.e., non-sedimentary parentage). Isotopic ratios and trace-element abundances (largely Nb, Y, Rb; Nb anomaly) and the Alleghanian syn-deformational emplacement history of the Rolesville batholith identify it as representing melts from ~600 Ma metamorphic crust that harbors compositional signatures of subduction and/or oceanic island-arc history. However, no whole-rock trace-element data are available to document that partial melting of this largely metavolcanic complex actually yielded Rolesville parental magmas.

ACKNOWLEDGMENTS

This study was supported by funds from various sources: to JK from the Department of Marine, Earth, and Atmospheric Sciences, North Carolina State University, for Sr-isotope ratio acquisition from the University of North Carolina, Chapel Hill; to JK from the North Carolina Department of Environmental, Health, and Natural Resources for oxygen isotope data acquisition from the University of Georgia; to RVF from the National Science Foundation, grant EAR8903704, for microprobe and xrf operations at NCSU; and indirectly to RVF from the U.S. Department of Energy via its reactor-sharing grant to Oregon State University radiation center for neutron activation services for trace element determinations. We are grateful to Drs. S.A. Goldberg and D.B. Wenner for enabling us to acquire isotope data in their laboratories, to personnel of Oregon State University radiation center for providing neutron activation services, and to E.F. Stoddard, Bill Meurer, and Jonathan Miller for critical reviews.

REFERENCES

Abdel-Rahman, A.F.M., 1994, Nature of biotite from alkaline, calc-alkaline, and peraluminous magmas: Journal of Petrology, v. 35, p. 525-542.

Becker, S.W., and Farrar, S.S., 1977, The Rolesville batholith, in Costain J.A., Glover, L., and Sinha, K.A., editors, Evaluation and Targeting of Geothermal Resources in the Southeastern United States, Progress Report to the U.S. Department of Energy, November 1, 1976-March 31, 1977: Virginia Polytechnical Institute, Department of Geological Sciences, Blacksburg, Virginia.

Bowman, J.T., 1969, Compositional variation in granite of eastern Wake and northwestern Johnston counties, NC: MS thesis, North Carolina State University, Raleigh, NC, 33 p.

Chappel, B.W., White, A.J.R., and Wyborn, D. 1987, The importance of residual source material (restite) in granite petrogenesis: Journal of Petrology, v. 28, p. 1111-1138.

Coler, D.G., Samson, S.D., and Speer, J.A., 1997, Nd and Sr isotopic constraints on the source of Alleghanian granites in the Raleigh metamorphic belt and Eastern slate belt, southern Appalachians, USA: Chemical Geology, v. 134, p. 257-270.

Eby, G.N., 1992, Chemical subdivision of the A-type granitoids: petrogenetic and tectonic implications: Geology, v. 20, p. 641-644.

Farrar, S.S., 1985, Tectonic evolution of the easternmost Piedmont, North Carolina: Geological Society of America Bulletin, v. 36, p. 362-380.

Feiss, P.G., 1982, Geochemistry and tectonic setting of the volcanics of the Carolina slate belt: Economic Geology, v. 77, p. 273-293.

Fullagar, P.D., and Butler, J.R., 1979, 325 to 265 m.y.-old granitic plutons in the Piedmont of the southeastern Appalachians: American Journal of Science, v. 279, p. 161-185.

Gromet, L.P., and Silver, L.T., 1982, Rare-earth element distribution among minerals in a granodiorite and their petrogenetic implications: Geochimica et Cosmochimca Acta, v. 47, p. 925-939.

Harmon, R.S., and Hoefs, J., 1996, Oxygen isotope hetrogeneity of the mantle deduced from global ^{18}O systematics of ballasts from different geotectonic settings: Contributions to Mineralogy and Petrology, v. 120, p. 95-114.

Harris, N.B.W., and Inger, S., 1992, Trace element modelling of pelite-derived granites: Contributions to Mineralogy and Petrology, v. 110, p. 46-56.

Horton, J.W., and Stern, T.W., 1994, Tectonic significance of preliminary uranium-lead ages from the eastern Piedmont of North Carolina: Geological Society of America Abstracts with Programs, v. 26, p. 21.

Inger, S, and Harris, N., 1993, Geochemical constraints on leucogranite magmatism in the Langtang Valley, Nepal Himalaya: Journal of Petrology, v. 34, P. 345-368.

McDermott, F., Harris, N.B.W., and Hawkesworth, C.J., 1996, Geochemical constraints on crustal anatexis: a case study from the Pan-African Damara granitoids of Namibia: Contributions to Mineralogy and Petrology, v. 123, p. 406-423.

Miller, C.F., Stoddard, E.F., Bradfish, L.J., Dollase, W.A., 1981, Composition of plutonic muscovite: genetic implications: Canadian Mineralogist, v. 9, p. 25-34.

Nash, W.P., and Crecaft, H.R., 1985, Partition coefficients for trace elements in silicic magmas: Geochimica et Cosmochimica Acta, v. 49, p. 2309-2322.

Parker, J.M., 1968, Structure of easternmost North Carolina Piedmont: Southeastern Geology, v. 9, p. 117-131.

Parker, J.M., 1979, Geology and mineral resources of Wake County, North Carolina: Division of Mineral Resources Bulletin 86, 112 p.

Pearce, J.A., Harris, N.B.W., and Tindle, A.G., 1984, Trace element discrimination diagrams for the tectonic interpretation of granitic rocks: Journal of Petrology, v. 25, p. 956-983.

Russell, G.S., Russell, C. W., and Farrar, S.S., 1985, Alleghanian deformation and metamorphism in the eastern North Carolina Piedmont: Geological Society of America Bulletin, v. 96, p. 381-387.

Samson, S.D., Coler, D.G., and Speer, J.A., 1995, Geochemistry and Nd-Sr-Pb isotopic compositions of Alleghanian granites in the southern Appalachians: origin, tectonic setting, and source characteristics: Earth and Planetary Science Letters, v. 134, p. 359-376.

Speer, J.A., 1994, Nature of the Rolesville batholith, North Carolina: *in* Stoddard, E.F., and Blake, D.E., editors, Geology and Field Trip Guide, Western Flank of the Raleigh Metamorphic Belt, North Carolina, Carolina Geological Society Guidebook, p. 57-62.

Speer, J.A., McSween, H.Y., and Gates, A.E., 1994, Generation, segregation, ascent, and emplacement of Alleghanian plutons in the southern Appalachians: Journal of Geology, v. 102, p. 249-267.

Stoddard, E.F., Farrar, S.S., Horton, J.W., Butler, J.R., and Druhan, R.M., 1991, The eastern Piedmont in North Carolina: *in* Horton, J.W., and Zullo, V.A., editors, Geology of the Carolinas, Carolina Geological Society Fiftieth Anniversary Volume, University of Tennessee Press, Knoxville, TN, p. 79-92.

Sun, S.-S., and McDonough, W.F., 1989, Chemical and isotopic systematics of oceanic basalts: implications for mantle composition and processes: *in* Saunders, A.D., and Norry, M.J., editors, Magmatism in the Ocean Basins. Geological Society of London, Special Publication, 42, 313-345.

SOUTHEASTERN GEOLOGY
V. 37, No. 2, October 1997, p. 109-114

IMPACT OF RECREATIONAL SUCTION DREDGING ON MOBILIZATION OF ANTHROPOGENIC MERCURY IN GOLD PLACERS

J. WILLIAM MILLER

Environmental Studies Program
University of North Carolina at Asheville
Asheville, NC 28804

JOHN E. CALLAHAN

Department of Geology
Appalachian State University
Boone, NC 28608

DOUGLAS J. HATTERSLEY

(Retired)
U.S. Department of Agriculture
Forest Service
1720 Peachtree Road, NW
Atlanta, GA 30367

JAMES R. CRAIG

Department of Geological Sciences
Virginia Polytechnic Institute and State University
Blacksburg, VA 24061

ABSTRACT

Dredging for gold prospecting and mining from placers has been prohibited since 1994 in national forests of North Carolina because of adverse mechanical and siltation effects on aquatic life.

Mercury has escaped from amalgamation activities during gold panning, mining, and processing and therefore is found in many gold placers. The source of most mercury in aquatic ecosystems enters by dissolution or sorption from the uppermost part of the stream bed or water column. Water and sediment samples were analyzed at two sites in Talladega Creek near Waldo, Alabama to examine the potential effect of suction dredging on mercury present in stream sediments.

Decanted water from the dredged sediment plume and from the site following dredging contained 0.3 - 0.6 ppb mercury which represented a slight decrease compared to water sampled before dredging. Panned concentrates of stream sediments contained 95-7585 mercury μg/kg before dredging, which indicates that mercury was present in the system. Most gold grains recovered from the stream bed varied from pure gold to 92.7% Au and 7.3% Ag by weight, and none contained mercury. Suspended sediments from the plume contained 255 - 2945 μg/kg mercury, compared to 180 - 530 μg/kg mercury found in mid-stream sediment taken from the top of the stream bed before dredging. The mercury-rich suspended sediments are spread thinly over the sediment bed downstream, making mercury more available to the stream ecosystem, in comparison to mercury residing in deeper stream sediments.

INTRODUCTION

The use of suction dredges for recreational gold prospecting in the National Forests in North Carolina has been prohibited for the past few years because such activities have greatly disturbed the aquatic environment and dispersed large quantities of fine silt that had adverse impacts on aquatic organisms. In 1994, the U.S. Forest Service decided to revisit the issue after receiving requests from citizens and hobby groups who wanted to collect gold using suction dredges. This study was initiated to determine the effect of suction dredging on mercury that might be present in the sediment-stream systems.

Mercury is found in association with many gold placers and is nearly always the result of materials lost into the environment from amalgamation activities that were used extensively in the extraction of gold in the middle 1800's through the early 1900's in the U.S. and more recently in other countries (Tümpling and others, 1995; Aula, 1994; Pfeiffer and others, 1993; Nriagu and others, 1992; and Pfeiffer and others, 1989). In the U.S. today, use of mercury continues by some recreational panners to enhance recovery of fine gold grains even though its use has been banned or discouraged. This study was initiated to determine whether or not suction dredging would dislodge mercury from the sediment and release it into the water or sediment plume and thus result in a greater dispersal than already exists.

Because of its high density and low solubility, mercury introduced by mining and processing remains in stream sediments of gold placers, especially in the heavy mineral fraction (Callahan and others, 1994). Once introduced into a stream system, the free metallic mercury may enter the water as dissolved elemental mercury (Hg^0), mercury chloride ($HgCl_n^{n-2}$), mercury hydroxide ($Hg(OH)_2$), methyl mercury (CH_3Hg^+), or other forms, depending on physicochemical (pH, Eh, dissolved ions) and biological conditions (Allard and Arsenie, 1991; Meili, 1991; Meili and others, 1991; Wang and others, 1991; Craig, 1986; Moore and Ramamoorthy, 1984; Benes and Havlík, 1979; Lockwood and Chen, 1973; and Hem, 1970). The rate of sorption is relatively fast in comparison to desorption (Moore and Ramamoorthy, 1984). Desorption is negligible for inorganic mercury in sands, clays, and organics, and low to negligible for $HgCl_2$ and methyl mercuric chloride in sands (1:10), clays (1:100), and organics (Reimers and Krenkel, 1974).

Mercury has resided undisturbed in the sediments of many streams for decades. The studies of Craig (1986) and Rudd and others (1980) have shown that most mercury enters the aquatic ecosystem from the water column and top of the stream bed rather than from subsurface sediments. Furthermore, the effective depth for sorption is less than 1 mm for sand, regardless of whether conditions were aerobic or anaerobic (Kudo and Hart, 1974). Some studies of sediments in highly polluted lakes have detected decreases in mercury levels over several years following cessation of mercury pollution (Lodenius, 1991). However, other studies have found lake sediments "more or less permanent" sinks for mercury (Johansson and others, 1991), where its release is extremely slow. These studies indicated that mercury should stay in deeper sediments and out of the overlying ecosystem for many decades or more if metallic mercury-rich sediments remain undisturbed. Most mercury lost into sediment from gold mining operations and panning undoubtedly occurs as elemental mercury. Although the mercury was lost in droplets of variable size, most of those observed are less than 0.5 mm in diameter, because small droplets were more easily lost during mining and panning. This small droplet size facilitates reaction with the surrounding environment due to large surface areas in comparison to larger droplets when sediments are disturbed. If bottom sediments with this mercury are excavated, as occurs during dredging, they will spread downstream and settle in thin layers on top of the stream bed. Most mercury in this redeposited sediment should then be available for dissolution, methylation, and bioaccumulation. To evaluate the effects of suction dredging on sediments polluted with mercury, we sampled and analyzed water and sediments before, during, and after suction dredging at two

sites near Talladega, Alabama, where gold placer mining had occurred in and near the National Forest (Figure 1).

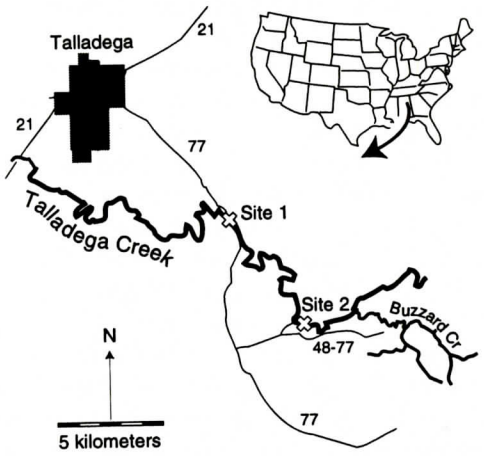

Figure 1. Site locations along Talladega Creek, Alabama. Separate numbers indicate state highways.

METHODS

Sampling

At the time of sampling during mid-summer, Talladega Creek was approximately 14 meters across, with an average depth of 18 cm. The average stream velocity was 0.4 m/sec, for an estimated discharge of 1 m^3/second. The pH of the water was 6.6.

Stream water, mid-stream sediment, which was dominantly clay and silt with some fine sand, and heavy mineral samples were obtained prior to suction dredging at each of two sites. These provided base-line values against which other samples could be compared (Table 1). Water was sampled directly in the stream, without filtering, to include the finest suspended sediments that likely are present during normal, undisturbed conditions. All water samples were collected in polyethylene bottles and preserved with nitric acid to pH < 2. Fine stream sediment was taken in mid-stream from the top 4 cm of the sediment bed, and heavy mineral samples were extracted from sediments in the stream bed, from the top to a depth of ~0.5 meter. Three 36-centimeter (diameter) pans of these sediments were panned in the stream, combined, and subsequently concentrated further in the laboratory.

A suction dredge with a 3-inch orifice, similar to those used by hobbyists, was run for approximately 15 minutes at three different spots in gravel bars at each site. While the dredge was in operation, suspended sediment was collected in three five-gallon polyethylene buckets from the center of the downstream plume, 1-2 meters from the dredge. The brownish-milky-white

Table 1. Mercury concentrations in Talladega stream water and sediment plume.

		Sample	Water (ppb)	Suspended Sediment (µg/kg)	Heavy Mineral Concentrates (µg/kg)	Mid-stream Sediment (µg/kg)
Site 1		TW1-be	.30			
	plume	TW1-a	.27	*	525.	180.
		TW1-b	<.25	380.	95.	
		TW1-c	<.25	255.	245.	
		TW1-af	.34			
Site 2		TW2-be	.55			
	plume	TW2-a	.32	2945.	580.	530.
		TW2-b	.44	605.	6990.	
		TW2-c	.26	1330.	7280.	
		TW2-af	.60			

*Not enough sample for analysis. Suffixes for water samples indicate the following: be = stream water before dredging; a, b, & c = decanted water collected in 5-gallon buckets from suspended sediment plume during dredging; af = stream water collected after dredging. Heavy mineral concentrates and mid-stream sediment sampled before dredging. Precision is ±10% of amounts with a detection limit of 0.1 ppb or 0.1 µg/kg.

plume was easily distinguished from the otherwise clear stream water. The collected suspended sediments were allowed to settle for approximately 20 minutes, and the water sampled and then poured off. The suspended sediments left at the bottom of the three buckets were collected with filters and combined into one composite sample. With this method, the finest suspended sediments would remain part of the decanted water, but the greatest proportion will settle and be captured by filters.

Laboratory

Water was analyzed for mercury at a commercial laboratory using cold-vapor (flameless) atomic absorption spectrometry (AA) with a lower detection limit of 0.1 ppb. The analyses were checked with control samples and corroborated with atomic emission spectrometric analysis (ICP-AES) of duplicate samples. Pan concentrates were sieved to minus 18-mesh (<1.0 mm), and the strongly magnetic fraction was removed with a Sepor automagnet. The remaining nonmagnetic concentrates were further concentrated with heavy liquid (sodium polytungstate), and gold grains were removed by hand-picking under a stereomicroscope. The concentrates and mid-stream sediments were ground to minus 80-mesh (< 0.177 mm) and sent to a commercial contractor for digestion and analysis. Each 0.5 gram sample was digested at 95° C for one hour with 3 ml of 3-1-2 HCl-HNO_3-H_2O which was then diluted to 10 ml with water before mercury analysis by cold-vapor AA.

RESULTS AND DISCUSSION

The results of mercury analyses of samples before, during, and after operation of the dredge are presented in Table 1. The mercury content of the sediments and water probably are due to the close proximity of site 2, one mile downstream from the confluence of Buzzard Creek with Talladega Creek. Buzzard Creek drains the Idaho gold district that was active in the 1890's and that included the Franklin mine, the largest open pit gold mine to use amalgamation for gold recovery in Alabama (Zwaschka and Cook, 1989).

Iron contents of suspended sediments averaged 3.5% (by wt.) for site 1 and 2.8% for site 2, and of panned concentrates 3.2% for site 1 and 4.4% for site 2. No correlation between Hg and Fe was apparent, which indicates mercury probably was not bound to the fine sediment fraction and implies that elemental mercury could have been present in sediments.

Apparently, no significant increase occurred in the mercury content in the water of the stream during or shortly after suction dredging created disturbance of the stream sediment. In contrast, a study of mercury contamination in the Arbacoochee gold district in east-central Alabama (Rippstein, 1995) discovered mercury concentrations in stream water 130 ppb during recreational dredging and 160 ppb shortly after cessation of dredging. Sediments in this region were much more highly contaminated, with as much as 90,000 µg/kg Hg in comparison to the maximum 530 µg/kg Hg sampled in Talladega Creek.

Suspended sediments from the dredging plume in this study contained much more mercury than water in the plume. Similar observations have been made near Monte Amiata, Italy, where suspended particulate matter contained "a significant load" of mercury, but aqueous transport was of "no importance" (Ferrara and others, 1991). Suspended sediments from the dredge plume in Talladega Creek also contained elevated amounts of mercury in comparison to the stream sediment. These suspended sediments represent samples of fine, mercury-bearing sediments that are widely dispersed as a thin veneer over the stream bed during suction dredging. Once these have been dispersed downstream and at the top of the stream bed, mercury has been deposited with them over a larger area downstream and into the active upper part of the stream bed where it may be released into the water through methylation or some other dissolution process (Craig, 1986; Kudo and Hart, 1974). Accordingly, suction dredging will likely accelerate the dissolution of mercury pollution introduced into streams during placer mining and result in assimilation

Table 2. Maximum amounts of mercury for Talladega compared to other sites. *

Location	In water (ppb)	In sediment (µg/kg)	In pan concentrate (µg/kg)	On gold** grains wt. %
Talladega, AL	0.55	530	7,585	<0.2
South Mtns., NC	<0.2	460	860	13.38
Robbins, NC	<0.2	700	784,000	45.36
High Point, NC	<0.2	7400	26,000	44.75

*North Carolina data from Callahan and others (1994)
**Spot analyses on mercury-richest parts of gold grains

of mercury into stream water and the surrounding stream habitat, much in the way that massive floods bring mercury to the sediment bed surface by scouring. Likewise, subsequent flooding could bury mercury-laden sediment previously excavated by dredging, if mercury has not migrated out of the sediment column.

Mercury is concentrated in the pan concentrates in comparison to the mid-stream sediment in all but one of six samples (Table 1). This has been demonstrated in previous work (Callahan and others, 1994) and should be expected because of the high specific gravity of mercury (13.5).

Gold Grains

Of more than 70 gold grains recovered from pan concentrates 38 were analyzed by energy dispersive analysis using a Camscan II scanning electron microscope; five were mounted and sectioned to reveal interior compositions, and the remainder were mounted to allow analysis of their exteriors. Of the polished grains, two contained small amounts of silver (5.8 and 7.3 weight percent silver), three were pure gold, and none contained detectable mercury (<0.2%). These analyses were mirrored by scans of the unpolished grains. Previous studies (Callahan and others, 1994) have shown irregular mercury rims on gold and electrum grains in heavy mineral concentrates from three locations in North Carolina (Table 2). At those locations, no mercury was detected in stream water, but some of the amounts of mercury in the sediments and heavy mineral concentrates were elevated. Beads of mercury (< 0.5 mm) were observed in heavy mineral concentrates from some sites in North Carolina, but none in six samples from Talladega Creek. Thus, it is likely that the gold grains with mercury coatings were in physical contact with small dispersed beads of mercury during mechanical agitation of the sediment during high rates of stream flow or dredging. Laboratory tests by the authors have shown that there is a rapid reaction of gold grains with mercury and that it creates small significant areas of gold amalgam that will then persist.

SUMMARY

Mercury in stream sediments is freed during dredging in old gold mining areas. The mercury-rich sediments in the dredge plume settle downstream in thin layers on top of the sediment bed which contains less or no mercury. Consequently, the mercury that has resided for decades or more in deeper stream sediments, where it has little entrance into the water column, is released into surface sediments where it may be readily dissolved or methylated and released for reaction with biota.

ACKNOWLEDGMENTS

We thank Ms. Jo Ellis of the U.S. Forest Service for bringing the problem to our attention, for information and helpful discussion. Thanks are due to Ms. Lora L. Combs for heavy mineral separations and gold grain extractions, and Ms. Barbara M. Miller for corroboration of mercury analyses. Also, we appreciate the reviews of J.C. Varekamp (Arizona State University) and L.S. Dean (Geological Survey of Alabama) that significantly improved the manuscript.

REFERENCES CITED

Allard, B., and Arsenie, I., 1991, Abiotic reduction of mercury by humic substances in aquatic system - an important process for the mercury cycle: Water, Air, and Soil Pollution, v. 56, p. 457-464.

Aula, I., Braunschweiler, H., Leino, T., Malin, I., Porvari, P., Hatanaka, T., Lodenius, M., and Juras, A., 1994, Levels of mercury in the Tucuru' reservoir and its surrounding area in Par‡, Brazil, *in* Watras, C.J. and Huckabee, J.W. (eds.), Mercury Pollution - Integration and Synthesis: Lewis Publishers, Boca Raton, p. 21-40.

Benes, P., and Havlík, B., 1979, Speciation of mercury in natural waters, *in* Nriagu, (ed.), The Biogeochemistry of Mercury in the Environment, p. 177-202.

Callahan, J.E., Miller, J.W., and Craig, J.R., 1994, Mercury pollution as a result of gold extraction in North Carolina, U.S.A.: Applied Geochemistry, v. 9, p. 235-241.

Craig, P.J., 1986, Organomercury compounds in the environment: *in* Craig, P.J. (ed.), Organometallic Compounds in the Environment, p. 65-110.

Ferrara, R., Maserti, B.E., and Breder, R., 1991, Mercury in abiotic and biotic compartments of an area affected by a geochemical anomaly (Mt. Amiata, Italy): Water, Air, and Soil Pollution, v. 56, p. 219-233.

Hem, J.D., 1970, Chemical behavior of mercury in aqueous media, *in* Mercury in the Environment: USGS Professional Paper 713, p. 19-24.

Johansson, K., Aastrup, M., Andersson, A., Bringmark, L., and Iverfeldt, A., 1991, Mercury in Swedish forest soils and waters - assessment of critical load: Water, Air, and Soil Pollution, v. 56, p. 267-281.

Kudo, A., and Hart, J.S., 1974, Uptake of inorganic mercury by bed sediments: Journal of Environmental Quality, v. 3, p. 273-278.

Lockwood, R.A., and Chen, K.Y., 1973, Adsorption of Hg (II) by hydrous manganese oxides: Environmental Science and Technology, v. 7, p. 1028-1034.

Lodenius, M., 1991, Mercury concentrations in an aquatic ecosystem during twenty years following abatement [of] the pollution source: Water, Air, and Soil Pollution, v. 56, p. 323-332.

Meili, M., 1991, The coupling of mercury and organic matter in the biogeochemical cycle - towards a mechanistic model for the boreal forest zone: Water, Air, and Soil Pollution, v. 56, p. 333-347.

Meili, M., Iverfeldt, Å., Håkanson, L., 1991, Mercury in the surface water of a Swedish forest lakes - concentrations, speciation and controlling factors: Water, Air, and Soil Pollution, v. 56, p. 439-453.

Moore, J.W., and Ramamoorthy, S., 1984, Heavy Metals in Natural Waters, Applied Monitoring and Impact Assessment: Springer-Verlag, New York Inc., New York, 268 p.

Nriagu, J.O., Pfeiffer, W.C., Malm, O., Souza, M., and Mierle, G., 1992, Mercury pollution in Brazil: Nature, v. 356, p. 369.

Pfeiffer, W.C., Lacerda, L.D., Salomons, W., and Malm, O., 1993, Environmental fate of mercury from gold mining in the Brazilian Amazon: Environmental Reviews, v. 1, p. 26-37.

Pfeiffer, W.C., De Lacerda, L.D., Malm, O., Souza, M.M., Da Silveira, E.G., and Bastos, W.R., 1989, Mercury concentrations in inland waters of gold-mining areas of Rondônia, Brazil: The Science of the Total Environment, v. 87/88, p. 233-240.

Reimers, R.S., and Krenkel, P.A., 1974, Kinetics of mercury adsorption and desorption in sediments: Journal Water Pollution Control Federation, v. 46, p. 352-365.

Rippstein, T.W., 1995, A geochemical study of mercury contamination and mobility in the Arbacoochee gold mining district, Cleburne County, east central Alabama: unpublished Masters thesis, The University of Alabama, Tuscaloosa, Alabama, 76 p.

Rudd, J.W.M., Furutani, A., and Turner, M.A., 1980, Mercury methylation by fish intestinal contents: Applied and Environmental Microbiology, v. 40, p. 777-782.

Tümpling, Jr., W. von, Wilken, R.-D., Einax, J., 1995, Mercury contamination in the northern Pantanal region Mato Grosso, Brazil: Journal of Geochemical Exploration, v. 52, p. 127-134.

Wang, J.S., Huang, P.M., Liaw, W.K., and Hammer, U.T., 1991, Kinetics of the desorption of mercury from selected freshwater sediments as influenced by chloride: Water, Air, and Soil Pollution, v. 56, p. 533-542.

Zwaschka, M.R., and Cook, R.B., 1989, Geology and preliminary exploration geochemistry of the Idaho district, Clay County, Alabama, *in* Lesher, C.M., Cook, R.B., and Dean, L.S. (eds.), Gold Deposits of Alabama: Alabama Geological Survey Bulletin 136, p. 83-100.